The Long-Term Interaction of Groundwater with Lake Naivasha, Kenya

A numerical simulation of the relationship between groundwater and lake allowing for fluctuating lake levels

Owor Michael

April 2000

The Long-Term Interaction of Groundwater with Lake Naivasha, Kenya

A numerical simulation of the relationship between groundwater and lake allowing for fluctuating lake levels

Owor Michael

April 2000

Thesis submitted to the International Institute for Aerospace Survey and Earth Sciences in partial fulfilment of the requirements for the Degree of Master of Science in Water Resources Surveys

THE EXAMINATIONS BOARD

Prof. Dr. A.M.J. Meijerink (HEAD, WREM)	Chairman
Dr. E. Seyhan (Free University of Amsterdam)	External Supervisor
Drs. R. Becht (ITC-Enschede)	Supervisor
Dr. A. S. M. Gieske (ITC-Enschede)	
Drs. D. F. Kovacs (ITC-Enschede)	Director of Studies
Dr. M. W. Lubczynski (ITC-Enschede)	

The Water Resources and Environmental Studies Division
INTERNATIONAL INSTITUTE FOR AEROSPACE SURVEY AND EARTH SCIENCES
Enschede, The Netherlands

To my parents
from whose support have drawn all
my motivation and strength thus far

Acknowledgements

The Netherlands Government through the Netherlands Fellowship Program has sponsored this study at ITC. I do appreciate on behalf of my government and myself in particular, the provision of the means to attain more awareness. I am grateful to my organisation for granting me leave of absence to pursue the extra studies, and for all the help they have rendered this far. I do thank Dr A. Muwanga, Dr. E. Barifaijo, Mrs I. Ssemmanda, and Mrs R. Serumaga.

I am immensely indebted to my supervisor Drs. Robert Becht, for enabling me carry out a virtually new study and diligently guiding me through it all. I am grateful for all the support he provided right from the outset, through the fieldwork and subsequent analyses, to the final write-ups. I would like to register special thanks with Drs. D. Kovacs for all the help during fieldwork and the critical reviews and comments during the data analyses and thesis writing. I would equally like to thank Dr. A. Gieske for helping out with the text editor program for reading out the time-series data. I extend special thanks to Mr. A. Lieshout, my first DOS, for all the help and guidance rendered in the first part of this course. I do acknowledge all the help of all the other ITC academic and support staff, especially the cluster manager, Mr. Polman. I thank the whole Examinations Board most especially Dr. Seyhan, the external examiner, for making the time to evaluate this study.

I do acknowledge and appreciate the invaluable help of the WRAP personnel and the field assistants during fieldwork. All the help and accessories provided by the District Water authorities and the entire local and government bodies in the area are equally appreciated. Special thanks are extended to all the local farms and communities who were so co-operative when approached and contacted.

I highly appreciate all the invaluable discussions and work I shared with Kibona. I do extend similar appreciation to all my colleagues of the Naivasha group: Mai, Jolicoeur and Ataya, and to the rest of the group: Bojana, Uria, Mogessie, Worku, Obakeng, Saveedra and Merka. I do salute the IGS-boys: Keeetile and Anthony, and the Ugandan community.

Last but not least I stretch out my hands to my family for always being there for me, and to my special friends Syliver and Theresa.

Owor Michael
Enschede, The Netherlands
April, 2000

I do extend a special word of valuation to Bojana, Patricia, Kibona, Carlos and Jolicoeur who with utmost dedication and commitment collectively helped put together this final report. May the good Lord bless them all!

Abstract

The long-term interaction of groundwater with Lake Naivasha allowing for fluctuating lake levels over 66 years (1932-1997), was numerically simulated under steady state and transient conditions. A Lake Package that simulates lake-groundwater interaction with MODFLOW was used.

The results show that the accuracy of the digital terrain model is important to consider so as to safeguard the integrity of the ensuring hydrologic model and its applications. Automatic calibration of a model of this complexity is fast, efficient and quantifies the degree of uncertainty in the model results. The similarity in the budget components of the steady state and transient runs indicate that the hydrologic system had nearly reached a state of dynamic steady state equilibrium prior to the onset of the present level of water abstraction. There is a temporal variation in groundwater seepage from the lake that responds to the peak hydrologic inflow events to the lake. The rise in lake levels are associated with only those periods when stream/runoff inflows to the lake are in excess of the outflows. Consistent net groundwater outflow from the lake that averages 4.76 million cubic metres per month is evident. The regional groundwater flow patterns indicates major outflow areas to the south and south-east of the basin and lesser to the north and north-east. Temporal and spatial variations in the nature and magnitudes of groundwater-lake interactions, vertical flow and storage, abound around the lake. The extent of the zone of influence of the lake varies with the direction. The northern and western parts of the lake show the highest fluctuations in lake-groundwater flow interactions. The response of the groundwater levels to selected periods of lake level rise, fall and stability shows mimicry. There is a significant amount of water abstraction that has been picking up since 1980.

The results are instrumental in providing a more realistic insight into the long-term interaction of the lake and groundwater for this kind of system affected by transience.

Table Of Contents

List of Figures

List of Tables

List of Appendices and Plates

List of acronyms and symbols

ARGUS-1	MODFLOW processor incorporated with the lake Package
DTM	Digital Terrain Model
GIS	Geographical Information System
GPS	Geographical Positioning Systems
GUI	Graphical User Interface
ILWIS	Integrated Land and Water Information System (ITC GIS package)
KWS	Kenya Wildlife Service
Lake Package	Processor for Lake transience used with MODFLOW
LNROA	Lake Naivasha Riparian Owners Association
Ma	million years
MAE	Mean Absolute error
Mamsl	metres above mean sea level
Mcm/mth	Million Cubic meters/month
Mcm	million cubic metres
ME	mean error
MODFLOW	Finite Difference Groundwater Flow Model
Naivasha D.O.	Naivasha Divisional Office
NA	no available data
PEST	Model-Independent Parameter Estimation
PMWIN	Processing MODFLOW for Windows
RMS	Root Mean square error
S	Storativity/Storage Coefficient (also used for lake stage; appropriately defined in those cases)
SENSAN	Sensitivity Analysis program
T	Transmissivity
USGS	United States Geological Surveys
WRAP	Water Resource Assessment Project

Thesis Structure

Chapter 1 deals with the general background and relevance of the study.
Chapter 2 gives a breakdown of the structure of the thesis, all the data and materials used in the data pre-processing stage and the actual fieldwork activities that were undertaken.
Chapter 3 deals with the analyses of the fieldwork and all achieved hydrological/hydrogeological data that were necessary for the modelling stage.
Chapter 4 handles the geologic and hydrogeological framework that was essential for defining the conceptual model.
Chapter 5 describes all the modelling aspects that were carried out.
Chapter 6 analyses the model simulation results.
Chapter 7 discusses the results pertinent with the modelling and all the preceding data handling processes and therefrom draws a number of conclusions with some recommendations.

Chapter 1

INTRODUCTION

1.1 Background

1.1.1 Location

The Lake Naivasha Basin covering an area of approximately 3400 km^2 is between latitudes $0^o30'$ to $0^o55'$ S and longitudes $36^o09'$ and $36^o24'$ E shown in Figure 1.1. It incorporates the lake, the Ndabibi Plains to the west of the lake and the Ilkek Plains immediately to the north. It is situated in the Rift Valley Province of south-western Kenya, within the administrative district of Nakuru. The basin lies about 100 km to the Northwest of Nairobi. It is accessible by the mainline of the East African railways and a major road that services the western part of the country. There is an even distribution of all weather roads within the area.

The study area encompasses the lake area at the central part of the basin stretching westwards to the Mau escarpment and eastwards to the South Kinangop fault. Due north it extends to the Eburru volcanic pile and south to the volcanic complexes of Olkaria and Longonot. The study area covers an area of about 1600 km^2.

1.1.2 Physical Environment

Physiography: Lake Naivasha dominates the central part of the Naivasha basin. It has a mean surface area of 145 km^2 at an average altitude of 1887.3 mamsl (Mmbui, MSc 1999). The Mau escarpment on the western fringe rises up to a maximum of 3080 mamsl with a N-NNW orientation and is over 3000 m for 36 km of its length on the western fringe of the study area. The escarpment is rugged and deeply incised with numerous faults and scarps that are prevalent. There is a rise of topography to the south towards the Olkaria volcanic cones of up to 2430 mamsl at Olkaria Hill. The Ndabibi plains extend up to 9 km west of the lake and separate the Olkaria and Eburru volcanic complexes. To the east is the broad Kinangop Plateau that rises to a maximum altitude of 2740 m. The NNW-trending South Kinangop fault scarp (100-240 m, Darling ET al., 1990) separates the plateau from the plain in a series of downthrown fault steps.
The plains are about 1980 mamsl (Clark ET al., 1990) along their western margin and slope gently eastward to the lake. The Ilkek plains extend up to 23 km north of the lake and range in width from 13 km near Naivasha town to 4 km wide near Gilgil town. The plains slope gently southward from a maximum elevation of 2000 m in the north.

Climate: The basin lies within the semi-arid belt of Kenya with average annual precipitation of 700 mm (Ewbank Preece Ltd, 1990). The rainfall pattern is bimodal with the main rainy period in April-May and the shorter one from October-November (Ase ET al., 1986), Figure 1.2. It is greatest along the Mau and Aberdare escarpments where it averages from 1250-1500 mm annually and is lower in valley areas where it averages about 650 mm at Lake Naivasha being noticeably a function of topography. There is an annual potential evaporation estimated at about 1700 mm (McCann, 1974). Monthly averaged potential evaporation on the floor of the basin exceeds

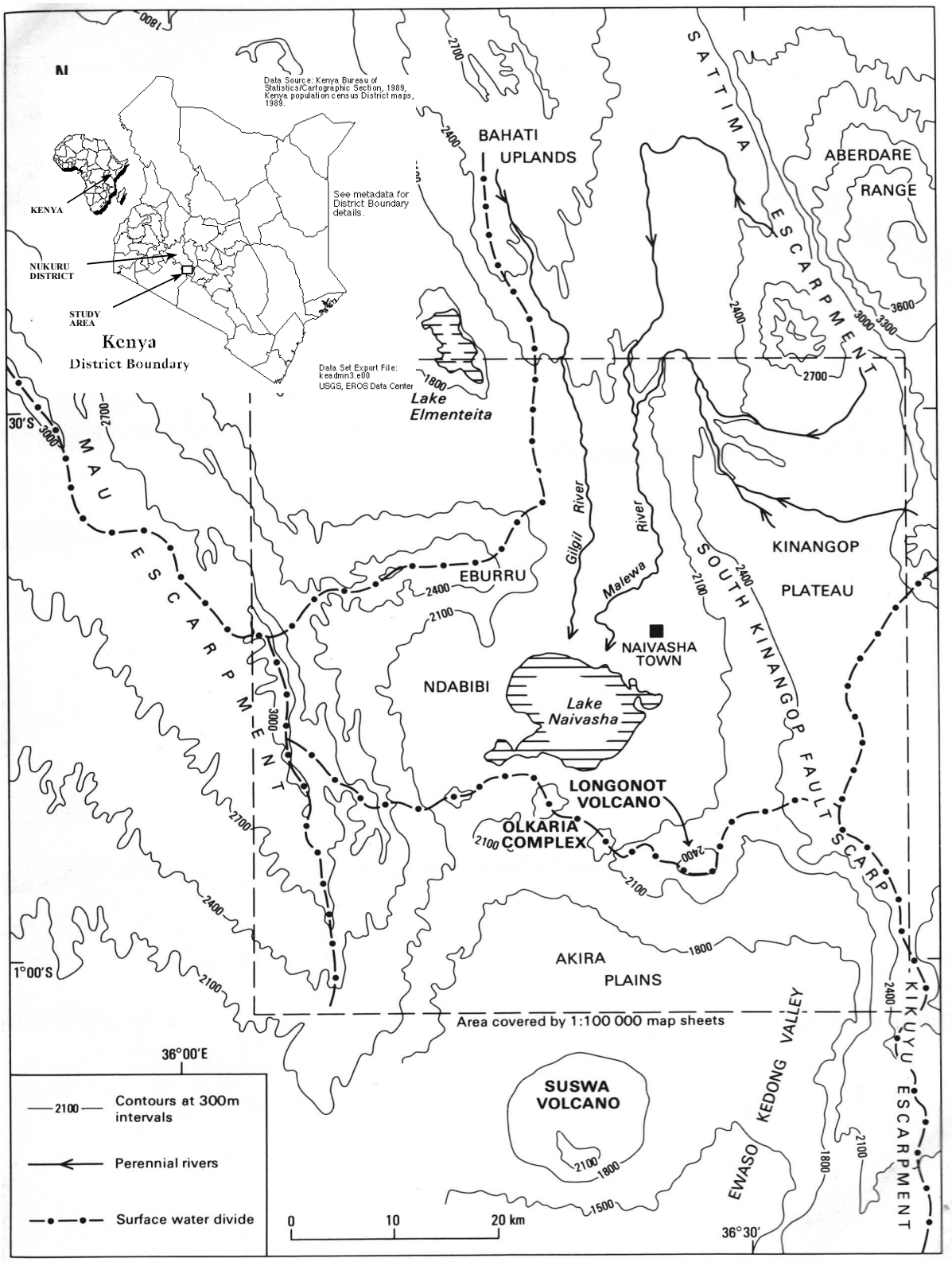

Figure 1.1: Detailed Physiographic Map of the Lake Naivasha Basin (after Clarke et al., 1990). Inset is the location of the study area in south-western Kenya.

rainfall by a factor of 2 to 8 for every month except April when the potential evaporation still exceeds rainfall save for the wettest years. Mean daily temperatures vary between 9^{o}C at night to 25^{o}C during the day. At Naivasha the relative humidity is less than 75%.

Hydrology: The Naivasha catchment is separated from the Nakuru-Elmenteita catchment mainly by the Eburru Volcanic pile which is linked to the Mau Escarpment by a ridge at an altitude of around 2600 mamsl. Between the Eburu and the Bahati Escarpment the surface drainage divide runs via Gilgil along a culmination of the Rift floor at an altitude of approximately 2000 mamsl. To the south of Lake Naivasha the surface water divide runs from the Mau Escarpment in the west, via the Olkaria and Longonot to the Kinangop Plateau and finally to the Nyandarua Mountains, see Figure 1.1.

Lake Naivasha: Lake Naivasha occupies the bottom of the rift valley and is in the middle of three major centres of geothermal activity: the Eburu Hills to the northwest, Mt Longonot to the southeast, and Olkaria to the south. The lake is the highest and freshest of all the lakes in the Gregory rift valley system. It consists of the main lake, a smaller sometimes separate Oloidien, and the Crater Lake Sonachi (the smallest of the three).

The lake level has been fluctuating thus affecting its area and volume and gradually declining over time. The bottom of the lake is predominantly very flat that may be due to the filling by large quantities of sediments that has resulted in the development of an even bottom topography. The two deepest parts of the lake have typical crater-shaped morphology indicating volcanic origin of formation (Ase ET al., 1986), Figure 1.3.

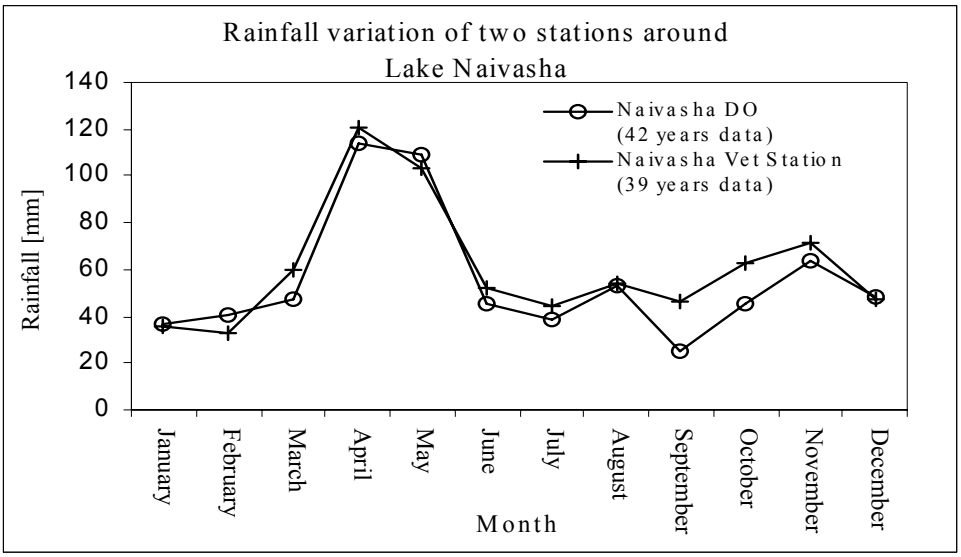

Figure 1.2: Rainfall variation of two stations around Lake Naivasha. Rainfall is bimodal with main pulses in April/ May and in November. The average rainfall on the lake for the period 1931-1960 was 608mm (East African Meteorological Dept.1966, after Ase ET al., 1986).

Rivers: The Malewa River is one of the two main perennial rivers that drain the lake and flow in a graben at the foot of the Kinangop plateau. The Malewa and Turasha Rivers have a combined drainage area of about 1,730 km^2.

The tributaries of the Turasha River (Makungi, Kitiri and Engare) deeply incise the Kinangop plateau flowing in a westerly direction. The Kinangop rivers are captured by the main Malewa River in the northeast of the basin. Further downstream the Malewa River is joined by the Turasha River and the two flow southwards.

The Gilgil River flows in a narrow basin to the north of the basin and is the second major perennial river that drains the lake. The Gilgil River has its headwaters high in the Bahati Highlands. Its main tributaries rise up to 2,772 mamsl and drain about 420 km^2.

None of the numerous streams that incise the Eburru ridge and drain the Ndabibi Plains reach Lake Naivasha.

Landuse and vegetation: The principle landuse is agriculture which includes irrigated crop farming (horticulture, vegetables, fruits) around the lake and mixed farming (wheat, maize, potatoes, beans and sunflowers) on the rain-fed slopes of the escarpment. Dairy farming is mainly practised on large estates on the north-eastern shores of the lake.

The low lying central parts of the catchments carry natural and semi-natural vegetation (grassland, bushland, acacia, cactus trees, savannah and shrub) that provide suitable habitat for wildlife and indigenous livestock farming. Game sanctuaries for wildlife are mainly set to the west of the area.

Settlements are mainly concentrated around the main towns with a few homes within the estates and farms.

The wetlands that are found around the shores of the lake are reputable for the existence of papyrus swamps. They are mainly used as indicators of hydrological regimes, modifiers of water quality and as habitats for numerous animals and birds.

The Eburru Hills, Mau, Longonot and Nyarandua escarpments are all hosts to indigenous hardwood forests that form the main watersheds of the lake basin. The bamboo forests are confined to the Nyarandua and Mau escarpments.

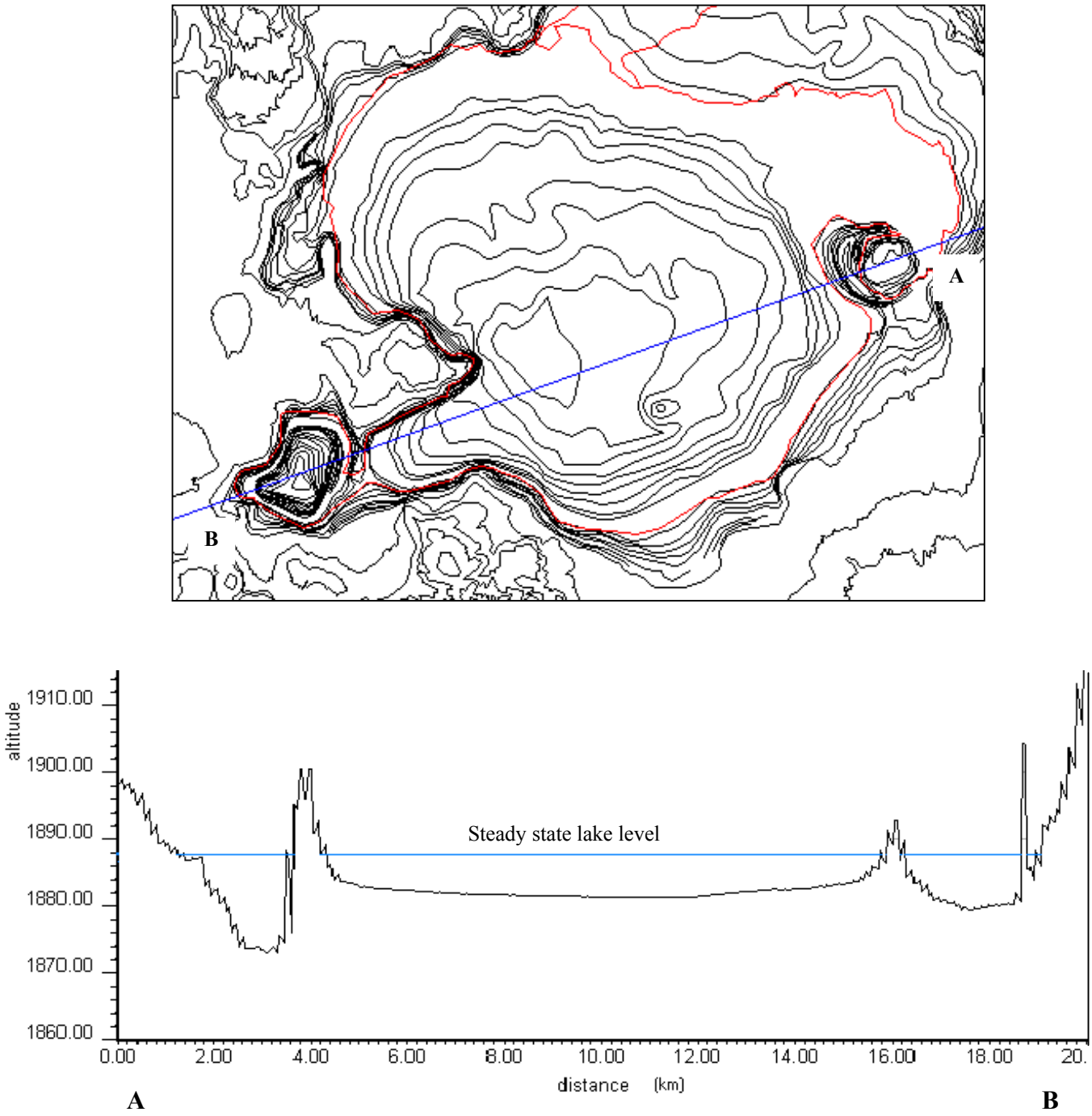

Figure 1.3: Bathymetric profile of Lake Naivasha from Crescent Lake, A (south-eastern), to Oloidien Bay, B (south-western) based on the existing contour maps that were modified during this study (see section 3.2). The Crescent Lake forms the deepest parts of the lake down to 1872 mamsl.

1.2 Importance

The quantity and distribution of suitable water determine the life and conditions of people, animals and vegetation. The type of water used by the human society is closely related to the progress or level of civilisation. Lake Naivasha is the only fresh water reservoir in the whole rift valley region. It supports the domestic, municipal and industrial needs of the town and countryside of Naivasha. Commercial irrigation agriculture thrives along its shores that is a major contributor to the nation's employment effort and socio-economic development. A rich abundance of wildlife and ecology abound in the basin. The Olkaria geothermal power project (generating about 18% of electricity) to the South of the lake indirectly derives its waters by recharge from the lake.
There is thus a big strain on the availability of water of suitable quality and adequate quantity to meet these diverse and conflicting demands.

The lake level has been fluctuating and declining over the years. The water balance and flow systems in the area have been altered. The lake has only an internal drainage that is hydrologically linked to the aquifers that underlie it. In view of the increasing demands and limited resources, there is need to obtain a reliable regional estimate of the groundwater fluxes and lake level fluctuations over time.

1.3 Research Problem

Numerical modelling is helpful in analysing field data and quantifying groundwater fluxes (Krabbenhoft ET al., 1990). A number of numerical models have been run to estimate the long-term water balance of the lake-aquifer systems of the Naivasha Basin. Numerical models used to quantify the water exchange between a lake and groundwater typically use a constant head condition to represent the average level of the lake (Winter, 1976). However, lake levels often show long and short-term transience. Precipitation to and evaporation from the lake surface, stream flow, and groundwater fluxes have to be considered. These flow components affect lake levels and changes in them lead to lake level fluctuations (Anderson and Cheng, 1993). A three-dimensional representation of the groundwater system is required to predict the flow system more accurately and provide a more realistic view of the lake settings.

In this study numerical simulations involved a Lake Package that incorporated the dynamic exchange of water between the lake and groundwater.
The model results were basically to be used as a tool to:

- provide enhanced insight into the intricacies of the system, and
- more efficiently plan detailed investigations, surveys and data collection in areas where the sensitivity of model performance to certain unknown factors were largest.

1.4 Objectives

The study was initiated essentially to develop a three-dimensional model to simulate the interaction of groundwater with the lake allowing for fluctuating lake levels.

The main goals of the study were:

- To describe more accurately the flow system around the lake.
- To construct a groundwater piezometric map derived from a single reference datum for the whole basin.
- To determine long-term water budget for the lake.
- To estimate water abstractions from both the surface and groundwater resources.
- To compare the Spreadsheet and MODFLOW Lake Package models.

1.5 General Approach

The Lake-groundwater interaction was three-dimensionally modelled over 66 years (since 1932) using a MODFLOW processor PMWIN. At the outset it was also intended to conjunctively make use of the ARGUS-1 GUI MODFLOW pre/postprocessor.

This was an integration of two previous studies: Long-term Water Balance of Lake Naivasha (Mmbui, MSc 1999), and Groundwater Flow Modeling of the Lake Naivasha Basin (Hernandez, MSc 1999).

The following activities were carried out:

- Time-series data on the climate, hydrology/hydrogeology and lake levels were assembled using available data and remotely sensed images.
- A hydrogeological model was developed giving groundwater heads and lake budgets/stages as output.
- The hydrological model was parameterised using available and assembled data sets (field measurements, maps, information derived by remote sensing) and implemented in a GIS environment.
- The model was calibrated and a sensitivity analysis of its results undertaken in response to a range of artificial changes introduced to the input data to measure and analyse the changes to the lake and groundwater levels, and to quantify the effect of these changes.

1.6 Previous Work

Lake Naivasha basin is a popular site for natural resources research due to its location in the Great Rift Valley of Kenya, its continuing freshness in an area of alkaline lakes, the mystery of its recharge together with its fame as a centre for recreation and wildlife.

1.6.1 Geology

The general geology of the Lake Naivasha area and its catchment as found in the papers of Thompson and Dodson (1963), Clark et al. (1990), and McCall (1967), is discussed in Chapter 3.

1.6.2 Precipitation

Richard and Richardson (1972) summarised the annual water input to the lake through rainfall as 608 mm.

1.6.3 Evapotranspiration

Tetley (1948) considered that evapotranspiration varied between 5.1 and 7.5 feet with an average annual figure of 6.0 feet (1.83 m). Ase (1986) calculated an average figure from pan evaporation of 1865 ±106 mm.
Chance (1944) calculated the evaporation for the lake as 74" (1850 mm).
England and Robertson (1959) using the Cochrane Formula calculated the evaporation rate at 63.6"±10% equivalent to 1358 mm.

1.6.4 River flows

Inflows from the Malewa and Gilgil Rivers for the 29-year period from 1936 to 1964 were calculated by England and Robertson (1969) to produce a change in volume of the lake of 209,000 acre feet, equivalent to 269 mcm, of which 89.9% was attributed to the Malewa. The same authors quoted flows for the Karati of less than 2000 acre feet in good years, equivalent to 26 mcm, when the river flowed for six months or less. As an inflow of 2000 acre feet in a month would result in lake level rise of only 0.07 feet, about 23cm (without adjustment for evaporation) this river's contribution to the lake can virtually be ignored for all practical purposes.
Ase et al (1986) use the data to provide water discharge values using a rating curve. The authors calculated the average annual flow for the 48-year period from 1932 to 1980 to be 153 mcm.
Tetley (1948) has also reported on the flow of the two rivers for the 10-year period from 1936 to 1947 as 137,960 and 12,322 acre feet respectively equivalent to 178 million and 16.55 mcm.
Lars-Erik, 1986 estimates the long-term (1932-1980) annual average from of the Malewa River Catchment (1553 m^2) at 153 mcm and from the Gilgil River catchmment at 24 mcm.

1.6.5 Lake Seepage

As early as 1922, Gregory suggested that there was an undiscovered outlet to the lake. Nilsson (1932) was the first to suggest that water entered and left the lake via underground seepage of some sort.
Gaudet and Melack (1981) and Ase (1987) showed that hydrologically Lake Naivasha was a seepage lake with input via underground seepage in the northern area.
Darling et al (1990) modelled the direction, quantity and character of underground flows in and out of the lake tracing the outflows up to 30 kms south. The northern flow is confined to the area between Eburu and Gilgil and the southerly outflow is

between the Olkaria and Longonot areas. Their estimates of outflow agreed broadly with the other workers: Sikes (1935), 43 mcm/year, McCann (1972), 34 mcm/year and Ase et al (1986) 46-56 mcm/year.
Clark ET al (1990) using water balance studies and the application of Darcy's law on groundwater estimated a total of 50 mcm/year outflow representing about 20% of total recharge. They estimated flow to the north of the lake at 11.3 mcm/year. McCann (1974) calculated a much greater flow to the north at 39 mcm/year. Ojiambo (1992, 1996) indicates that Lake Naivasha has a subsurface outflow of about 40 mcm/year from its eastern and south-western shores. The flow to the south may account for 50-90% of the total flow.
Howard (1993) has estimated that 16% of total inflow into the lake comes from underground. Gaudet and Melack (1979) have estimated an inflow of 58.5 mcm/year in their water balance.
Viak (1975) estimated groundwater inflow to lake at 1.8 mcm/year.

1.6.6 Surface Water Abstraction

The water bailiff's total of permitted extraction directly from the lake amounted to 32.7 million per year. Agriculture uses approximately 35 million m^3 per annum from the lake (Goldson, 1993).
A considerable proportion of water from the supplying rivers does not reach the lake, as it is abstracted upstream for various domestic and agricultural purposes. The permitted abstraction figures for the Malewa of 1990 (Water Bailiff, 1993) that cover 80 extraction rights total 21.6 mcm/year for domestic, flood flow and subsequent storage.
Clark et al (1990) calculated discharge of the Olkaria field based on data of well head steam provided by Bodvarsson (1987) at 3 mcm per year. They pointed out that this was only a small percentage of total material southerly flow from Lake Naivasha, thought to be in the region of 50 mcm. They concluded that any geothermal production influence on lake levels was likely to be masked by the effects of natural rainfall over the catchment.
Krhoda, 1995 estimated the safe abstraction limit from the lake at 12 mcm/year for a lake area of 140 km^2.

1.6.7 Lake Water balance

The following estimates have been made of the Lake Naivasha water balance, Table 1.1.

1.6.8 Groundwater

Clark, 1990 considered the lake sediments to be a patched aquifer with hydraulic conductivities varying from 12-148 m/day from the NE to the NW of the lake.
Viak estimated aquifer transmissivities between 200-500 m^2/day.
Ojiambo, 1992 noted the existence of three main aquifer systems: lake sediments, shallow volcanic aquifers and deep geothermal aquifers.
Krhoda, 1995 estimated the lacustrine sediment yields from 100-2000 m^3/year and away from the lake at <100 m^3/year. He calculated recharge rates of 0.10 to 1.59 m/year with a mean of 0.52±0.40 m/year.

McCann, 1972 estimated the mean annual recharge of the basin at 9.2% of total precipitation. McCann, 1974 estimated shallow outflow to the south from the rift areas and the lake at 250 mcm/year.

parameter	McCann (1974) 1957-1967	Gaudet and Melack (1981) 1973	Ase, Sernbo 1972-1974	And Syren (1986) 1978-1980	ITC calculated average
INPUT					
Precipitation	132	103 (range 77-114)	115 (range 84-149)	142 (range 127-167)	121
River discharge	248	185 (range 90-260)	187 (range 156-263)	254 (range 143-383)	212
Surface runoff	NA	0.6 (range 0.4-0.7)	NA	NA	0.6
Seepage-in	NA	49 (range 41-58)	NA	NA	49
TOTAL INPUT	380	338 (range 208-433)	302 (range 240-412)	396	382.6
OUTPUT					
Evapotranspiration	346	313 (range 289-324)	308 (range 294-332)	301 (range 272-339)	294
Seepage-out	34	44 (17-78)	NA	NA	39
Irrigation+ Industrial	NA	12 (range 7-15)	NA	NA	12
TOTAL OUTPUT	380	369 (range 313-417)	308 (range 294-332)	301 (range 272-339)	345
Storage change	NA	-31	0.4	95	37.6

Table 1.1: Estimates of the Lake Naivasha water balance from previous studies in million cubic metres per year

NA: no available data

1.6.9 Recent ITC Hydrological Studies

Mmbui, MSc 1999 studied the long-term water balance of the basin and calculated a groundwater outflow of 4.6 million m^3 per month and lake abstraction of about 57 mcm/mth. He estimated a long-term average total combined inflow from the Rivers Malewa, Gilgil, Turasha, Karati and surface runoff into the lake at about 2.26 mcm/mth.

Behar, MSc 1999 in the study of surface water-groundwater interaction found a similar lake seepage loss of 55 mcm per annum since 1958.

The groundwater flow modeling of the Naivasha basin by Ramirez, MSc 1999 found aquifer transmissivity values varying from less than 1 m^2/day to more than 5000 m^2/day. He estimated storativity values between 0.01 and 0.15.

Trottman, MSc 1998 in the study of the groundwater storage change in response to fluctuating levels of the lake found active groundwater storage zones of up to 1-2 km from the lake shores. Podder, MSc 1998 estimated the long-term average inflow from the Malewa catchment 1960 – 1990 into Lake Naivasha at about 215 mcm /year. Groundwater recharge estimation of the Malewa catchment by Graham, MSc 1998 found annual baseflow contribution to the lake to average 60 mm/year representing about 8% of effective precipitation. Baseflow and surface inflow to lake was about 137 mm/year. Ashfaque, MSc 1999 estimated daily average evaporation from the lake at 5.96 mm using the evaporative fraction approach, whereas the pan evaporation gave 5.46 mm with a standard deviation of 1.28 mm for the period 1958-1999.

Chapter 2

METHODOLOGY

2.1 Work Plan

The schematic representation of the breakdown and sequence of the study process is shown in Figure 2.1.

2.2 Data Preparation

In the preliminary stages of the study a literature review and preparation for fieldwork was carried out. The existing well database was updated and reorganised. Available data were screened and pre-processed, field survey points mapped out, mapping units delineated and appropriate field materials and tools identified.

The following materials were used:

2.2.1 Topographic Maps

Naivasha, sheet 133/2, 1975, 1:50 000 (UK Ordnance Survey Overseas Survey Department maps).

Longonot, sheet 133/4, 1975, 1:50 000 (UK Ordnance Survey Overseas Survey Department maps).

Kipipri, sheet 120/3, 1975, 1:50 000 (UK Ordnance Survey Overseas Survey Department maps).

Nakuru, sheet 119/3, 1974, 1:50 000 (UK Ordnance Survey Overseas Survey Department maps).

Gilgil, sheet 119/4, 1975, 1:50 000 (UK Ordnance Survey Overseas Survey Department maps).

2.2.2 Geologic Maps

Geological Map of Longonot Volcano, the Greater Olkaria and Eburru Volcanic Complexes and adjacent areas, 1988, 1:100 000, Government of Kenya, Ministry of Energy Geothermal Section.

2.2.3 Satellite Images

LANDSAT TM images (bands 1, 2 and 3), 21 January 1996 (western part) and 25 February 1987 (eastern part).

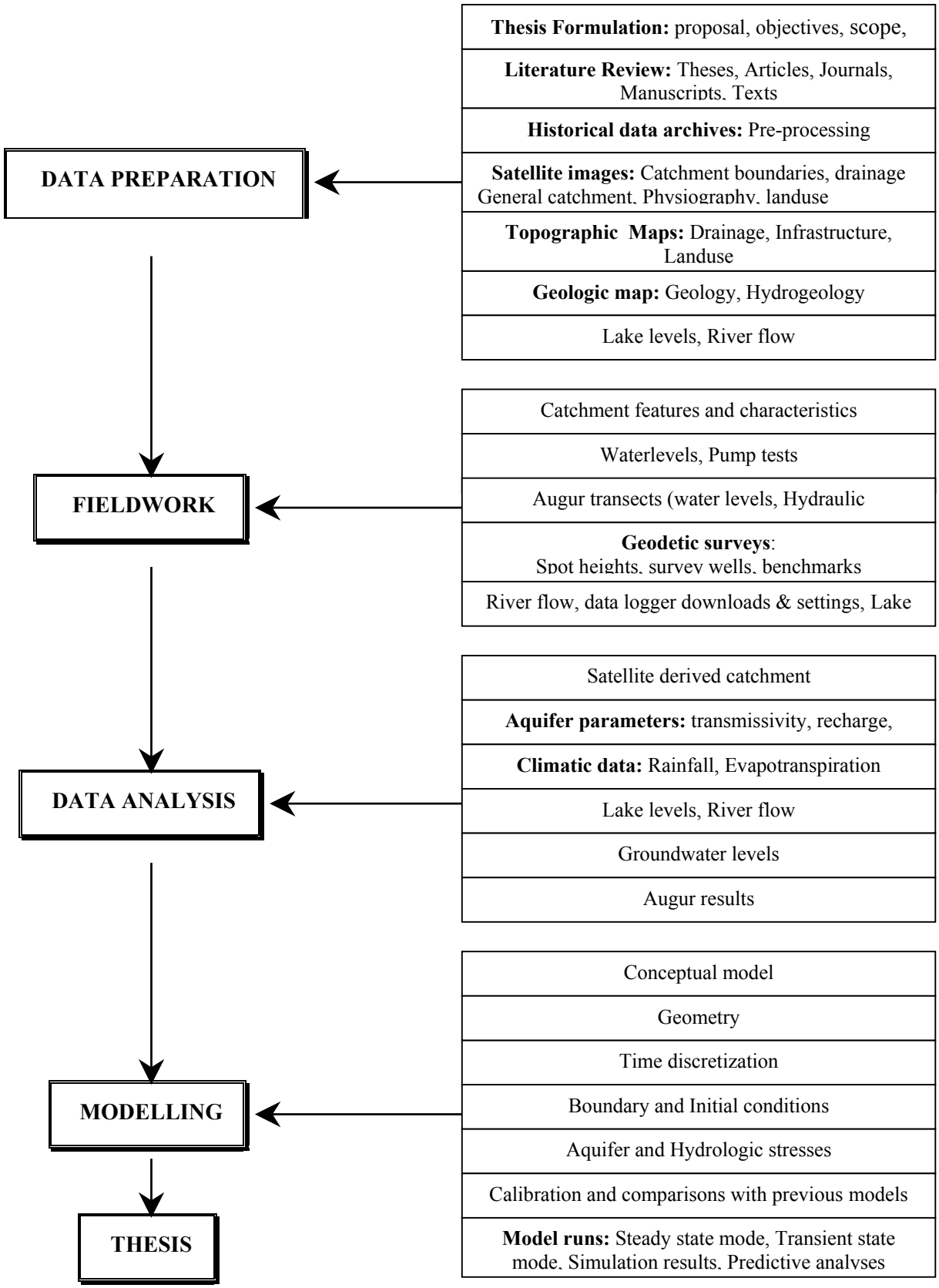

Figure 2.1: Schematic representation of the sequence of the study process.

Rainfall data,
Lake evaporation/evapotranspiration data,
Lake Naivasha levels data,
River discharge data for the Rivers Malewa, and Gilgil.

2.2.5 Groundwater well records

Borehole pumping tests data,
Well completion records,
Well water levels monitoring data.

2.2.6 References

A number of research papers, MSc theses, consultant reports, manuscripts, and journal articles from past works in the Lake Naivasha Basin were used in this study (see the References).

2.2.7 Equipment

The following equipment and materials were used in the field:
Water level transducers
Geodetic GPS meters
Field geological equipment
Hand Augurs

2.3 Fieldwork

A 3-week fieldwork was carried out from the first week of October 1999, after the data had been pre-processed and preparations made. The following activities were carried out in the field:

2.3.1 Geodetic Surveys

A Geodetic GPS of the Leica GPS Receiver type (tripod-mounted) was used to survey the wells and benchmarks in the area. A GPS is a three-dimensional positioning system that can naturally provide heights and/or height differences referred to a selected ellipsoid.
In the field the antenna was centred above the station on a tripod and the height to the antenna phase centre was measured. All the cables were connected and the receivers were initialised so that visible satellites were acquired. When the tracking had begun, it was ensured that the receiving device was functioning properly and that both measurements and broadcast ephemeris were recorded. The tracking performance was then monitored by watching receiver signal quality indicators. Logbooks were maintained to record any operator errors, receiver problems, tracking problems, obstruction diagrams, and weather data. When the predetermined amount of data had been collected, the antenna height and centring was checked, the antenna taken down, and the equipment moved to the next site.

The relative positioning in a network mode was used as the basic mode for the geodetic survey resulting in a geodetic levelling network. The concept of the relative (differential) positioning uses one stationary antenna as a reference point. The stationary antenna's receiver then tracks at least the same satellites (preferably all visible satellites) as the moving receiver does. Accurate knowledge is assumed of the stationary receiver's position and clock behaviour.
The precision with which positions are determined depends on two factors:
1) the satellite configuration geometry that changes with time and with position, as the satellites travel along their orbits, and
2) the measurement accuracy that represents the combined effect of ephemeris uncertainties, propagation errors, clock and timing errors, and receiver noise.

The raw geodetic survey data had to be pre-processed to obtain the correct positions of the reference points in the local UTM co-ordinate system. A reference benchmark was used to compute co-ordinates of the other user-defined stations using baseline processing and single point processing where required. After the whole data had been processed, the interpolation method was used to relate and transform the co-ordinates from the Cartesian WGS84 system to the local Cassini system. The two co-ordinate systems were then matched using common tie points to obtain the transformation parameters. The transformation parameters were necessary to transform the co-ordinates from one datum to another. Using SKI software, the transformed co-ordinates in the local system were obtained from the Cartesian WGS84 co-ordinates, Appendix 3.

2.3.2 Groundwater Levels

Water level measurements of a number of boreholes with access openings and for open wells were carried out, Figure 3.10. The water levels where ever possible were taken relative to the top of the access holes. In cases where the access holes were not available, the water levels were measured relative to the top of the concrete slab embankment. In a few cases access holes were welded into the borehole casings to enable the measurements be taken.

2.3.3 Pump Tests

Most recent data used were obtained from Kibona, MSc 2000 who carried out pumping tests in a couple wells at the Three-Point Ostrich farm on the north-eastern part of the lake, Figure 3.9. Data from all the previous work done in the area were also used to have a better feel of the spatial distribution of the aquifer characteristics.

2.3.4 Transect Augers

Water levels were measured for the test holes within the KWS-Annex and in the Manera Farm augured by Behar, 1999, shown in Figure 3.3. Of the KWS-Annex monitoring holes only one was traced back and so new ones were augured along a similar transect.
All the holes at the second transect in the Manera Farm were traced and the water levels measured. The current and previous water levels were compared for groundwater fluctuations, Figure 3.11a and b.

Augur holes were made on the banks of the River Malewa by Kibona, MSc 2000 to estimate the hydraulic conductivity of the river using the auger-hole and inverse auger-hole methods, Table 3.2.

This was close to the augers made by Behar, MSc 1999 to study the interaction of the river with the groundwater Figure 3.3.

2.3.5 River Flow

Data from the Ministry of Water Development, Nairobi were screened for anomalous entries. Gauging stations were visited to ascertain their status and extra data collected. The main River Malewa gauging station (2GB1) had wooden planks placed across its width to dam and divert the flow. This obstruction was clearly interfering with the rating curve/equation (stage-discharge relationship) for this section of the river reach, that was currently in use, Plate 2.

2.3.6 Lake Levels

Virtually all the lake level data used in the study were historical and already digitally archived. Some lake level data were collected and the gauging stations visited to measure the current levels.

Chapter 3

DATA ANALYSIS

The screening of hydrological data is a prerequisite to the successful design and implementation of water development schemes (Dahmen ET al., 1990). The previous workers had already screened most of the data that has been used in this study. All the spatial data have been stored in the ILWIS for fast and efficient acquisition, pre-processing, management, retrieval, manipulation, analysis and result generation.

3.1 Catchment Characteristics

The general topographical and hydrological background from available records, maps aerial photos and satellite imagery were described. The LANDSAT TM images (composite of bands 3, 4 and 5) that had been georeferenced using tie points within the ILWIS package (Ramirez, MSc 1999) were used to delineate the catchment boundaries, Figure 3.1. Drainage lines were also drawn for the Rivers Malewa and Gilgil, the Lake Naivasha boundary in 1996, included too were the necessary infrastructure and base/reference stations.

3.2 Digital Terrain Model

The DTM is a numerical representation of the relief of (part of) of the earth's surface. Different maps and survey data have been used to generate the DTM, Figure 3.2. The base system of the lake bathymetry was originally surveyed in the old feet system in 1957 by the Ministry of Works.

The contours digitised from the 1:50 000 scale topographic map sheets of Naivasha, Longonot, Gilgil and Nakuru had their reference datum raised by 3.5m to the level of the lake bathymetry. The contours of a map of the Naivasha area that was mapped by Viak, 1975 were also raised by 2m to the level of the lake bathymetry. The three vector contour maps were glued together and rasterized. The resultant map was then combined together with the rasterized altitude map. Contour interpolation was then performed in one algorithm. The algorithm first interpolates values for all the pixels (image element or cell) that are located on the segments and points. Then values are calculated for the pixels that fall in between the two. For each undefined pixel, the distance is calculated towards the two nearest contour lines and/or points. The distances are calculated backwards and forwards until no more changes occur. Then a linear interpolation is performed using the two distance values. This returns the value for the undefined pixel (Gorte ET. al., 1990). The final DTM indicating the spatial distribution of the relief attribute of the area was calculated with a 50m-cell size. The positions of the surveyed reference benchmarks and wells are shown in the satellite image of the area in Figure 3.1.

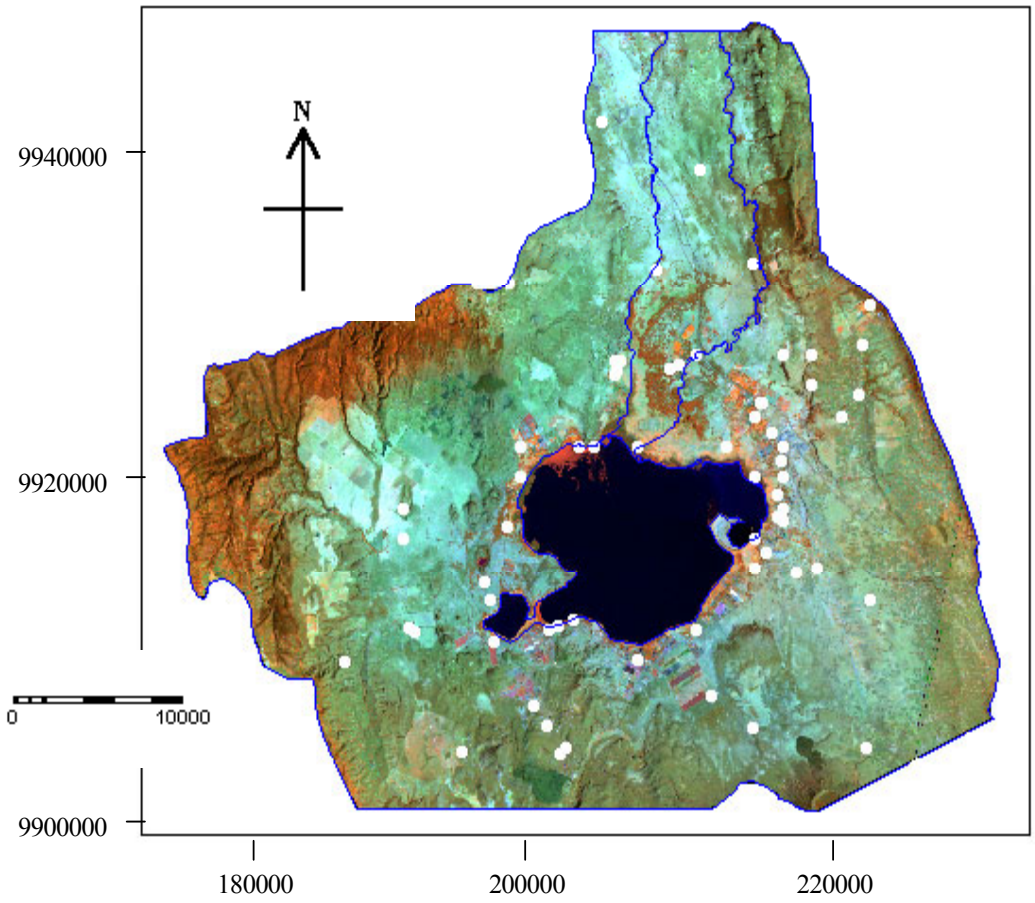

Figure 3.1: TM image showing the distribution of surveyed wells and benchmarks in the catchment.

O Positions of surveyed wells and benchmarks (some of the outlying wells have been surveyed by previous workers.

3.3 Climatic Data

3.3.1 Precipitation

Rainfall data was obtained from the Naivasha District Office for the duration 1910-1997. The data gaps for the 1977 period was infilled using a station on the western shores of the lake (Mmbui, MSc 1999) Figure 3.3. The rainfall data considered include that for the direct precipitation into the lake and for the general catchment area that has been used for the runoff and recharge estimates.

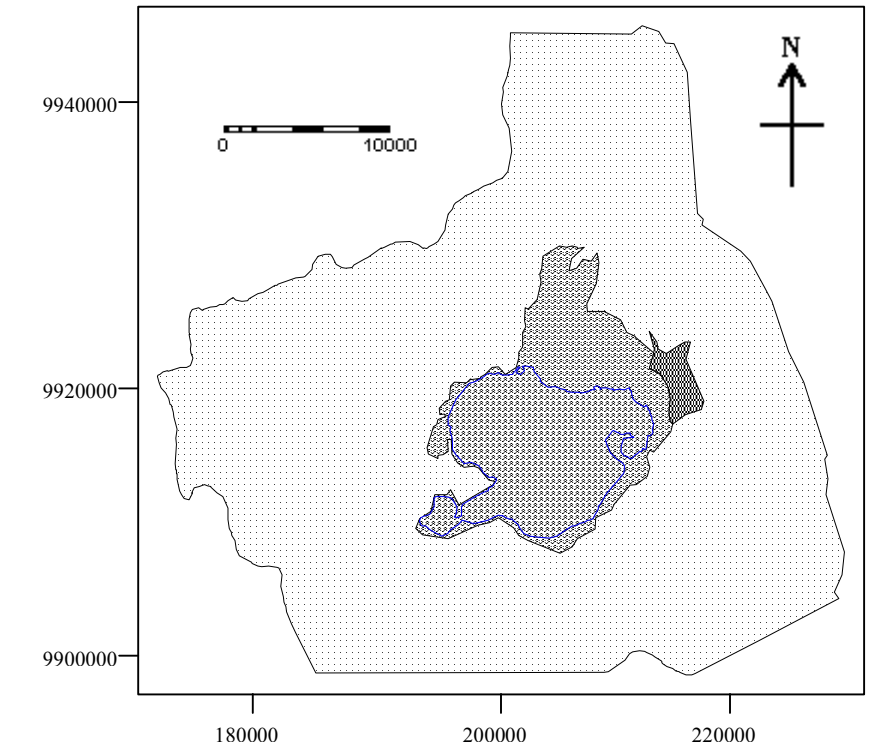

Figure 3.2: The layout of the different maps and corrections made to generate the DTM.

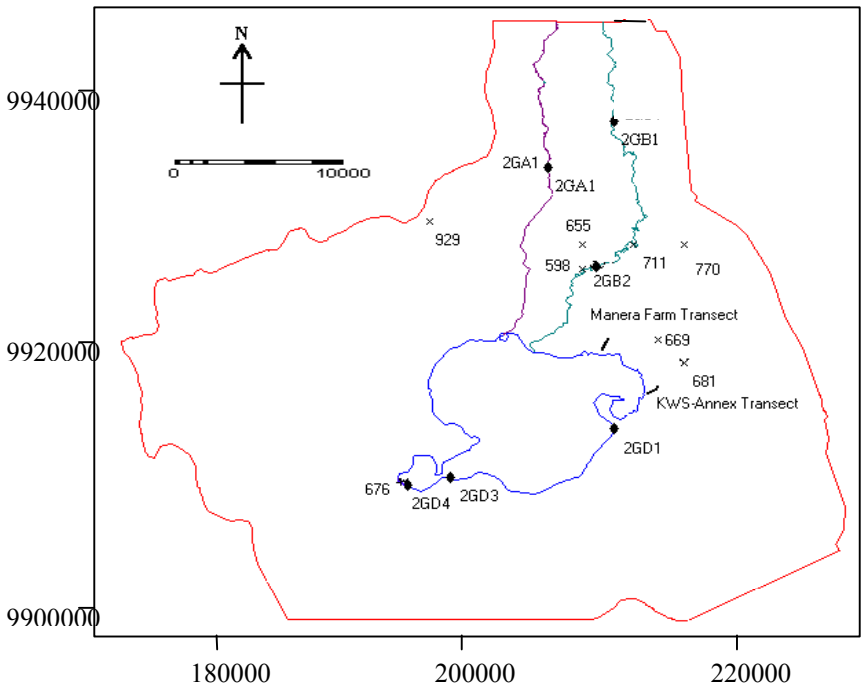

Figure 3.3: Location of rainfall (×), discharge (GA- and GB- numbers) and lake (GD- numbers) stations within the study area.

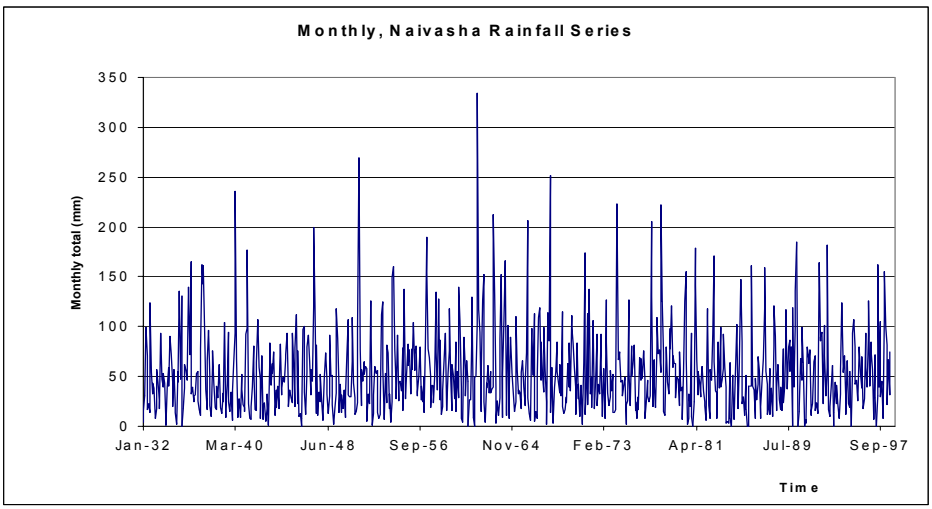

Figure 3.4: Long-term monthly rainfall (direct rainfall into the lake: 1932-1998, after Mmbui, MSc 1999).

3.3.2 Evaporation

The evaporation data was obtained from the Naivasha Water Development Department. The existing data from 1952-1990 had been screened for outliers and typing errors using scatter plots. The long-term monthly averages were used for infilling the months with missing data and backdated to 1932 using linear regression (Mmbui, MSc 1999), Figures 3.5a and b.

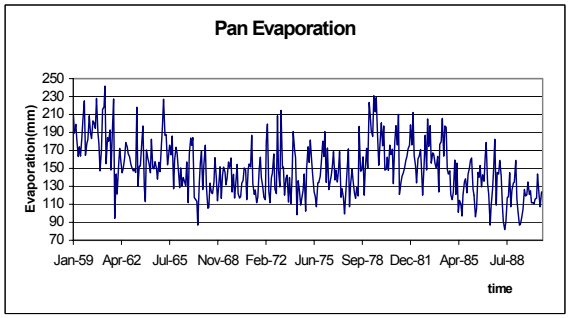

Figure 3.5a: Long-term monthly average lake pan evaporation, 1959-1990 (Mmbui, MSc 1999).

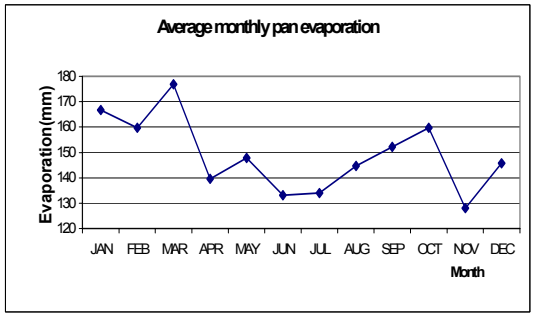

Figure 3.5b: Long term average monthly pan evaporation.

3.4 River flow/runoff

The Stream discharge stations 2GB1(1931 to present), 2GA5 (December 1959 to present) and 2GD2 (1952-1982) on Rivers Malewa, Gilgil and Karati, respectively were used to quantify the stream input into the lake. They were chosen for their proximity to the lake to reduce the need for estimating the amount of river diversions (Mmbui, MSc 1999), Figure 3.3.

Using linear interpolation, simple and multilinear regression with the neighboring stations, the data gaps were infilled, the results of which are shown in Figure 3.6. The

Karati River drains the smallest of the three catchments and its contribution to the lake was considered to be negligible.

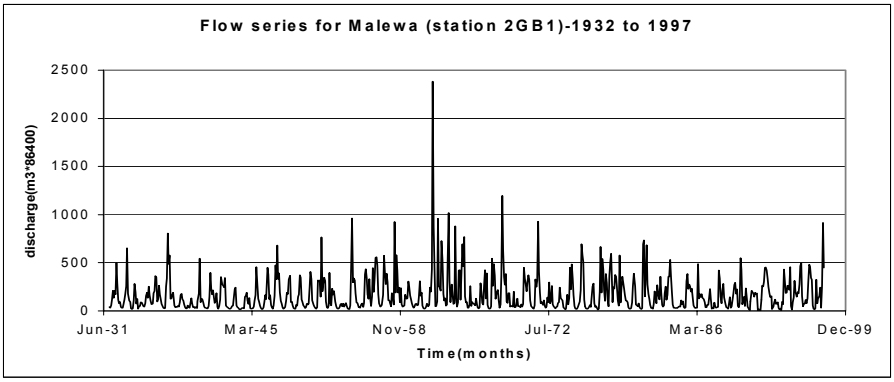

Figure 3.6: River Malewa Flow series for the main station 2GB1 (1932-1997), Mmbui, MSc 1999.

3.5 Lake Levels

Three main lake level stations were used for lake level estimates, namely: 2GD4, 2GD6 (1967-1987) and 2GD1 (1900-1961), Figure 3.3 (Mmbui, 1999). Also included were private monitoring stations at the Sulmac and Vaughan farms. These stations have been operational at various times. The 2GD1 station data existing as hardcopy hydrographs were digitized into the required format and with the aid of the ILWIS and a spreadsheet the water levels were aggregated into monthly levels. The 2GD6 data was screened for typing errors and outliers using time scatter plots and aggregated into monthly averages after linear regression. A plot of the 2 stations showed a high correlation in times of overlap after shifting the 2GD1 station datum by 3.6m to those of the 2GD6. The two series were then combined to extend the levels from April 1982 to 1987. The Sulmac series were from 1984 – 1993 fitted the adjusted 2gd6 data perfectly and was used to extend the water levels to 1993 (Mmbui, MSc 1999). The Vaughan series fitted the reconstructed lake levels and was used to extend the levels to 1998. Data gaps in these series were filled with those of Min. of Water Development from 1997. The complete reconstructed lake levels for the period 1900 to 1998 is shown in Figure 3.7 (Mmbui, MSc 1999). Lake level data is indicated in Appendix 2.

Rating equations (curves) were derived form the bathymetric surveys carried out by WRAP, 1998 showing the Lake stage – volume and Lake stage – area relationships, indicated in Figure 3.8.

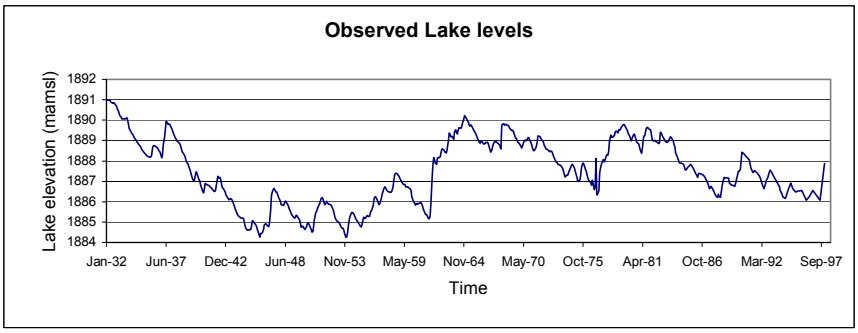

Figure 3.7: Reconstructed observed average monthly lake levels from 1932 to 1998 (Mmbui, MSc 1999).

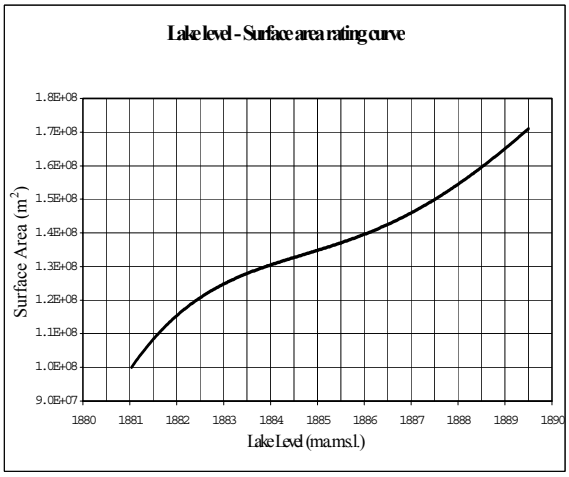

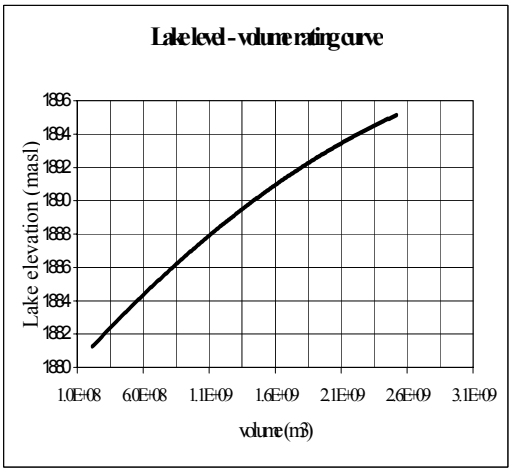

Fig. 3.8a: Lake surface area-stage rating curve. Fig. 3.8: Lake surface volume-stage rating curve.

Figure 3.8: The Rating Curves (equations) computed from the 1998 bathymetric surveys of WRAP, Kenya.

3.6 Groundwater Characteristics

3.6.1 Groundwater Levels

The wells with available groundwater levels in the area are shown in Figure 3.10. The groundwater levels of the wells have been obtained as altitudes in mamsl derived as the depth to the water surface from the DTM-defined ground surface. These values were used to derive the piezometric surface as inferred from their distribution. Within the vicinity of the lake area, average attitudes of 1886 mamsl are evident, that significantly reduces or increases in the outlying areas.

The scale chosen for the piezometric map of the study area was 1:2 000 with a contour interval of 25 m.

Clark ET al., 1990 in the construction of a piezometric map for the basin noted that: The problem with collecting hydrogeological data in the Rift Valley is that few wells

have access for the water level measurements, either because a piston pump is installed or because the borehole is blocked. Therefore water levels are taken from borehole records. These data refer to levels at the time of well completion that is a period spanning over 50 years for boreholes in the project area. This introduces errors in defining piezometric contours, because of the seasonal and longer-term variations in groundwater levels.
The scale of such errors may be found by comparing borehole water levels at the time of completion with levels measured recently. While differences measured are not insignificant, such variations are small when compared with the large spatial variation in surface topography and water table geometry encountered in the Rift, and can therefore be ignored when groundwater movement on the scale of the Rift is considered. Other errors are introduced into piezometric map construction by using borehole rest-water levels that may represent a local averaging of several piezometric surfaces where different aquifers are intersected by a borehole.

3.6.2 Groundwater Flow

The groundwater flow directions as inferred from the piezometric surface discussed in section 3.6.1 is included in Figure 6.21 (section 6.2.3) for the initial flow directions under the natural setting. The shallow regional groundwater flow as it was prior to the onset of all the activities that have changed the original pattern can be surmised as follows: The first component of lateral flow into the basin was from the Mau scarp that dispersed into three arms. NE wards towards the Eburru hills, SE wards to the Olkaria geothermal range, and directly E wards that recharged the lake sediments. The second lateral flow was from the Kinangop and Aberdare escarpments that dispersed again into three arms: N and NW wards to the Eburru and Bahati uplands, E wards to the Lake, and SW wards through the Longonot plains. The bulk of this second flow to the catchment seems to have been impeded by the South Kinangop fault and mostly recharged the deeper southern geothermal aquifers. Axially, the bulk of the flow from the lake was to the south through the Olkaria-Longonot volcanic complexes. There was a local NW flow into the lake from the southeast lying area of Kedong.
Northward flow from the lake was towards and through the Eburru hills and Elmenteita Lake basin (Darling et al., 1996, Clark et al., 1995).

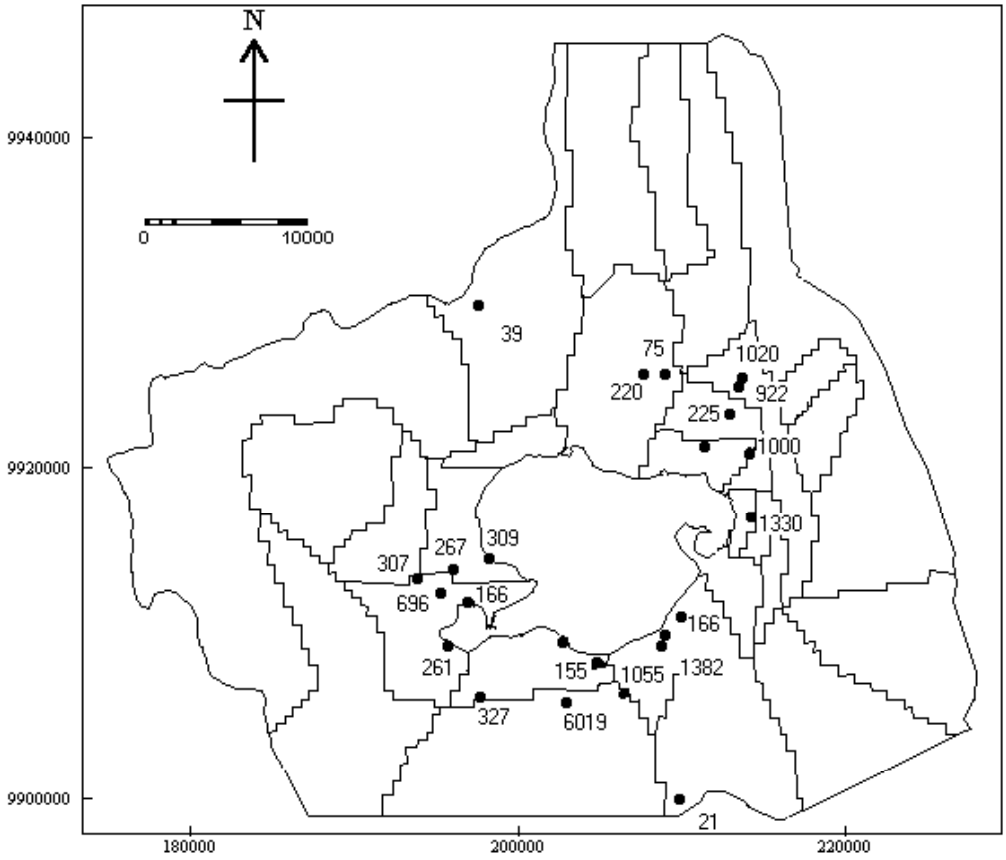

Figure 3.9: Distribution of transmissivity values in wells in the catchment.

3.6.3 Pump Tests

The pump test results have been obtained from a number of sources; most recent of which is Kibona, (MSc 2000). For well BH C at Three Point Ostrich farm within the lake sediments She estimates using the Hantush method a transmissivity of 1150 m^2/d and a storativity of 3.95×10^{-3}. With the Cooper-Jacob yields a transmissivity of 462 m^2/d and storativity of 1.46×10^{-3}. The results of all the available data from previous studies have been tabulated in Appendix 1. The distribution of the wells with pump test results is shown in Figure 3.9.

Area	Lithology	Geometric mean estimated Transmissivity m^2/day	Geometric mean estimated permeability m/day	Total number of boreholes
NE Naivasha	Sediment & volcanics	307 (1170)	12 (33)	35
SE Naivasha	Sediment & volcanics	502 (3082)	20 (114)	22
SW Naivasha	Sediment & volcanics	297 (940)	63 (196)	17
NW Naivasha	Sediment & volcanics	1601 (5308)	148 (818)	26

Table 3.1: Average aquifer characteristics of the selected areas and lithologies from borehole data (figures in brackets are geometric means), Clarke et al., 1990.

Clarke et al., 1990 estimated a regional distibution of transmissivity values for the whole of Lake Naivasha Basin from a number of boreholes, the results are summarized in Table 3.1.

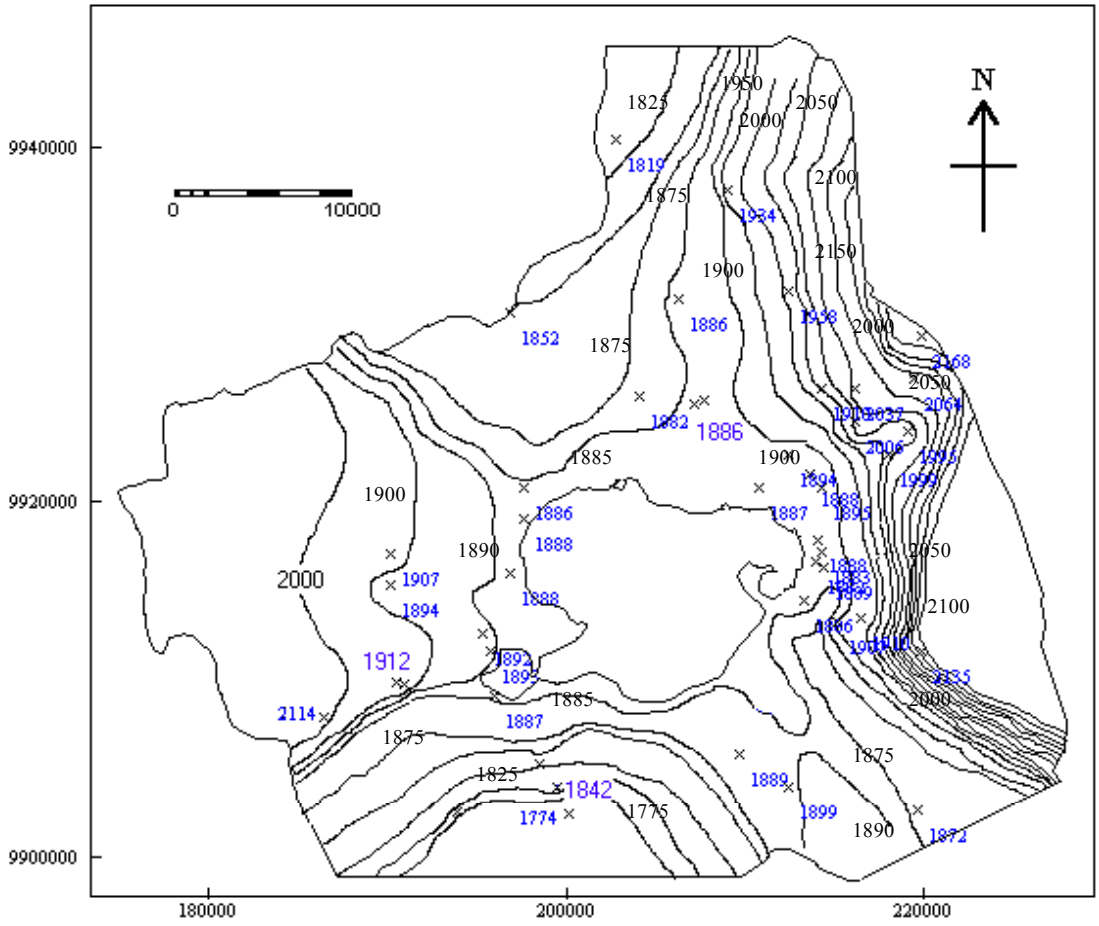

Figure 3.10: The inferred piezometric surface of the area under the natural setting (prior to the 1980 period). The map is drawn with a 25m contour interval. The crosses indicate borehole positions.

3.6.5 Auger Transects

Water Level Fluctuation: The water levels in the Behar transects (MSc 1999), Figures 3.11a and b were measured to check on the groundwater level change in the past year. Figure 3.11a shows the fluctuation in levels between the two periods of measurements at the KWS-Annex and Manera farm stations. As noted by Behar, it can be seen that the water levels in the wells of each of the transects are below the lake level, and have generally dropped by about 1.5 m in the past year. These transects reflect the local flows from the lake that are a response to the lower groundwater levels in the north-eastern parts due to the substantial amounts of abstractions taking place there.

Hydraulic Conductivity: The hydraulic conductivity of the river sediments on the banks of the River Malewa has been estimated by a number of previous studies.

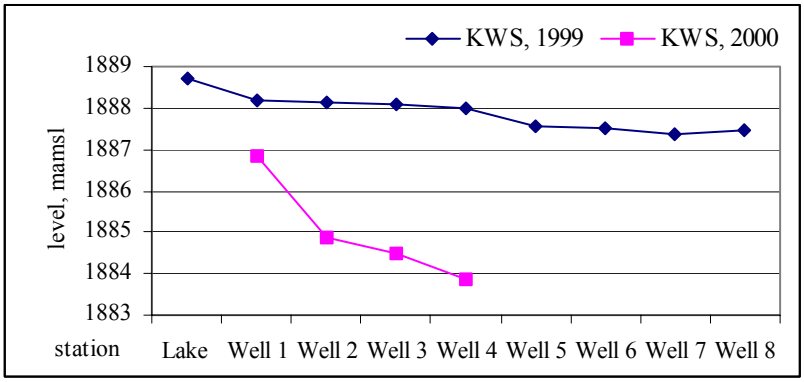

Figure 3.11b: The water levels in the KWS-Annex wells for the two periods October 1998 and October 1999. Notable are the lower levels in the latter year and the lower levels away from the lake in both instances.

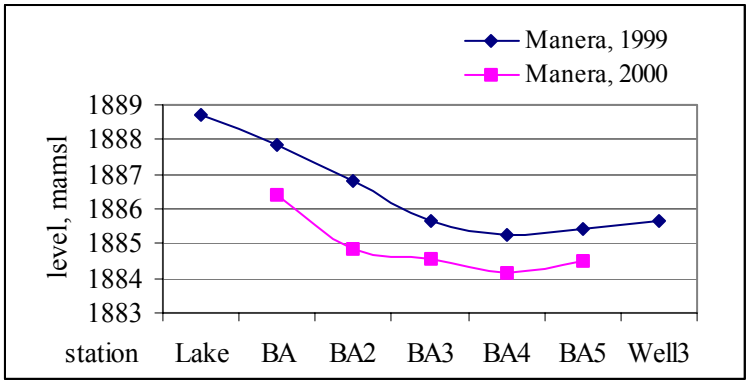

Figure 3.11a: The water levels in the wells in October 1998 and in October 1999. The lower levels in the latter year are notable.

3.7 Groundwater/Lake Abstractions

Its been noted by most of the previous workers that the activities that have imposed a lot of stress on the lake and groundwater picked up after 1980. Prior to this period the effects of the activities that were being carried out in the basin on the water balance were negligible. Estimates of water abstractions have been taken from previous workers (see section 1.6.6).

Identification	Distance from Malewa River (cm)	Depth of the hole (cm)	Coordinates		Hydraulic Conductivity (K, m/d)
			X	Y	
The Auger-hole method					
Auger-hole A	110	186.5	211900	9927739	0.1
Auger-hole B	110	174	211900	9927739	0.42
The Inverse Auger-hole method					
Inverse Auger-hole C	330	330	212717	9928025	0.23
Inverse auger-hole D	100 cm	110 cm	212717	9928025	0.28 m/d
Inverse auger-hole E	270 cm	71 cm	211489	9927104	0.38 m/d

Table 3.2: Hydraulic conductivity results using the Auger-hole and Inverse Auger-hole methods (Kibona, MSc 2000).

Chapter 4

HYDROGEOLOGIC SETTING

4.1 Geologic setting

Stratigraphy: Thompson et al. (1957), tentatively classified the rock succession of the Naivasha area as:

Age	Rock type
Holocene	volocanics, lake and fluviatile sediments
Upper Pleistocene	volcanics and lake sediments
Upper Middle Pleistocene	volcanics and lacustrine sediments
Lower Middle Pleistocene	volcanics and lake sediments
Pleistocene	volcanics

They noted that the volcanic rocks in the area consist of tephrites, phonolites, ashes, tuffs, agglomerates and acid lavas rhyolite, and comendite and obsidian. The lakebeds are mainly composed of reworked volcanic material or sub-aqueously deposited pyroclastics, and a few diatomaceous beds are known to occur. Despite their extensive distribution the exposed lakebeds are not thick and rarely exceed 100 ft (30 m). The structures of the area comprise faulting on the flanks and in the floor of the Rift Valley, and slight folding in the Njorowa gorge. Slight unconformities are present in the lake beds, and can most clearly be seen along the Malewa River drainage. The simplified geology of the catchment area is shown in Figure 4.1.

Two cross sections AB and CD are taken to the north and south, respectively shown in Figure 4.1. Section AB shows that up to a depth of 500m, the western part is underlain by mostly the Eburru pumice intermixed with pantellerite. To the east is mostly underlain by Limuru trachyte and Kinangop tuff that is overlain by alluvial and lake sediments in the valleys. Section CD has a mixture of mostly Maiella pumice to the west and longonot pumice and ash to the east.

The four major episodes of both volcanic activity (V1-V4), and faulting (D1-D4), based on work done by Baker et al (1988) include:

Episode		Activity	Age range (Ma)
V4		late Quaternary to Recent Salic Volcanoes	0.4-0
	D4	extensive minor faulting of the rift floor	0.8-0.4
V3		Quaternary flood lava of rift floor	1.65-0.9
	D3	renewed faulting of rift margins	1.7
V2		early Quaternary flood trachytes	2.0-1.8
	D2	formation of step faults (narrowing of graben)	3-2
V1		Pliocene ash flows	3.7-3.4
	D1	major faulting of eastern rift margin	4-3

Clark et al. (1995) described that west and southwest of the Kinangop plateau, the soft volcanic rocks that form the plateau have been down-faulted in a series of steps.

These include ignimbrite succession, mostly welded tuffs, palaesols and weathered zones at the top of most beds. The maximum exposed thicknesses are about 150 m.

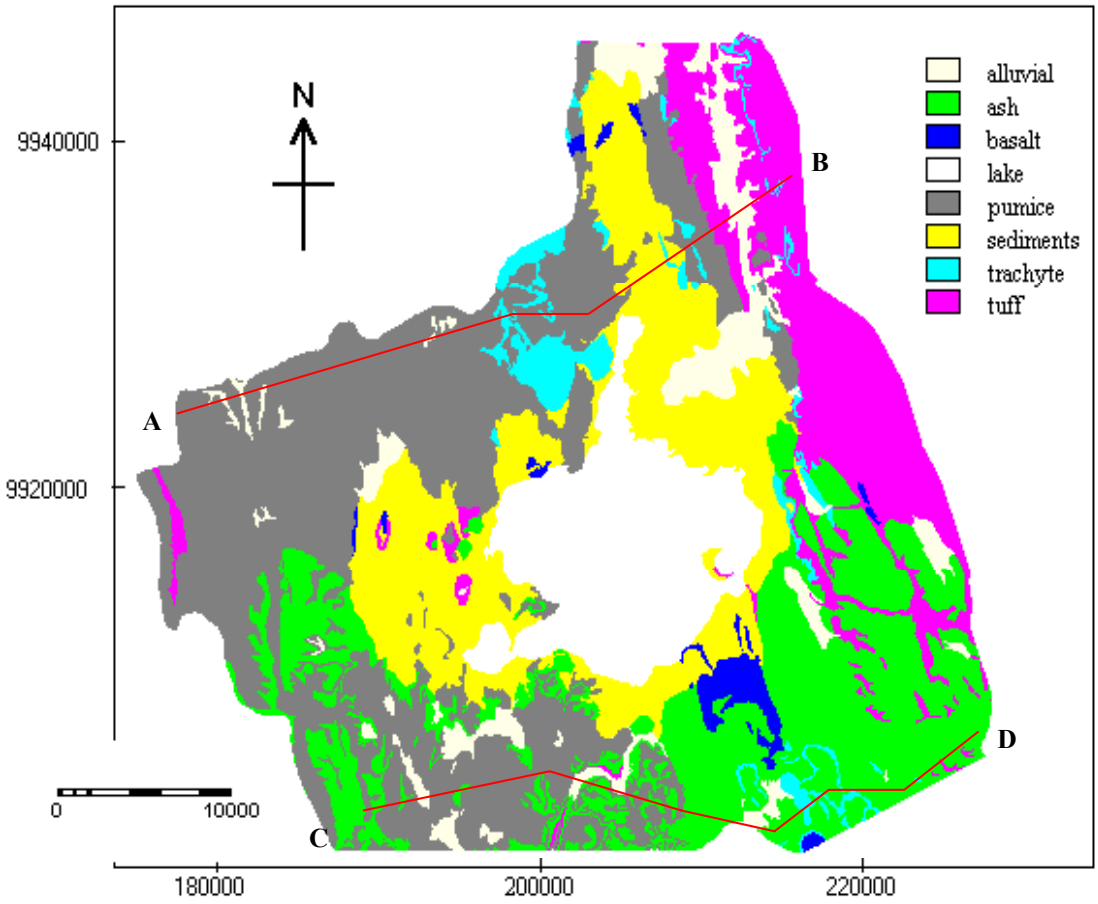

Figure 4.1: Simplified geology of the catchment area derived from the Geological Map of Longonot Volcano, The Greater Olkaria and Eburru Volcanic Complexes, and Adjacent Areas.

The Mau escarpment is largely composed of the ignimbrite succession dominated by tuffs with only rare outcrops of agglomerates and lavas. The rifting has produced blocks down-faulted to the east along the escarpment. The maximum exposed thickness is about 100 m.

The rift valley floor is largely covered with sediments that accumulated in the lakes during the Gamblian stage of the Pleistocene period. They contain a large proportion of their volcanic material, and a few diatomaceous beds are known to occur. The floor abounds with the greatest variety of topographic features caused by earth movements: craters, remnants of pre-existing craters, fault scarps, fissures, and steam-jets. The rocks found on the Rift floor vary from undersaturated tephrites to highly acid rocks such as rhyolites and sodic rhyolites.
The lake beds are mainly composed of pumiceous granules (pebble gravel, diatomites, coarse sand, silt and clay). The maximum thickness of exposed beds is about 15 m.
Along the Malewa River valley are alluvial deposits that include silt, fine sand, some ferruginous coarse sand and boulder gravel.

Structure: North to north-west-trending faults define the eastern and western rift margins, and most of this faulting has probably occurred prior to the development of volcanic centres on the rift floor. At least three distinct periods of faulting have occurred within the period 0.4 to 4 Ma. And these followed the periods of volcanism that gave rise to Kinangop Tuff, Limuru Trachyte and Gilgil Trachyte.

4.2 Hydrogeologic Setting:

Aquifer Systems: Clark ET al. (1995) noted that aquifers are normally found in fractured volcanics, or along weathered contacts between different lithological units. These aquifers are often confined or semi-confined and storage coefficients are likely to be low. Aquifers with relatively high permeabilities are found in sediments covering areas around the Lake. They are often unconfined and will have relatively high specific yields. This is in agreement with McCann, 1974; Ojiambo, 1992 who also noted that the wells near the Lake Naivasha shore yield water from lacustrine deposit aquifers and usually have higher discharge yields and transmissivities than wells further away from the lake. Most of the production in the Olkaria reservoir is from fractured trachytes and basalts and from contacts between these lavas and pyroclastics (Merz & McLellan/VIRKIR, 1986, Ewbank Preece Ltd, 1989; Ojiambo, 1992).

Tectonic movements of the Rift Valley have important effects on aquifer properties, both on a small scale by creating the local fracture systems which comprise many aquifers, and on a large scale by forming regional hydraulic barriers or shatter zones of enhanced permeability.

Piezometry: Clark ET al. (1995) noted that the area has a complex hydrogeology, because while it is lower than the Rift escarpments it is at the culmination of the Rift floor. Flow towards Lake Naivasha from the Mau Escarpment and the Kinangop Plateau is unambiguous and some of the groundwater from the western side of the Rift must eventually form part of the discharges at Olkaria and Eburru. However the longitudinal flows in this area are more difficult to assess.

The piezometric surface has an uninterrupted fall from Lake Naivasha, around the east side of Eburru, towards Lake Elmenteita, indicating flow in this direction. It is probable that while shallow groundwaters on the south side of Eburru move locally towards Naivasha, deeper flows are substantially northwards.

Around Lake Naivasha itself the groundwater level is between approximately 1880 and 1900 m, similar to that of the lake itself. East and west of the lake the groundwater contours rise, indicating flow towards the lake, while to the south they remain at about the same level as far as the latitude of Longonot and Olkaria complexes. South of this region the piezometric surface must drop by several hundreds of metres because the few boreholes drilled between Longonot and Suswa have all proved to be dry, or have produced steam.

Groundwater certainly flows away from Lake Naivasha because the lake water is fresh, even though the lake has no outlet and lies in an area of high evaporation. Northerly flow may occur both via Gilgil and under Eburru. Southerly flow must also occur, following the hydraulic gradient, but the high values of the gradient suggest that values of permeability in the Olkaria-Longonot region are low.

McCann, 1974 in the Hydrogeological study of the groundwater level changes in the Naivasha catchment noted that seasonal water level changes ranged from 0.5 to 0.25 m in response to groundwater recharge. Changes were greater in the highland areas and less in lowland areas surrounding Lake Naivasha. Net annual water level changes were less than 0.2 m that was probably related to below normal rainfall rather than the effects of groundwater extractions from water wells. He went on to describe the relationships between precipitation, streamflow and changes in groundwater levels and noted that there was a lag in groundwater level response to precipitation that ranged from one week to several months. He also noted that the well hydrographs also showed the effects of evapotranspiration and soil moisture deficiency by their limited response to precipitation following dry periods.

Aquifer properties: Clark ET al., (1995) found that in the majority of wells only a yield and pumped water level at equilibrium have been noted only in few cases have recovery data been recorded. The highest vales of permeability are found in reworked volcanics composing the sediments of Naivasha area, where the specific capacities of wells often exceed 3 l/s/m and where estimated hydraulic conductivities of greater than 10 m/d are common. On the rift escarpments, the permeabilities of different rock types are uniformly low. Mean borehole specific capacities and estimated hydraulic conductivities range from 0.21 l/s/m and 0.1 m/d for the Kinangop Tuff to 0.2221 l/s/m, and 1.1 m/d for the Limuru Trachyte to the east of Suswa and the Mau Tuff. These figures are only applicable to the drilled depths of boreholes, normally less than 250 m. Below this depth the permeabilities will fall, mainly as a result of the closure of fissures by the overburden stresses.

Groundwater flow: The structure of the Rift Valley and in particular major marginal Rift faults and the system of grid faulting and the Rift floor undoubtedly have substantial effect on the groundwater flow systems of the area.

In general faults are considered to have two effects on fluid flow. They may facilitate flow by providing channels of high permeability, or they may prove to be barriers to flow by offsetting zones of relatively high permeability.

In the Rift Valley the main direction of faulting is along the axis of the Rift, and this has a significant effect on the flows across the Rift. It is apparent from the high hydraulic gradients that are developed across the Rift escarpments that the effect of the major faults is to act as zones of low permeability.

The effect of faulting is to cause groundwater flows from the sides of the Rift towards the centre to flow longer paths reaching greater depths, and to align flows within the Rift along its axis. McCann, 1974 noted that the intense faulting between Lake Naivasha and the Kinangop Plateau also appeared to control the movement of groundwater in the southeast part of the Naivasha catchment. Darling ET al., (1990) used stable isotope techniques to show that lake water appeared to be detectable at least 30 km to the south at the Suswa volcano (see Fig. 1.1). They showed that the reservoir fluid could be explained by a 2:1 mixture of lake water with unmodified meteoric recharge from the rift wall area. Isotopic evidence from the Eburru well EW-1 (Figures 3.1 and 3.10) shows that lake water also passes beneath the Eburru volcanic ridge (Darling ET al., 1996).

4.2 Conceptual Model

The focus of this analysis was the zone of impacted shallow and near-surface groundwater close to the Lake Naivasha in the shallow lake sediments and reworked volcanic materials. The lake sediments have a thickness ranging from approximately 15m in areas of low thickness (thins out towards the scarps) to over 50m beneath the lake. They consist of thin and low permeability clay, silt interbedded with thicker layers of sand and coarser material. The depth to groundwater in the sediments is typically 20-30m below land surface and the aquifers are usually unconfined. The shallow reworked volcanics have an average saturated thickness of 10-15m and are usually intensely fractured or weathered at the contacts with other lithologies (water levels over 50m below ground surface). These aquifers are often confined or semi-confined and the storage coefficients are likely to be low.

The hydraulic conductivity of the upper sediment hydrostatic unit is low. Based on an analysis of inverse auger data results conductivity values are in the order of 0.1-0.4 m/d (Behar, MSc 1999, Kibona, MSc 2000).

Recharge rates to the upper sediments is generally low (30-60 mm/year) with localized areas of preferred recharge near water sources, local surface depressions and fracture zones. Higher recharge also occurs in localized areas of higher permeability sediments.

Given the nearly flat topography and the extensive fracturing of the reworked volcanic outcrops, it is highly possible that localized recharge rates are expected to be high in these areas. Highest recharge estimates are envisaged for the highland areas of the Mau Escarpment and the southern geothermal volcanic complexes of Olkaria and Longonot. Groundwater percolation to the deeper lying regional flow systems occurs through a thick layer of acid volcanic rocks, lavas and trachytes.

A total lake outflow of 4.6 million cubic metres per month has been considered (Mmbui, MSc 1999). Total outflow from the catchment estimated to average 89 million cubic metres per annum (McCann, 1974, Clark ET. al., 1995, Ojiambo, 1992) has the bulk (about two-thirds) to the south through the Olkaria-Longonot volcanic area and the rest flows northwards and north-eastwards including underneath the Eburru hills. Inflow from the Kinangop plateau is impeded by the South Kinangop fault (about 30 mm/year), most of it deeply percolates to the geothermal flow system. A schematic diagram of the conceptual representation of the model set-up is shown in Figure 4.2.

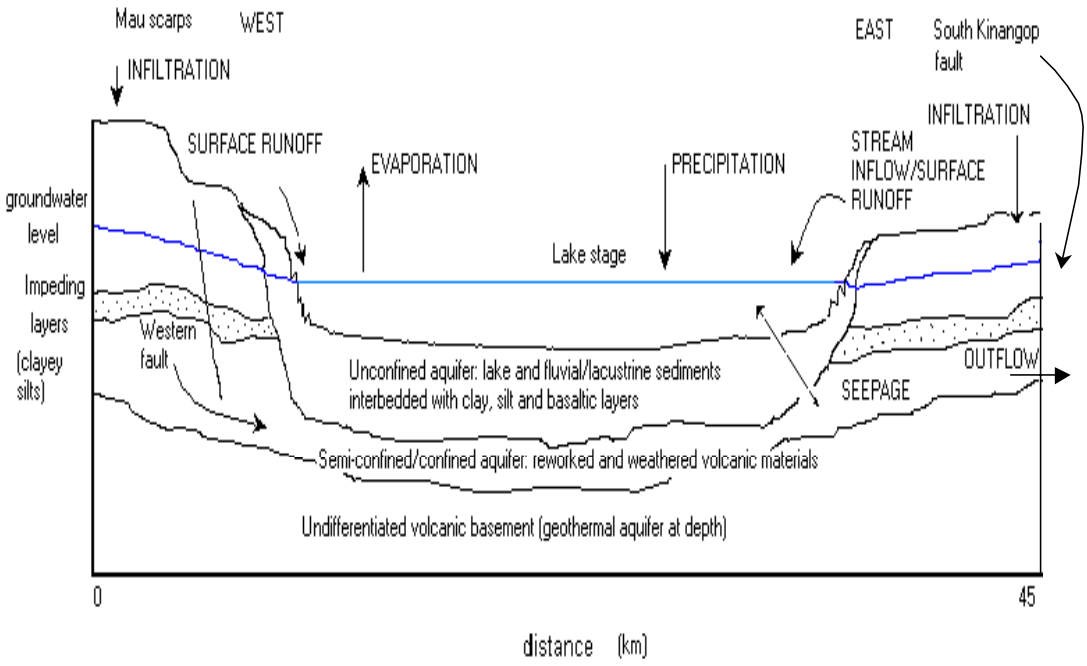

Figure 4.2: A 2D schematic cross section of the conceptual model drawn from the Mau Scarps(western) to the South Kinangop Fault (eastern) through the Lake Naivasha basin. Not drawn to scale.

Chapter 5

MODELLING

5.1 Modeling Protocol

Modeling gains its importance from the fact that models help in predicting the behaviour of groundwater systems in response to future stresses as well as understanding the cause and progress of past stresses (Akber ET al., 1998).
The protocol for the modelling included code selection, model design, calibration, sensitivity analysis, and finally prediction. The steps followed are summarised in Figure 5.1.

5.2 The MODFLOW LAKE PACKAGE

5.2.1 Conception

Three-dimensional incomprehensible groundwater flow through porous material is governed by the partial-differential equation (McDonald and Harbaugh, 1988)

$$\frac{\partial}{\partial x}\left(K_{xx}\frac{\partial h}{\partial x}\right)+\frac{\partial}{\partial x}\left(K_{yy}\frac{\partial h}{\partial y}\right)+\frac{\partial}{\partial z}\left(K_{zz}\frac{\partial h}{\partial z}\right)-W=S_s\frac{\partial h}{\partial t} \qquad \text{Eq. 5.1}$$

where K_{xx}, K_{yy} and K_{zz} are values of hydraulic conductivity along the x, y, and z coordinates axes, which are assumed parallel to the principal directions of hydraulic conductivity; h is the hydraulic head; W is discharge per unit volume, which represents sources and/or sinks of water; S_s is the specific storage of the porous material; and t is time. The equation 5.1 together with the boundary and initial conditions constitutes a mathematical representation of groundwater flow system.
In equation 5.1 the dependent variable, h [L], is a function of space and time. The independent variables are the spatially variable hydraulic conductivity (K_{xx}, K_{yy} and K_{zz}) [L/T] and S_s [L^{-1}] fields. Together with intitial conditions for head and various boundary conditions, MODFOW uses discretized, algebriac form of equation 5.1 to solve for potentiometric head at every model cell at time steps within each simulated period. In MODFLOW space is described in Cartesian co-ordinates.

A surface water body such as a lake (Figure 5.2) contributes water to the groundwater system or drains water from it depending on the head gradient between them. Such water exchange affects lake and groundwater levels. Lake water fluctuations result in changes in the hydraulic gradient between the lake and the groundwater even if the groundwater heads remain the same. The changes in hydraulic gradient, in turn, lead to changes in water exchange between the lake and the groundwater system. Therefore, unless a groundwater flow model incorporates lake level fluctuations, it will not predict groundwater heads near a lake accurately.It is for this purpose that the lake package (1) incorporates the dynamic water exchange between the lake and

groundwater system, and (2) calculates groundwater fluxes and lake level fluctuations over time.

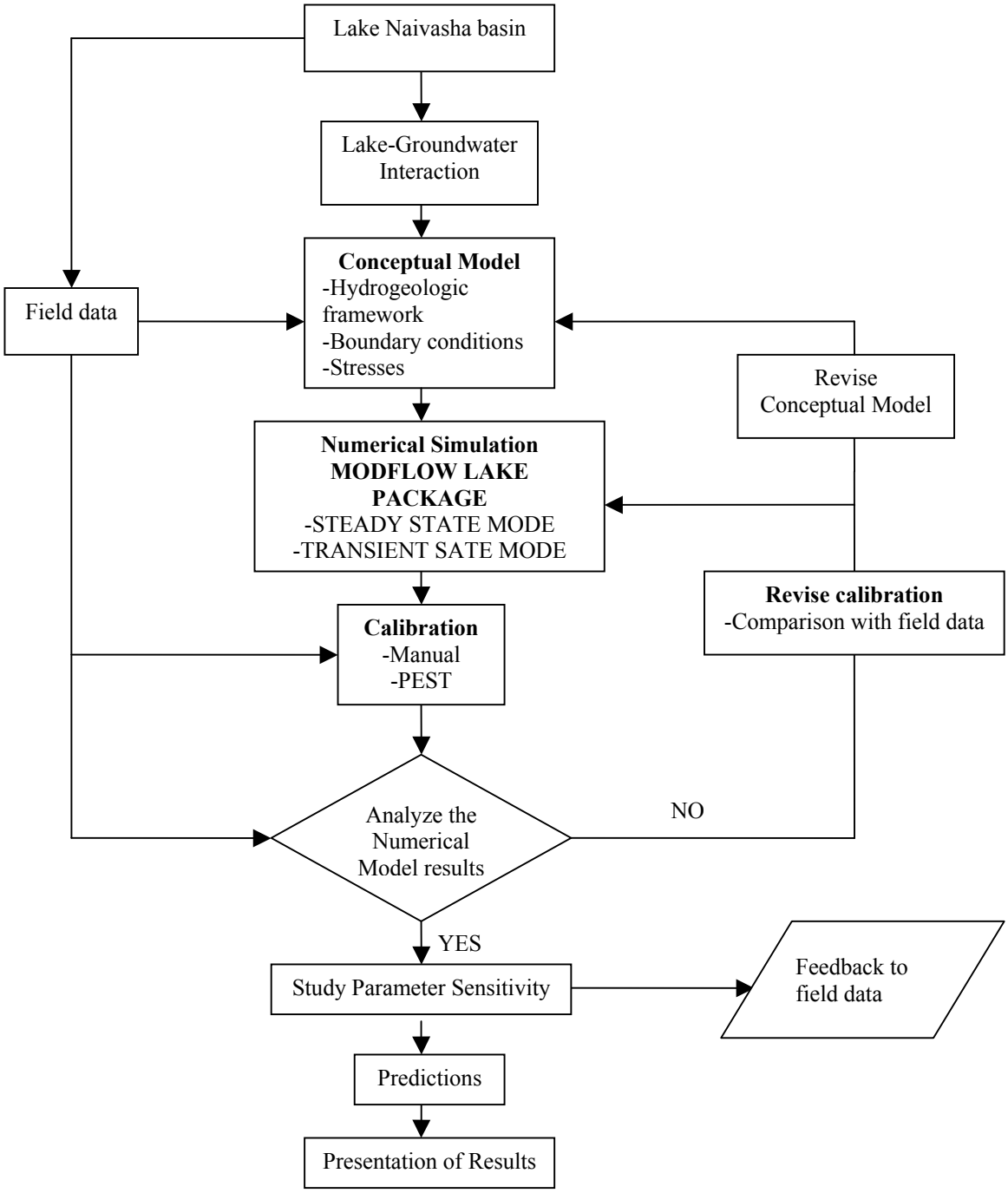

Figure 5.1: Synthesis of the modelling process.

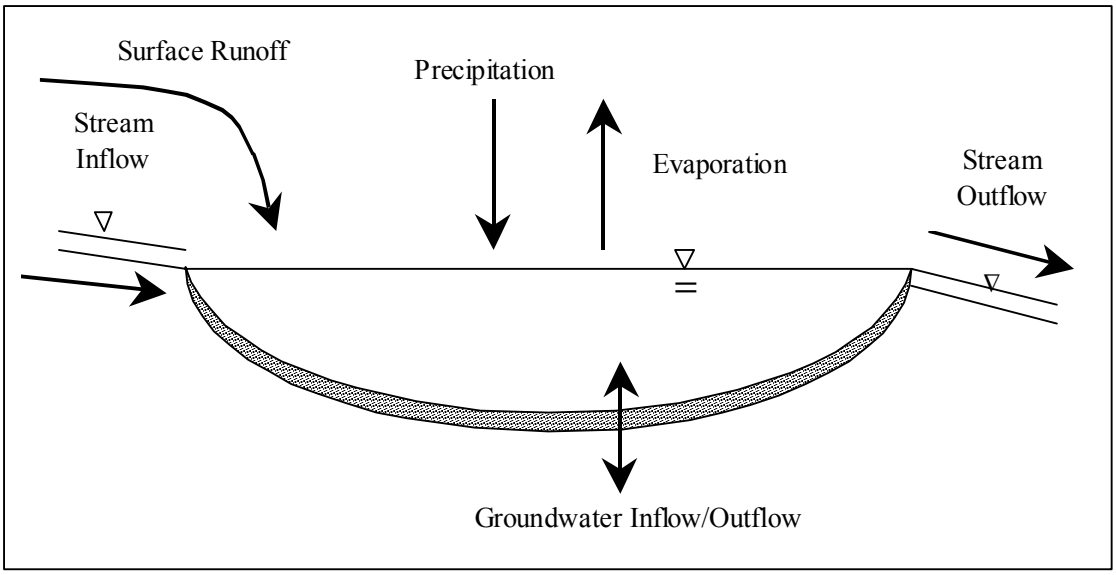

Figure 5.2: Cross-sectional view of a lake showing its volumetric budget components.

5.2.2 Algorithm

In general a lake is abstracted as a lake-region, which mostly consists of more than one cell of the flow model. On these cells the lake package is linked to the groundwater flow. Following McDonald and Harbaugh (1988) and Prudic (1989), it is assumed that there is no significant head loss between the bottom of the lakebed layer and the point represented by the underlying model node.
The flow over a cell interface is calculated as (Figure 5.3a):

$$q_i = COND_i\left(S - h_{ijk}\right) \qquad \text{Eq. 5.2}$$

q_i	-	flow (seepage) between lake and aquifer
$COND_i$	-	vertical or horizontal hydraulic conductance of the lakebed
S	-	lake stage
h_{ijk}	-	groundwater head in cell i, j, k (row, column, and layer)

This formula possesses its validity on condition that groundwater level and lake stage are above the bottom of the lakebed.
In other cases there are three special types:

a) filled lake, groundwater table below the bottom of the lakebed (maximum seepage), Figure 5.3b:

$$q_i = COND_i\left(S - BOT_i\right) \qquad \text{Eq. 5.3}$$

BOT_i	-	average level lakebed bottom cell of the flow model

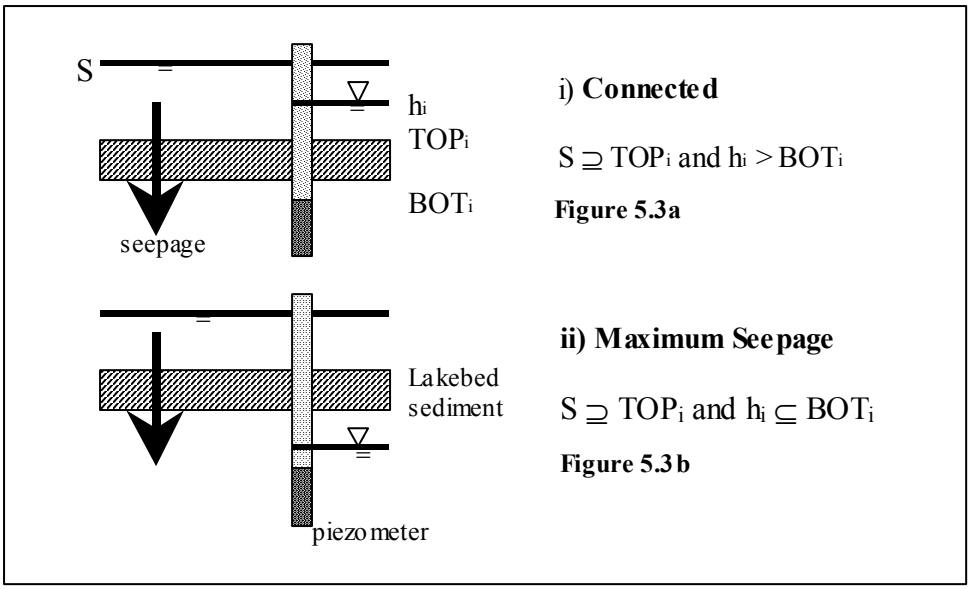

Figure 5.3: Computation of Lake-to-Groundwater Flux (Council, 1998).

b) empty lake, groundwater table below lakebed bottom:

$$q_i = 0 \qquad \text{Eq. 5.4}$$

c) empty lake, groundwater table above lakebed bottom:

$$q_i = COND_i\left(BOT_i - h_{ijk}\right) \qquad \text{Eq. 5.5}$$

Cases a) and b) get a constant flow from the lake to aquifer on condition that the groundwater heads are below the lakebed bottom in the cell.

The conductance is calculated as:

$$COND_i = \frac{KA}{TOP_i - BOT_i} \qquad \text{Eq. 5.6}$$

A	-	surface area of the lake cell (projected on a horizontal plane)
TOP_i	-	average level lakebed bottom cell of the flow model
K	-	hydraulic conductivity of the lakebed

For the transient simulation, the lake package calculates lake level by using a water balance equation 5.7:

$$S_{i+1} = \frac{S_i + \Delta t\left\{Q_{in} - Q_{out} + \sum_{L=1}^{n}\left[(P_i - E_i)A_i - q_i\right]\right\}}{A_T} \qquad \text{Eq. 5.7}$$

Q_{in} , Q_{out}	-	total stream inflow and outflow, respectively,
Δt	-	time step,
P_i, E_I	-	precipitation and evaporation rates. The evaporation rate is set to zero for a cell if the lake level drops below the elevation of the top of the lakebed (i.e. that part of the lake becomes dry),
A_i	-	area of the lakebed in contact with a lake,
A_T	-	total area calculated by the lake package, which can change when lake levels fluctuate,
S_{i+1}	-	lake stage at the new time step; The product of A_T and the difference between S_{i+1} and S_i reflects the change in lake storage during one time step.
n	-	is the total number of aquifer cells in contact with the lake.

Equations 5.2 and 5.3 are substituted into equation 5.7 for q_i and the lake package solves for the unknown lake level, S_{i+1}.

5.3 The Concept

The conceptual model approach that has been used to construct the model in MODFLOW involved the use of the ILWIS tools. The location of sources/sinks, layer parameters such as transmissivity, model boundaries, and all other data necessary for the simulation were defined at the conceptual model level. Once the model was complete, the grid was automatically generated so that it fit the conceptual model. The grid was created such that there was a uniform grid size even around the well points, and the cells lying outside the model boundary were inactivated (Richards, et al, 1996). The sources/sinks and boundary conditions in the conceptual model were then automatically assigned to the appropriate cells on the grid. The conceptual model approach consisted of the following steps:

1. Using the background map image within the ILWIS, the model boundaries and features were defined with points, segments and polygons.
2. Attributes were assigned to the ILWIS objects.
3. The created data were imported into the MODFLOW model.
4. The grid was automatically created and the attributes to the appropriate grid cells were mapped.

The conceptual model approach had several advantages. The model definition process was fast, easy and intuitive. This became especially apparent the more complex the model became. Furthermore, once the simulation was performed, changes to the conceptual model could be made and the numerical model regenerated in a short while. Because the grid generation and attribute mapping was automatic and almost instantaneous, even major modifications to the model could be made more rapidly.

5.4 Model Design

MODFLOW, a three-dimensional finite difference groundwater flow code (McDonald and Habaugh, 1988), with BCF2, a block-centred flow package (McDonald et al., 1991) and LAK2, a Lake Package developed by Council et al., 1998 were used.
The wetting capability of the Block-Centered Flow 2 package (BCF2; McDonald et al. 1991) allows the simulation of a rising water table into unsaturated (dry) model layers.
A cell falls dry when the head is below the bottom elevation of the cell. When a cell falls dry, there is no flow or the cells become inactive, all conductances to the dry cell are set to zero. No water can flow into the cell as the simulation proceeds and the cell remains inactive. To overcome this problem, a computer code uses this value to decide, whether a dry or an inactive cell can be turned into a wet (active) cell.

The following two solvers were used: the PCG2 (Preconditioned Conjugate-Gradient Package) and the SIP (Strongly Implicit Procedure Package). The PCG2 solver was preferred because it is very insensitive to the "Head change criterion for convergence"; i.e. this criterion can vary from 0.01 to 0.00001 and still converge to identical solutions (Osiensky et al., 1997).

5.4.1 Geometry

The modeled area covers an area of 1603 km^2. The model grid contains 100 rows, 120 columns and two layers, Figure 5.4. Although there may be variation from one cell or node to another, it is assumed that within a nodal area the hydraulic characteristics off the system are constant and time-independent. The lake is located at the centre of the first layer with the two inflow Rivers Malewa and Gilgil, as shown in Figure 5.4. The horizontal spacing is uniformly equal to 500 metres. Layer 1 is unconfined (simulated as confined) and layer 2 is confined. Layer 1 has an average thickness of 50 metres and layer 2 has an average thickness of 10 metres. For this discretization, 880 cells are in contact with the lake (Lake Naivasha and the Oloidien Lake are joined together), 49 cells are with the River Gilgil and 60 cells with the River Malewa. 45 monitoring wells have been used in the calibration process, Figure 3.10.

5.4.2 Time steps

Data was available from 1932 to 1998 spanning over 66 years that included monthly lake levels and stream flow data over the whole duration. The groundwater levels in the wells were available over shorter and inconsistent periods. Monthly stress periods have been used with four time steps each and the time steps were uniform for each stress period. A trade-off had to be made with the time-step size to achieve convergence and mass balance, the length of the model run time, and bulky input and output files that were generated.

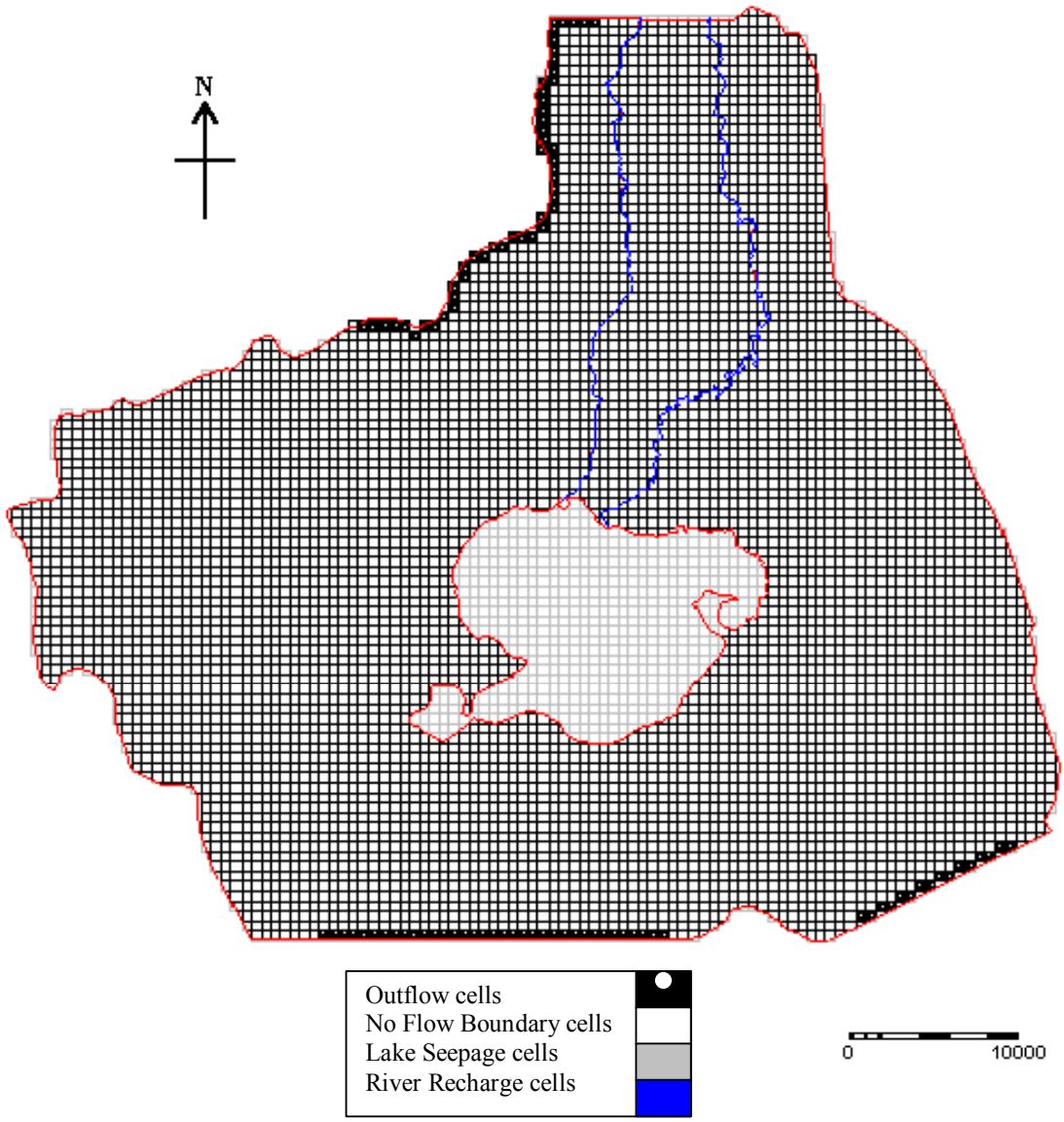

Figure 5.4: Finite difference grid layout of the modelled area (500-m square) showing the boundary conditions.

5.4.3 MODFLOW Lake Package Modifications

In order to run the Lake Package within the normal functionality of MODFLOW a number of modifications were made.

1. A Lake Package input file that incorporated time-series data was prepared (see Appendix 2) and included in the MODFLOW name file which was run using a special version of MODFLOW that had the Lake Package.
2. In the Lake Package the active MODFLOW cells that were connected to each modelled lake cell were specified.
3. The RUNOFF variable was used to add the known stream inflows to the lake's budget (instead of using the stream inflow calculated by the Stream Routing Package). This modification reduced the huge space requirements necessary to generate the Stream Routing Package MODFLOW input files. The River Package was then used to cater for river recharge.

4. A conceptualisation where precipitation was applied to the wetted lake area (like evaporation) was accomplished by setting precipitation to zero and specifying the net precipitation (precipitation minus evaporation) for evaporation. Under this conceptualisation, precipitation falling on shore cells is not accounted for in the lake volumetric budget (it may be considered to immediately evaporate), and the net precipitation is applied over the current wetted lake area.
5. The Lake Package cannot automatically handle coalescing of two nearby lakes when the stage rises to a certain level so the two lakes (Lake Naivasha and Oloidien Lake) were merged together to form a single large lake.

5.4.4 Boundary and Initial Conditions

The boundary conditions

The boundary conditions were defined as follows:
Western part: The watershed boundary that peaks at the Mau scarp was taken to be a no flow boundary. Most of the flow from this area has been inferred to be impeded by the fault associated with the Eburru volcanic complex to the west of the basin (trending north-south), and it disperses north-eastwards through the Eburru Hills and south-eastwards through the Olkaria region (McCann, 1974, Clarke et al., 1990). What little finds its way into the lake is by deep percolation. There is no clear cut, exhaustive work in this area that definitely confirms this view. Considering that there is outflow from the lake through the Eburru complex area, it has been assumed reasonable enough to consider that, part of the flow from the Mau scarp gets to the lake.
Northern part: The north-eastern boundary is spanned by the Eburru hills beneath which is acknowledged to be outflow to the Elmenteita Lake basin (Darling et al., 1996). Due north of the basin, there is some outflow on its western fringe to the east of the Eburru Hills (Clarke et al., 1990).
Eastern part: The South Kinangop fault trending due NNW is considered to impede most of the inflow from the Kinangop plateau. Most of the flux is considered to take place in the deeper horizons. Minimal flow through this area has been considered negligible.
Southern part: Flow through the Olkaria and Longonot volcanic complexes has been considered to be the conduit for most of the lake outflow from the basin most of which percolates into the deeper geothermal systems. To the southeast of the Longonot volcano, some considerable outflow from the basin has been considered to account for the fluxes from the Kinangop plateau that get into the basin in a southwestward direction and digress southeastwards.
The basement: The bottom of the system has been considered to be composed of undifferentiated volcanic materials that have a very low ($K_{zz} << K_{xx} \approx K_{yy}$) deep percolation of groundwater. This could also be attributed to the high pressures exerted by the deeper lying, highly volatile, multiphase geothermal systems that impede flow of water to the deeper horizons. It has been considered reasonable enough to be a no flow boundary over a long-term period.
The Surface: The lake surface at the centre of the domain is a time variant boundary whose transience has been accounted for within the Lake Package. The rivers are considered to be recharge boundaries (Behar, MSc 1999). Recharge zones have been accounted for in the different areas of the catchment.

The initial conditions

The initial conditions have been considered to be the hydrologic stresses (lake levels, river flows) at the 1932 period. The initial groundwater levels have been derived as a long-term average value from 1932 to 1979 interpolated within the model to obtain the initial piezometric surface (see Figure 3.10). This was so done because (1) levels within this duration correspond to the natural stresses that were acting in the system then, (2) lack of enough data to adequately describe the piezometric surface at the start of the simulation period.

5.4.5 Hydrologic Stresses and Aquifer Parameters

The lake-level data series over the 66 years used in this study were reconstructed by Mmbui, MSc 1999. The same author also prepared the flow data for the two main rivers over the same period. The river flow data also included estimates of the contribution of the much smaller Karati River and surface runoff. Direct rainfall and evaporation from the lake surface over the same period also included estimates for swamp evapotranspiration on the lakeshores.
The groundwater hydraulic parameters were obtained from the results of work previously carried out by various authors in the area. The distribution of the transmissivity characteristics of the aquifer systems by previous authors is shown in Figure 3.9. These values were used to map the initial estimates for the zones that were basically derived from the geologic map of the area. In the estimate for recharge an initial value of 30 mm/year equivalent to about 5% of average precipitation within the rift area was taken. The western scarp area of Mau stretching north to the Eburru area was considered to have a higher recharge of about 100 mm/year, with about 75 mm/year in the region around the southern volcanic complexes. Previous work by Wilberg, 1976 estimates recharge at 50 mm/year (not defined what methods he used). McCann (1974) noted that the Pleistocene pyroclastics that flank the Mau and Aberdare escarpments appear relatively absorptive and doubtless transmit infiltrating precipitation and runoff to the underlying fracture and fissure systems of less absorptive and permeable rocks. Such recharge also takes place where Quaternary pyroclastics occur such as in the Eburru area.

5.4.6 Parameter Zonation

Once the parameters to be varied were selected, defining zones for each parameter became the next critical step. These zones were made based on the hydrogeology and on the observed variations in field data. The number of zones defined for each parameter was also an important consideration for running PEST. Again, the more zones there were, the longer it took to perform one optimization iteration. However, enough zones needed to be defined so that spatial variation of the parameter was allowed in the model. For this set-up, zones were assigned for recharge, transmissivity, and storage coefficient (see Figures 6.17, 6.18, and 6.23, respectively). These zones were delineated based on previously described and known site hydrogeologic conditions, data from pump tests, and estimations of specific material characteristics (see Appendix 2). The vertical conductivity was assumed to be uniform over each of the two layers of the area.

5.5 Steady State Run

The long-term average stresses on the lake (precipitation, evaporation and stream flow) were imposed on the system for this run. To reduce instability, the initial conditions for the aquifer head were obtained by running the model using an interpolation of the observed aquifer heads (before the 1980 period) with the lake stage fixed (at a long-term average value of 1887.68 mamsl). The results of this run were then used for the steady state run. The water balance error was the criterion used to gauge the convergence of the runs (percentage error being less than 1%). The simulations of the steady state runs were matched to the observed average well levels prior to the 1980 period.

5.6 Transient State Run

The simulated steady state aquifer heads were used as initial aquifer heads for this run. The average observed well data after the 1980 period and the observed monthly lake levels over the 66 years were used to match the simulated aquifer heads and lake stages, respectively. The stress period step-size was increased to a monthly basis to match the available lake data with the aquifer heads generated for only the desired period (last 10 years). The PCG2 solver criteria had to be relaxed to achieve convergence due to the non-linearity of the simulation problem.

5.7 Model Calibration

5.7.1 Overview

Estimates of hydraulic parameter values obtained from field investigations are often poor or non-existent. The calibration and modeling process is a tool to fill in these gaps.
The model was originally calibrated by the traditional “best-estimate” in which values of transmissivity, or hydraulic conductivity, and recharge were manually modified until the differences between the observed and calculated aquifer head values were reduced to an acceptable level. It was not possible to obtain the desired level of agreement between the modeled and simulated aquifer heads and lake levels.

It was therefore imperative to further automatically calibrate PEST to achieve the desired error variance. PEST is a powerful numerical tool that can greatly improve the calibration of a complex, transient model. There are a number of considerations, however, which must be evaluated while setting up and running PEST.
Non-uniqueness of the calibration solution is an important one. There is a correlation between the effects of some model parameters in terms of their effect on the calculated head. Therefore, more than one parameter combination can result in essentially the same model result. Recognition of this possibility is important for determining the reasonable range of variation and the number and location of zones for each parameter. Setting upper and lower bounds is important to prevent parameter values from becoming unreasonable.

Although PEST is a powerful tool, automatic calibration were monitored for some of the following occurrences:

- The model forcing parameter values beyond the set, allowable range.
- The stabilisation of the parameter values.
- The oscillation or divergence due to numerical difficulties of the weighted sum of square error, which is PEST's indicator of when automatic calibration should stop.

PEST was extremely useful for the calibration of a model of this complexity, resulting in significant savings in effort and time.

5.7.2 Implementation

PEST requires three types of input file that had to be modified to accommodate the lake data. These are:

- template files, one for each model input file on which parameters are identified,
- instruction files, one for each model output file on which model-generated observations are identified, and
- an input control file, supplying PEST with the names of all template and instruction files, the names of the corresponding model input and output files, the problem size, control variables, initial parameter values, measurement values and weights, etc (Appendix 1).

In the steady state runs PEST was applied in an iterative fashion on the transmissivity, and recharge of the system. During the transient state runs, PEST was applied on the storage coefficients and lakebed conductance of the system. The outflow terms from the area were later separately optimised (due to computer memory problems) to fit the above calibration parameters.

A PEST run continued for as long as the weighted sum of squared errors continued to decrease. By inspection of the PEST record, it was possible to identify and fix (hold constant) parameters that had reached their reasonable lower or upper limits or were not changing between PEST runs. By holding these parameters constant and adjusting some of the allowable ranges for the other parameters, the optimisation process was reinitiated. Figure 5.5 shows the flow chart outlining the steps that were taken in order to arrive at the calibration solution.

The optimisation process was terminated after the lowest 3 objective function values were within a relative distance of 0.01 of each other. The objective function is a derivative for which the model-generated observations are as close as possible to the experimental observations in the least squares sense. After completing the parameter estimation process, PEST lists the optimised parameter values and calculates 95% confidence limits for the adjustable parameters.

5.7.3 Parallel PEST

An attempt was made to use Parallel PEST for the automatic calibration. In most cases by far the bulk of PEST's run time is consumed in running the model. It follows that any timesavings that are made in carrying out these model runs will result in dramatic enhancements to overall PEST performance.
Parallel PEST achieves such performance enhancement by carrying out model runs in parallel when these runs are undertaken to fill the Jacobian matrix. When derivatives are being calculated using finite parameter differences, successive model runs are

independent, i.e. the parameters used for one particular model run do not depend on the results of a previous model run. If installed on a machine that is part of a local area network, Parallel PEST is able to carry out model runs on the different machines that make up the network (including the machine that PEST itself is running on). If model run times are large and the number of parameters is greater than four or five, overall PEST run times can be reduced by a factor almost equal to the number of machines over which Parallel PEST is able to distribute model runs. As well as allowing distributing model runs across a network, Parallel PEST can also manage simultaneous model runs on a single machine. This can realize significant increases in PEST efficiency when carrying out parameter optimization on a multi-processor computer by keeping all processors simultaneously busy carrying out model runs.

Test model runs were carried out on different processors. But it was not possible to read the output files from the different runs across the network. So the efficiency that would have been gained from running a model of this complexity using this facility was not realized.

5.8 Sensitivity Analysis

Many model parameters did not justify calibration because of the empirical nature of the site data. It was therefore necessary to evaluate the effect of uncertainty on these parameters using a sensitivity analysis. Parameters evaluated in the sensitivity analysis included transmissivity, recharge, vertical hydraulic conductivity, storage coefficient, outflow, and lakebed conductance. The model sensitivity to each of these parameters was evaluated both individually and in couples for the aquifer heads and lake levels. The effects of varying these parameters (singly and then in duos) through a wide range of potential values was evaluated by observing the resultant aquifer heads and lake stages using firstly the steady state and then the transient state calibrated models.

5.8.1 Implementation

Two types of outcomes were evaluated: relative differences between the initial observation values and subsequent changes; and the “sensitivities” with respect to parameter variations from their base values.

The relative differences between initial observation values and the new outcomes were also calculated. If, for a particular model outcome, O_b represents the base value, and O_p represents the value for a certain set of alternative parameter values, then the value written out for that model outcome and parameter set is (equation 5.8):

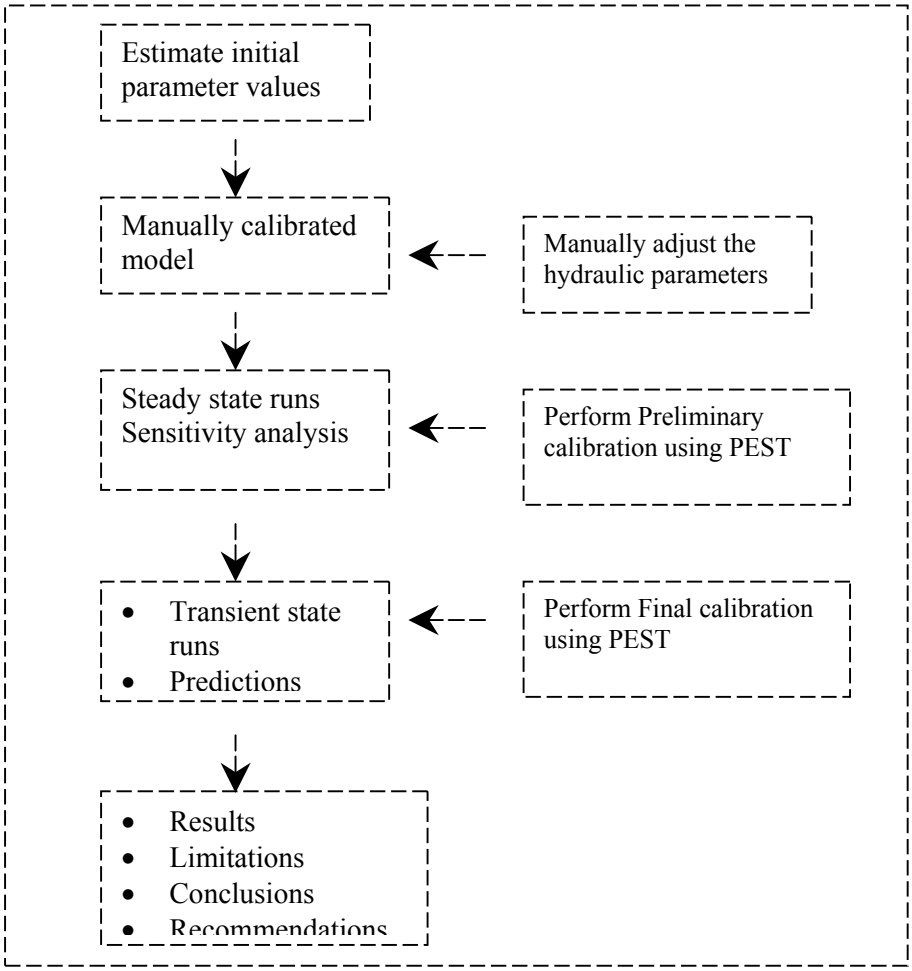

Figure 5.5: Flow chart of the outline of the steps used to calibrate the model.

$$\frac{O_p - O_b}{O_b} \qquad \text{Eq. 5.8}$$

Sensitivity for a particular outcome was calculated as the difference between the model outcome and the pertinent model outcome base value, divided by the difference between the current parameter set and the parameter base values. The latter was calculated as the L_2 norm, i.e. the square root of the sum of the squared differences between a current parameter set and the base parameter set. Thus if only a single parameter p differed from the base set, the sensitivity for a particular observation O was as defined equation 5.8.

$$\frac{O - O_b}{p - p_b} \qquad \text{Eq. 5.9}$$

where O_b and p_b are model outcome and parameter base values and O and p are the model outcome and parameter values pertaining to a particular model run.

5.9 Predictions

It was not possible to verify the model because only one set of field data was available which was needed for the calibration process. A calibrated but not verified model can be used to make predictions as long as careful sensitivity analyses of both calibrated model and predicted model are performed and evaluated. Predictions resulting from calibrated but unverified models generally will be more uncertain than predictions derived from the verified models Two major pitfalls are involved in making predictions: uncertainty in the calibrated model and uncertainty about future hydrologic stresses (Anderson ET al., 1992).

The purpose of this process was to introduce abstraction in the areas where there presently is intense use of water for various activities. The results of these new extra stresses were then compared with observed lake levels and aquifer heads after the 1980 period when these activities are known to have picked up.

5.9.1 Implementation

The simulation runs were made in the abstraction areas used by Ramirez, MSc 1999. The total discharge rates were stepped up from 18,000 m^3/day to 50,000 m^3/day, the bulk of which was concentrated in the north-eastern parts of the area.

A Sensitivity analysis was carried out on the effects of one of the predictive simulations to test the effect of uncertainty in the calibrated parameters.

5.10 The ARGUS-ONE

At the outset of the research study, the ARGUS-1 GUI was exhaustively tested to explore the possibilities of conjunctively using it with the PMWIN so as to exploit the strengths of either model.

The ARGUS-1 is a Graphical-User Interface for the U.S. Geological Survey Modular Three-Dimensional Finite-Difference Groundwater Flow Model (MODFLOW-96). It is a programmable GIS that has automated gridding and meshing capabilities to link geospatial information with finite-difference and finite-element discretization, as well as several means of importing geo-spatial information. The programmable nature of Argus-1 allows geo-spatial information and simulation parameters to be exported to ASCII files that can be by the numerical Plug-In Extensions (PIEs), which are executable codes loaded into the memory of Argus-1 such that they appear as part of Argus-1, even though they have been developed independently. The Lake package is included within the normal functionality of the ARGUS-1 domain.

5.10.1 Results

The Argus-1 input files were quite identical to those of PMWIN and both gave similar results in the test runs. There were slight differences due to the ways the two models defined their grids. The Argus-1 grids are more flexible and it therefore reduces the errors that PMWIN includes because of the rigid nature of its grid description.

5.10.2 Strengths

Argus-1 generates the grid after the parameters have been prescribed for user-defined regions. The PMWIN requires that the grid be laid out right at the outset and is not flexible enough to allow grid variations. This can only be achieved later on during the grid refinement stage. Even then, it includes areas where the refinement is not required.

The ARGUS-1 generated grid did not overshoot the model boundaries as is the case with the PMWIN discrete grid. The description and positioning of points or regions in ARGUS-1 could be identified within the grid cell. This is advantageous because positioning errors arising due to the discrete nature of the grid cells are well taken care of. The smallest area PMWIN can use to describe points or regions is the grid cell.

The inclusion of the Lake package within the normal functionality of Argus-1 was a lot more flexible to modify. The PMWIN does not accommodate the Lake Package that has to be separately attached.

The GIS capabilities of ARGUS-1 means that there is faster and more efficient generation, retrieval and manipulation of the spatial data. PMWIN requires that the GIS data be pre-processed prior to being used in it. This results into simulation delays and errors due to the transformation/importation of the input files.

5.10.3 Limitations

The Argus-1 input files had no provision to accommodate time-series data. It was not possible either to manipulate the input files so as to include the time series data as was the case with the PMWIN-generated MODFLOW input files.

It was not possible to import PMWIN generated input files into ARGUS-1. The ARGUS-1 spatial data had to be meticulously edited before being imported into PMWIN. Even then, the data ended up being distorted.

Thus the possibility of conjunctively using and comparing the results of either model was not adequately exploited or realised.

Chapter 6

SIMULATION RESULTS

6.1 Comparison with the Spreadsheet Model

6.1.1 Rating Equations

From the DTM, the lake spatially extends more towards the northern and north-eastern parts of the area for a lake stage of 1895 mamsl (within the limitations of the DTM), Figure 6.1.

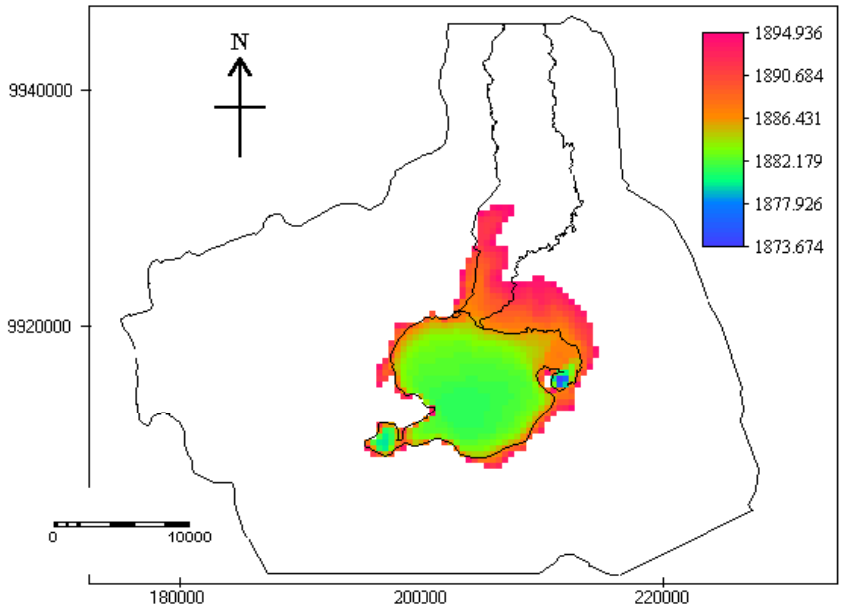

Figure 6.1: The spatial extent of the lake at a level of 1895 mamsl (within the limitations of the DTM)

Prior to running the model, a stage-area rating equation (curve) was generated using the DTM-derived Lake bathymetry. This was later compared with the rating curve generated by the MODFLOW Lake Package (hereinafter known as the Mflake) and that used by the Spreadsheet Model, Figure 6.2. The graphs show a close match indicating that there are no significant differences in the way the two models evaluate the stages from the given areas of extent. The rating curves compare well with that of WRAP, 1998 (see Figure 3.8a). The area of coverage of the lake from a summation of the lake cells of the DTM (from a possible minimal lake stage of 1882 mamsl to a maximal of 1895 mamsl) compared with those generated by the two models (Spreadsheet and Mflake) is shown in Appendix 2.

6.1.2 Lake Stage – Time Relationships

The initial simulation results show the significant influence of excluding groundwater seepage as was realised from the first model run, Figure 6.3. There is already a sizeable difference in the stages generated by the two models especially in the later

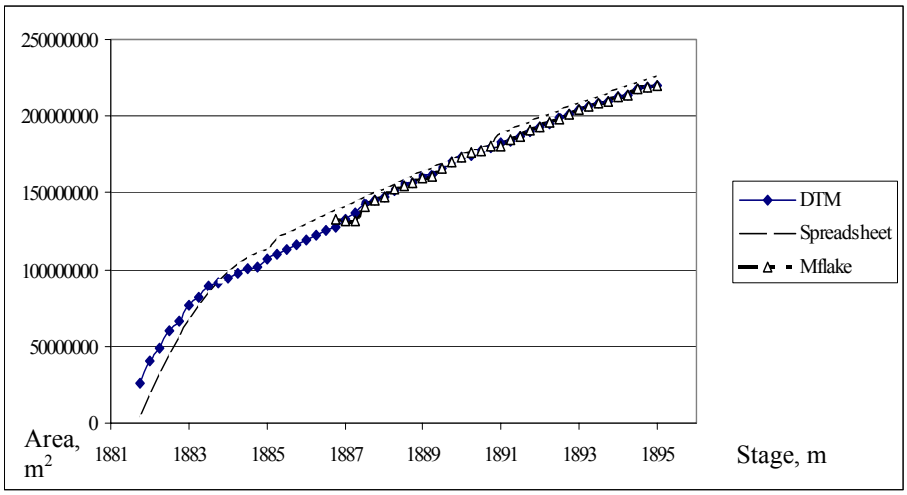

Figure 6.2: The Stage-Area Rating Curves generated by the DTM, Spreadsheet and Mflake models.

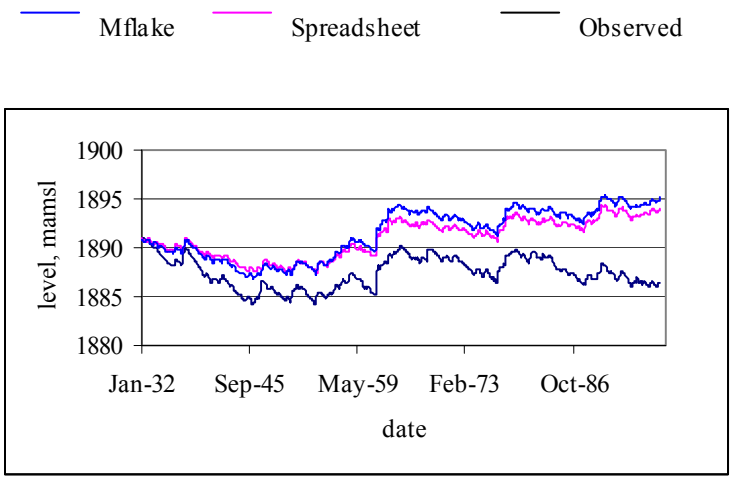

Figure 6.3: No Groundwater seepage included in the lake stages generated by the Spreadsheet and Mflake models. The deviation from the observed levels is evident (average of a 4-m difference).

periods. In the earlier periods closer fits are achieved that later on spread out as Mflake overshoots the Spreadsheet estimates by an average of 0.5m. This is attributed to the difference by which each method computes the new stage value from the preceding one. The Spreadsheet model sums up the net flow to the lake (from the precipitation, evaporation and stream flow and surface runoff terms) and obtains the change in storage from the previous month's storage. A new surface area is then derived and from which, using the rating curve, a new lake level is computed

(Mmbui, MSc 1999). The Mflake model on the other hand, accumulates using the newly estimated head values and the old stage value, a net flow into the lake at the end of the time step. The net flow is multiplied by the length of the current time step to get the change in lake volume, and the new "target" volume of the lake. The lake stage is then iteratively adjusted until the target volume is obtained. At each iteration, the next guess for the correct stage is calculated by subtracting the target volume from the current volume, dividing by the current wetted area, and adding that amount to the current stage (this is Newton's method with the wetted area as the derivative of volume with respect to stage), Council, 1999.
These adjustments made by Mflake result into lake stage round off errors that build up over time and significantly deviate away from the Spreadsheet lake level estimates.

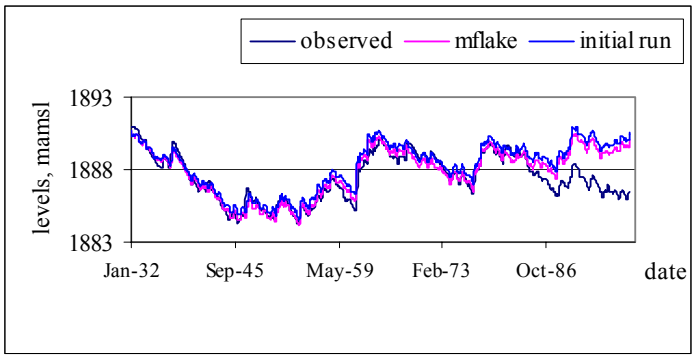

Figure 6.4: The initial run (optimised storage and conductance) for the Mflake model compared with the final run (optimised outflow).

When seepage between the lake and aquifer is introduced and optimised the resultant temporal lake level fluctuations shown in Figures 6.4 and 6.5 are obtained. Figure 6.4 shows a comparison of first and second of the final two runs: initial run(optimising storage coefficient and lakebed conductance), and Mflake (optimising outflow), respectively.

The closeness of fit between the observed and the simulated lake levels is apparent up to 1980. After that period the deviation between the two becomes apparent which time is linked to the start of intense abstraction of water from the lake and the riparian areas. In Figure 6.6, a comparison between the two models (Spreadsheet and Mflake) is made. The Mflake simulated lake levels on average fit those of the Spreadsheet with a less then half-metre discrepancy. This difference could additionally be attributed to the individual cell-by-cell flow terms of the groundwater-lake water balance that when summed over the whole lake interface exceeds that of the Spreadsheet. The steady state lake level (1888.4 mamsl, Table 6.1) is close enough to the simulated long-term average transient lake level (1888.2 mamsl).
The variation of the difference between the observed and simulated lake levels is on average less than 0.5m up to 1980. Thereafter, the difference widens to a maximum of nearly 4m in 1997, Figure 6.7. This digression is again related to extra water use from this point in time. A scatter plot of the same lake levels shows a fairly linear relationship, Figure 6.8 with a square of the Pearson product moment correlation coefficient (R^2) of 0.9494. More of the estimates are seen to be a little above the direct relationship line showing that the model on average tends to overestimate the observed lake levels.

The better simulation of the observed lake levels by the Spreadsheet model (Mmbui, MSc 1999) during certain periods as compared to the Mflake model is embedded in the basic assumptions underlying its inception. It does not account for the physical anomalies associated with the lake bathymetry that affects the evaluation of the lake stage fluctuations.

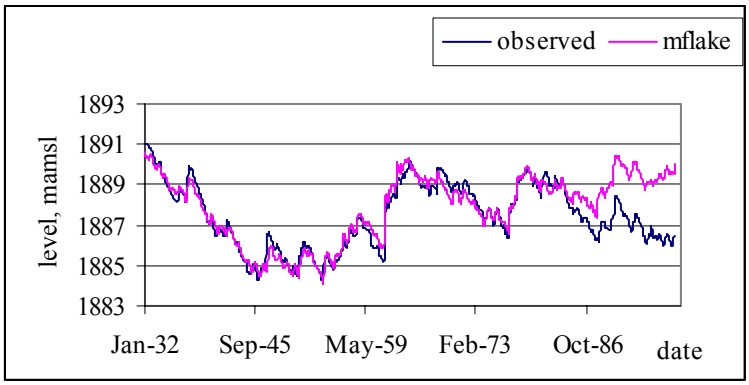

Figure 6.5: The final Mflake model run over the whole simulation period.

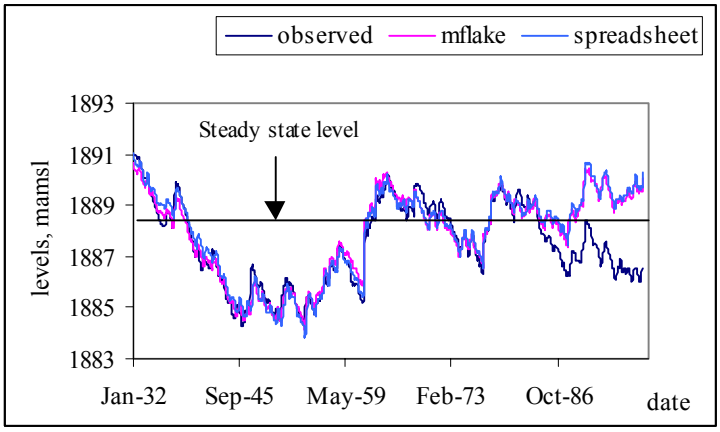

Figure 6.6: The final simulated lake levels by the two models (groundwater seepage incorporated) compared with the observed levels.

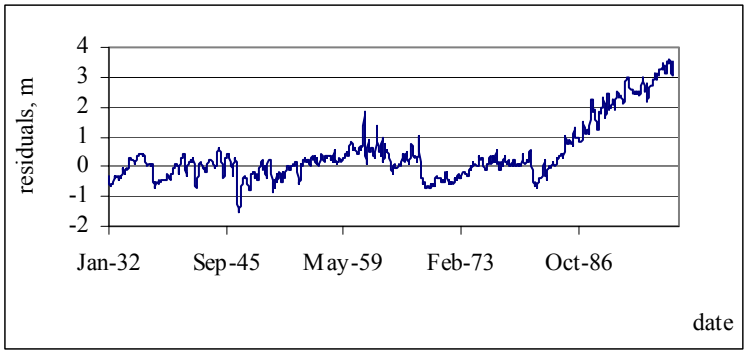

Figure 6.7: Temporal distribution of the differences between simulated and observed lake levels.

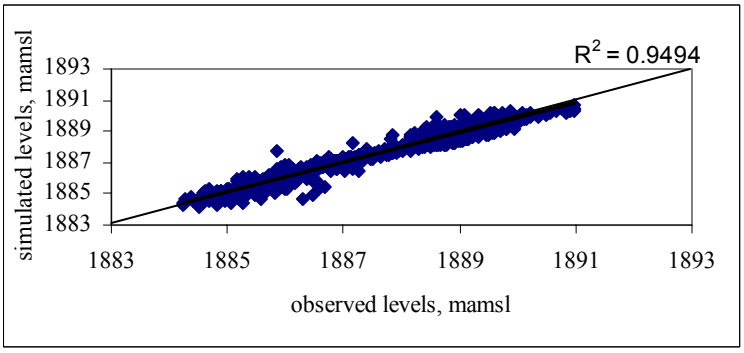

Figure 6.8: Scatter Plot of observed and simulated lake levels before 1980 (natural setting).

6.1.3 Lake Storage – Time Relationships

There is a temporal fluctuation of the total amount of water seeping to the aquifer from the lake, Figure 6.9. It is noted that the maximum quantities of seepage to the groundwater are during those periods of consistent lake stage rise (for example from October 1961 to March 1965). It amounts to over 25 mcm/mth during these peak events. The net flow depends on a cell-by-cell relative difference between the aquifer head and the lake stage summed over the whole lake-aquifer domain (equations 5.3 through 5.5). The steady state net lake seepage (4.3 million m^3/mth, Table 6.1) is quite comparable to that of the average transient flow (4.76 million m^3/mth).

Spreadsheet Modification: A temporal cumulative seepage plot of the two models (Mflake and Spreadsheet) shows good conformity, Figure 6.10. In order to compare the two models, a modification had to be made to the Spreadsheet model. The Spreadsheet model uses a single groundwater node to externally extract a known amount of seepage rate to the groundwater from the lake (4.6 mcm/mth) from the transient flow budget over the whole simulation period. This seepage rate component was shifted and incorporated into the flow budget for each simulation period. This was then optimised to ascertain if it would yield a better fit with the observed lake levels. The result did not improve the previously optimised values. The modification ensured that the Spreadsheet model had similar flow components with the Mflake model for deriving the storage volumetric budget for each simulation period.

The Spreadsheet and the Mflake models give long-term average lake seepage of 4.54 million and 4.76 million m^3/mth, respectively, Figures 6.9 and 6.10. The lake levels are sustained during those periods when the total inflow (stream flow, runoff and rainfall) exceeds the total outflow (lake seepage and evapotranspiration). These periods are linked to consistent inflows into the lake possibly during the high rains after the dry spells (see Figure 3.4, section 3.3.1). It is then that the lake levels are observed to rise over their preceding levels.

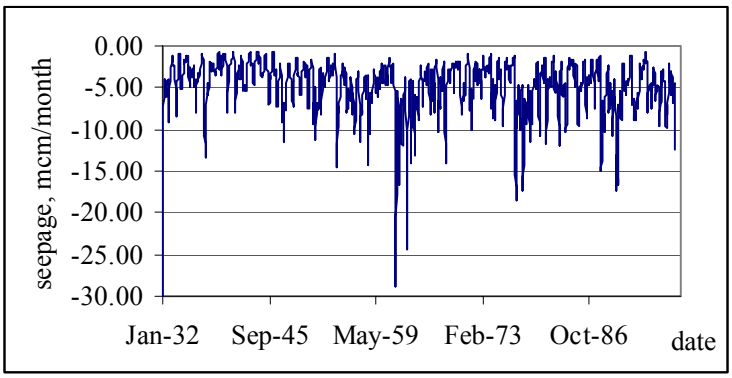

Figure 6.9: Temporal groundwater seepage over the simulation period.

The lake storage volume mimics the temporal lake level fluctuations, Figure 6.11. The closeness of fit between the two models is again apparent. The simulated volumes start diverging away from the observed volume after 1982. The closeness of fit between the simulations of the two models is again apparent. From the temporal differences between the observed and simulated lake storage volumes, a maximum deficit of nearly 500 million mcm/mth (17 mcm/day) is evident in 1997, Figure 6.12. This value gives an insight into the order of magnitude of water abstraction from the lake at that time. The steady state storage volume (7.1 mcm/mth, Table 6.2) is quite close to the average transient storage volume (6.9 mcm/mth obtained from the water balance record of the final transient run).

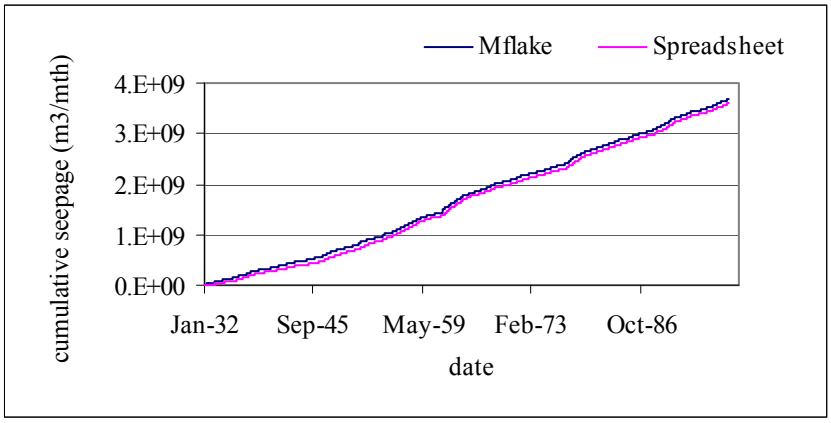

Figure 6.10: Temporal cumulative lake seepage to the groundwater as simulated by the models. The Spreadsheet and Mflake average 4.54 million and 4.76 million m^3/mth, respectively.

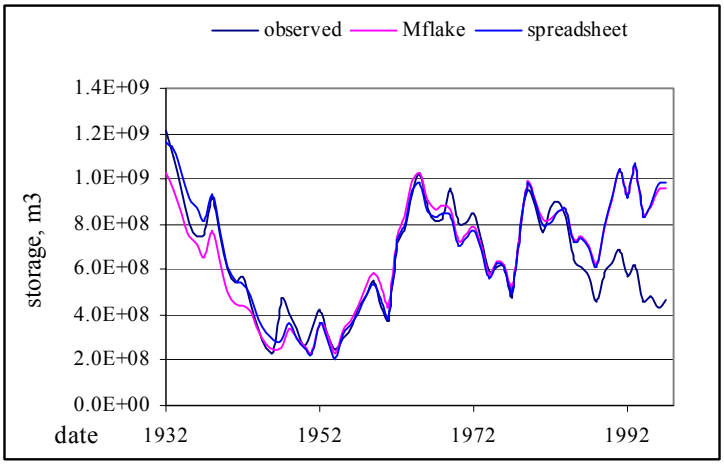

Figure 6.11: Temporal distribution of the lake storage volume over the 66 years. The deviation between the observed and simulated levels is apparent after 1980.

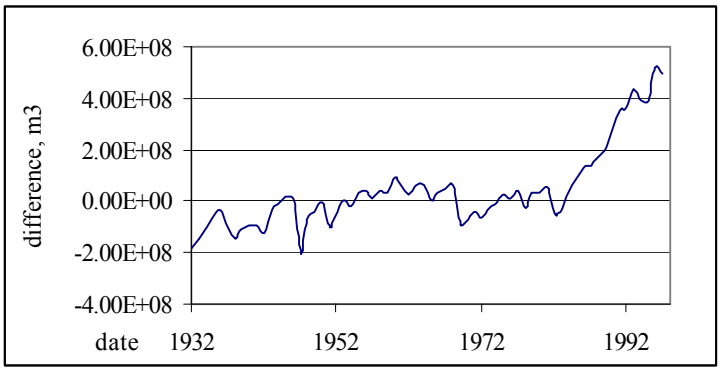

Figure 6.12: The temporal differences between the observed (derived from the WRAP, 1998 volume-stage rating curves, see Figure 3.7; section 3.5) and simulated lake storage volumes.

6.1.4 The Long-Term Water Balance

The long-term water balance for the lake is shown in Table 6.1. A consistent net groundwater outflow from the lake is evident. The storage change results are comparable with those of the Spreadsheet except in the months of June and September when there is a large discrepancy. It is most likely due to computational errors resulting from the evaluation of the amount of long-term monthly seepage from the lake. The summation of the storage change term results in a lake level fall error of about 1cm. Figure 6.13 compares the long-term components of the lake volumetric budget. The months with least net evaporation (precipitation minus evaporation) correspond to when there is most stream inflow. There is a time lag response of the groundwater seepage to high stream inflows.

Month	Precipitation minus Evaporation m^3/mth	Stream Inflow m^3/mth	Net Groundwater Seepage m^3/mth	Lake Area long-term monthly average m^2	Storage e Chang m^3/mth	Mflake Lake Level change (area=145km^2) M	Mflake Lake Level change (monthly area) m	Spreadsheet Lake Level change (area=145km^2) m
January	-2.01E+07	7.40E+06	-4.94E+06	1.49E+08	-1.76E+07	-0.122	-0.118	-0.097
February	-1.84E+07	7.31E+06	-2.98E+06	1.48E+08	-1.41E+07	-0.097	-0.095	-0.103
March	-1.80E+07	9.74E+06	-2.72E+06	1.47E+08	-1.09E+07	-0.075	-0.075	-0.097
April	-3.69E+06	2.39E+07	-2.83E+06	1.46E+08	1.74E+07	0.120	0.120	0.097
May	-1.04E+07	3.42E+07	-5.75E+06	1.47E+08	1.80E+07	0.124	0.123	0.131
June	-1.31E+07	1.90E+07	-6.76E+06	1.49E+08	-8.64E+05	-0.006	-0.006	0.012
July	-1.43E+07	1.98E+07	-5.15E+06	1.49E+08	3.52E+05	0.002	0.002	0.003
August	-1.48E+07	2.49E+07	-4.90E+06	1.49E+08	5.17E+06	0.036	0.035	0.029
September	-1.57E+07	2.44E+07	-5.38E+06	1.49E+08	3.32E+06	0.023	0.022	0.110
October	-1.62E+07	2.03E+07	-5.34E+06	1.50E+08	-1.23E+06	-0.008	-0.008	-0.013
November	-1.01E+07	2.10E+07	-4.87E+06	1.49E+08	6.01E+06	0.041	0.040	0.034
December	-1.58E+07	1.39E+07	-5.48E+06	1.50E+08	-7.47E+06	-0.052	-0.050	-0.054
Net Storage loss (m^3/mth)		-1.88E+06						
Net Lake Level fall (m)		-1.27E-02						

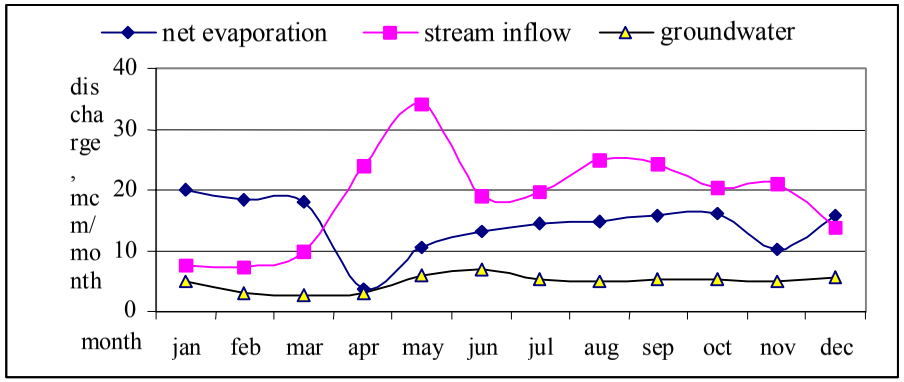

Table 6.1: The long-term water balance for the lake.
Figure 6.13. Comparisons of the long-term volumetric components.

6.2 The Steady State Mode

6.2.1 The Steady State Zones

Recharge: To make a reliable assessment of the groundwater recharge normally requires an adequate amount of good quality data on geology, geomorphology, hydrology, vegetation, topography and climate, Meijerink, ET al., 1994. The previous estimates of recharge have been quoted in section 1.6.9 and 5.4.3. These were taken as initial model input values.

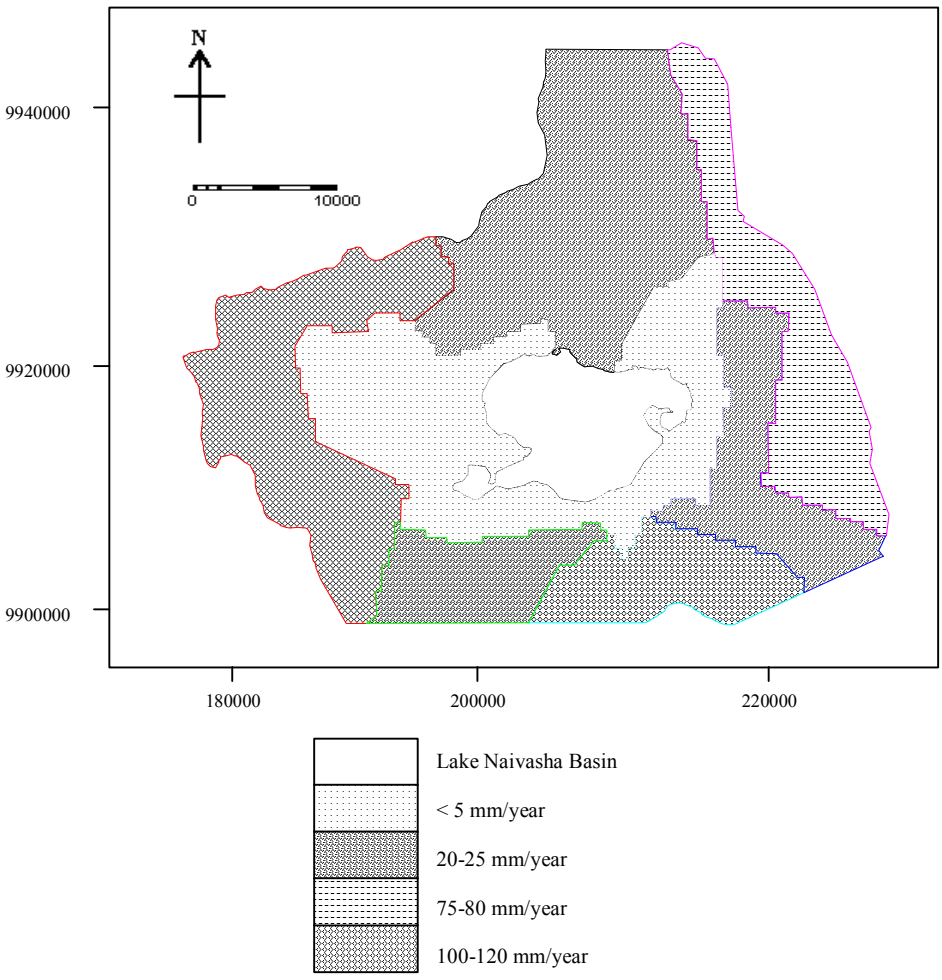

Figure 6.14: The spatial distribution of recharge derived from the optimisation of recharge estimates for the area.

The distribution of recharge zones is shown in Figure 6.14. There were basically four types of recharge zones recognised and taken to be constant throughout the model runs. The scarps to the west and the highlands to the south constituted the areas with most of the recharge (100-120 mm/year). The model was calibrated for low recharge values in the lake sediments in the vicinity of the lake (<5 mm/year, about 1% of average study basin rainfall). Jolicoeur, MSc 2000, studied the saturated hydraulic conductivity of soil types up to a depth of 6 m around the lake area. Values of 4

cm/day up to 80cm depth were found in clays southeast of the lake. A maximum value of 161 cm/day was found in sandy loams to the southwest (Appendix 2).

It is plausible that given the temporal and spatial heterogeneity of the sediments fairly low average recharge values are characteristic of the area. Nevertheless, it is still fairly low, which was deemed necessary in order to keep the transmissivity values reasonably close to quoted estimates.

The volcanic tuffs intercalated with ash that are bounded by the South Kinangop fault to the east are most likely deriving their waters through the extensive fracture systems characteristic of this area (75-80 mm/year). Considering the low gradient of the rest of the area, and the mixture of sediments and reworked volcanic material that underlie it, the quantity of recharge here is also quite sizeable (20-25 mm/year)

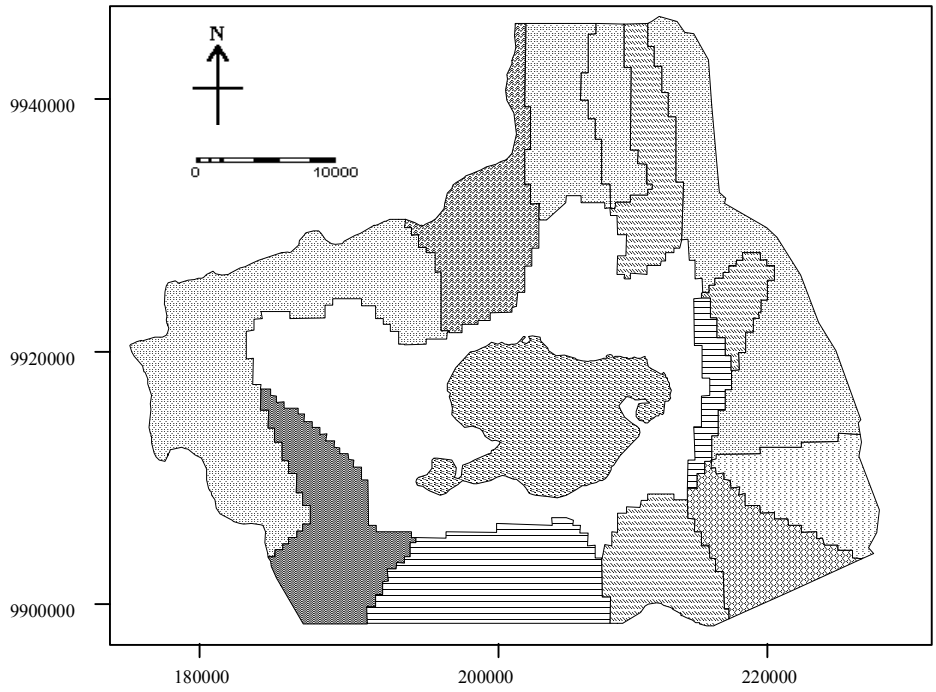

Figure 6.15: Transmissivity distribution for layer 1 of the modelled area.

Transmissivity: The transmissivity zones shown in Figures 6.15 and 6.16 for layers 1 and 2 (same legend shown in Figure 6.16), respectively are based essentially on the lithostratigraphy (Figure 4.1).

The first and second layers have been fitted to the observed lake levels and groundwater heads, respectively. Modifications had to be made for variations in aquifer properties within the same formation. Initial estimates were derived from Figure 3.9 and Table 3.1 (geometric mean was calculated for the different directions around the lake, Fetter, 1994) and from estimates from similar formations elsewhere, (see references cited).

Vertical Conductivity: The vertical conductivity of the formations are not well known. Previous studies indicate it to be in the order of magnitude of 10% of the

horizontal hydraulic conductivity. Values of 0.1 were initially considered that were later modified for calculating the vertical leakance between the two layers.

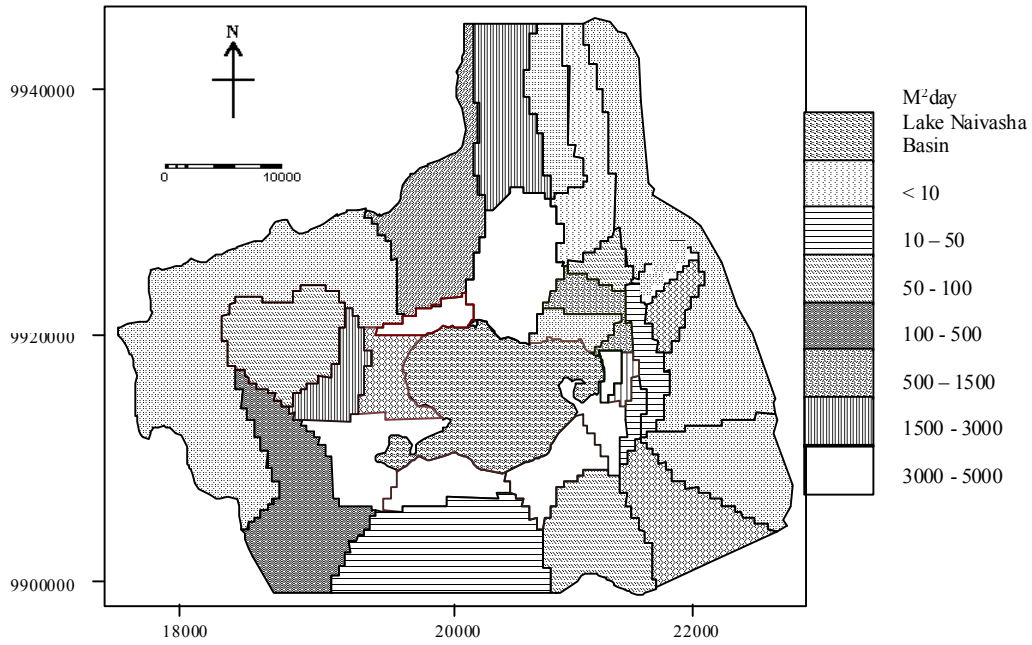

Figure 6.16: The distribution of Transmissivity zones in layer 2 of the modelled area.

6.2.2 The Piezometric Contour Map

A contour piezometric map was drawn for the simulated aquifer heads, Figure 6.17. Both layers have a similar spatial piezometric configuration. The lack and inadequate distribution of observation points has contributed to anomalies in the outlying areas, Figure 6.19 (residuals in metres). The piezometric heads around the vicinity of the lake drop towards 1885 mamsl (for the areas to the north and south of basin) and rise to 1990 mamsl (for the western and eastern parts). Away from the lake horizons, the aquifer hydraulic properties that determine the gradient of the piezometric surface has been affected by a number of factors, chief of which are the heterogeneity of the lithostratigraphy, structural differences, and various forms of measurement errors.

6.2.3 Steady State Flow

The steady state flow components and lake stage is quite close to those for the average long-term transient simulation indicating that the system may have reached a dynamic cyclic steady state (Anderson and Woessner, 1992), Table 6.1, and Figures 6.6, 6.11. The steady state groundwater seepage from the lake amounts to 4.48 mcm/mth and seepage into the lake is about 0.22 mcm/mth.
Significant inputs to the flow system of the area include recharge and lake seepage (sustained by the excess of the stream inflow-precipitation over evapotranspiration). The outflow to the south and north of the basin provides the main output from the area.

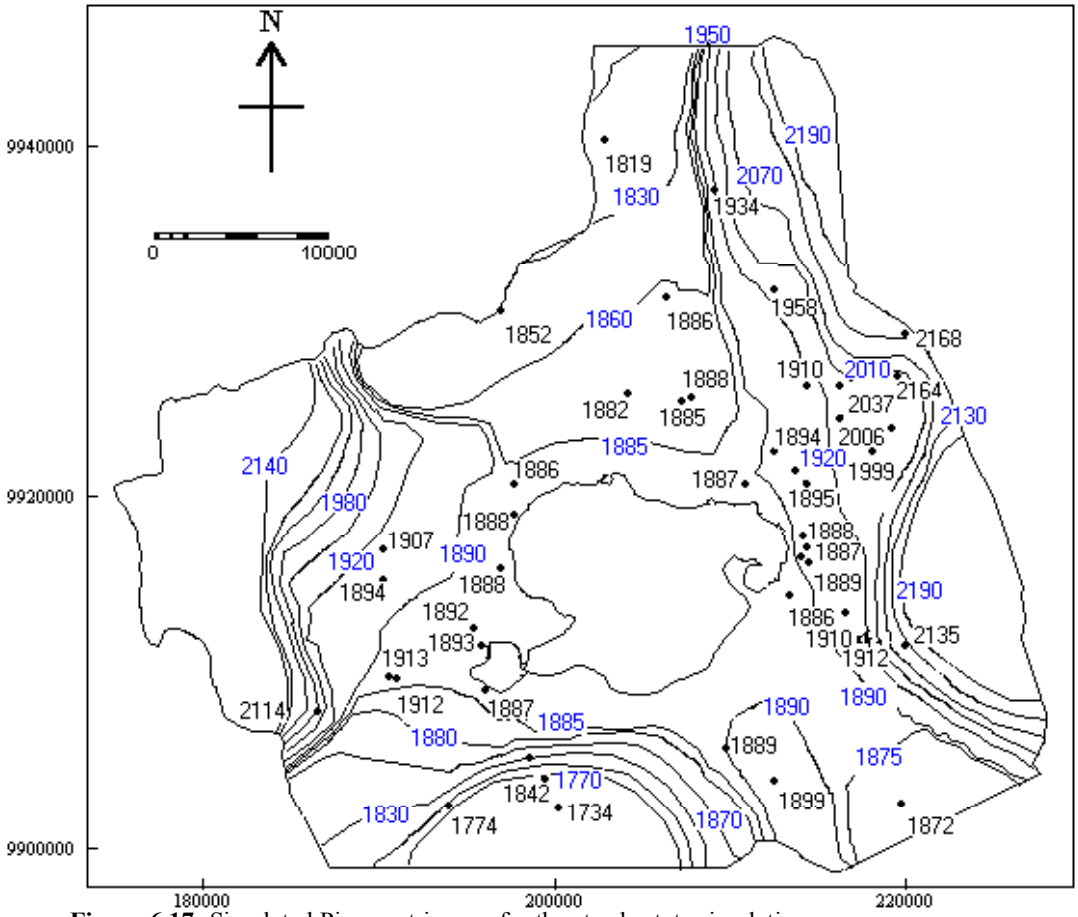

Figure 6.17: Simulated Piezometric map for the steady state simulation

The final calibration showed fairly good general agreement between observed and simulated aquifer heads. Residuals (observed minus simulated heads) ranged between –16.16m and 25.72m). The mean residual, mean absolute residual, standard deviation about the mean, and the sum of squared residuals were 0.99m, 6.57m, 9.65m, and 4138.5m, respectively. The head values around the lake vicinity show very good agreement. Residuals ranged between –2.74m and 3.834m. The mean residual, mean absolute residual, standard deviation about the mean, and the sum of squared residuals were 0.43m, 1.44m, 1.88m, and 48.54m, respectively. The main discrepancy in heads was in the outlying areas in the western and eastern scarp areas and in the southern geothermal-underlying areas. These areas have aquifer heads either much higher or lower than the average lake level values, respectively. It was not possible to adequately fit these areas too because of the anomalies of the system and the measurements. These points have been included to make it possible to establish the general trend and pattern of flow in the whole area taking into account acknowledged local and regional flow systems of the basin.

STEADY STATE VOLUMETRIC BUDGET

LAKE VOLUMETRIC BUDGET FOR LAKE NAIVASHA

STAGE	=	1888.40
WETTED AREA	=	1.542500E+08
VOLUME	=	7.060308E+08

	INFLOW	OUTFLOW
PRECIPITATION-EVAPORATION:	0.000000	-492058
STREAM INFLOW/RUNOFF:	627415.	0.000000
SEEPAGE:	7317.25	-147163
TOTAL:	634732.	-639221

ERROR	=	-4488.31
STEADY-STATE ERROR	=	-0.70%

VOLUMETRIC BUDGET FOR ENTIRE MODEL

CUMULATIVE VOLUMES	M3	RATES FOR THIS TIME STEP	M3/D
	IN:		IN:
CONSTANT HEAD =	0.0000	CONSTANT HEAD =	0.0000
INFLOW =	0.0000	INFLOW =	0.0000
RIVER LEAKAGE =	2219908.0000	RIVER LEAKAGE =	92.0803
RECHARGE =	4898189820.0000	RECHARGE =	203173.5780
LAKE LEAKAGE =	3547866110.0000	LAKE LEAKAGE =	147163.0630
TOTAL IN =	8448275970.0000	TOTAL IN =	350428.7190
	OUT:		OUT:
CONSTANT HEAD =	0.0000	CONSTANT HEAD =	0.0000
OUTFLOW =	8266466820.0000	OUTFLOW =	342887.4060
RIVER LEAKAGE =	6746499.0000	RIVER LEAKAGE =	279.8402
RECHARGE =	0.0000	RECHARGE =	0.0000
LAKE LEAKAGE =	176407200.0000	LAKE LEAKAGE =	7317.2500
TOTAL OUT =	8449620480.0000	TOTAL OUT =	350484.5000
IN - OUT =	-1344512.0000	IN - OUT =	55.7813
PERCENT DISCREPANCY =	-0.02	PERCENT DISCREPANCY =	0.02

Table 6.2: The steady state volumetric budget for the entire model (levels, flow volumes and flow rates in m, m^3 and m^3/day, respectively).
Negative values indicate discharge out of the lake domain.

The flow patterns of the immediate lake horizons as inferred from the aquifer head distribution (Figure 6.17) are shown in Figures 6.20 and 6.21. There are two main inflow paths, the bulk of which is to the north-east. Very little of the flow from the scarp to the west gets into the lake, most of it is dispersed southwards. The main outflow paths

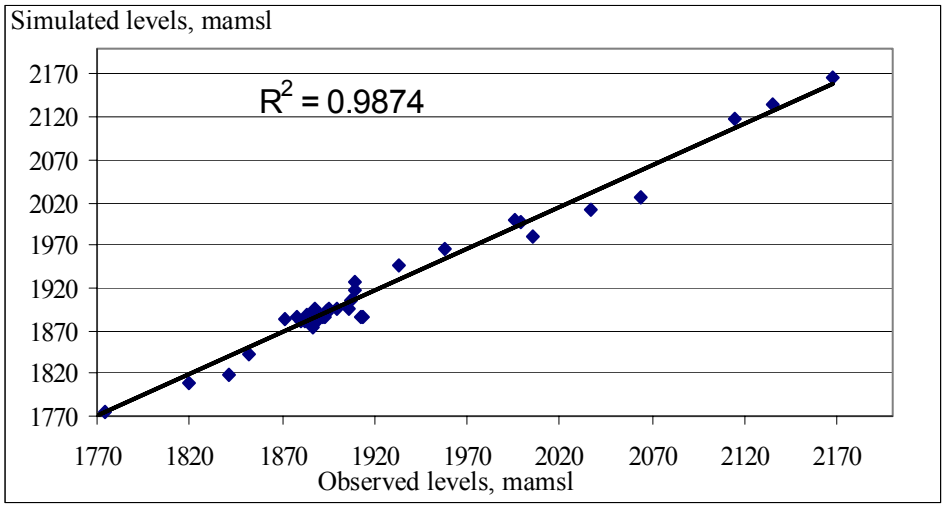

Figure 6.18: Scatter Plot of observed against calculated aquifer heads in the steady state mode (45 observation points, Figure 6.17)

from the lake are to the south-east and due north of the lake. There is a small component of outflow to the south-east of the lake that joins up the flow from the scarp to the north-east that is digressed south-eastwards.

6.3 The Transient State Mode

6.3.1 Initial Estimates

Storage Coefficient: The transient run involved making estimates for the storage coefficients of the aquifer. This was the least known parameter in the system. The values that were initially considered were taken from previous studies by: Wilberg, 1976 (0.0015), Ojiambo (0.0044), Trotman, MSc 1998 (0.12 for the unconfined aquifer, and 0.0001 for the confined aquifer), Ramirez, MSc 1999 (0.01-0.15) and Kibona MSc 2000 (0.00146-0.00395 for the sediments), and from a literature review of the characteristics of similar formations elsewhere in the world, Appendix 2.

The storage coefficient values have been generally lumped into two main zones to represent the lake sediments/alluvial materials, and the reworked volcanic materials Figure 6.21. There is a further subdivision to cater for the extra variations envisaged within each layer. It is assumed that within the limits of uncertainty, the variations in storage coefficients in the different hydrogeologic units will not have a significant influence in the final optimisation results. The small order of magnitude of variations within each kind of formation does not warrant further subdivisions. Both layers have been zoned in a like manner. There was a general lack of certainty in the making of the initial estimates.

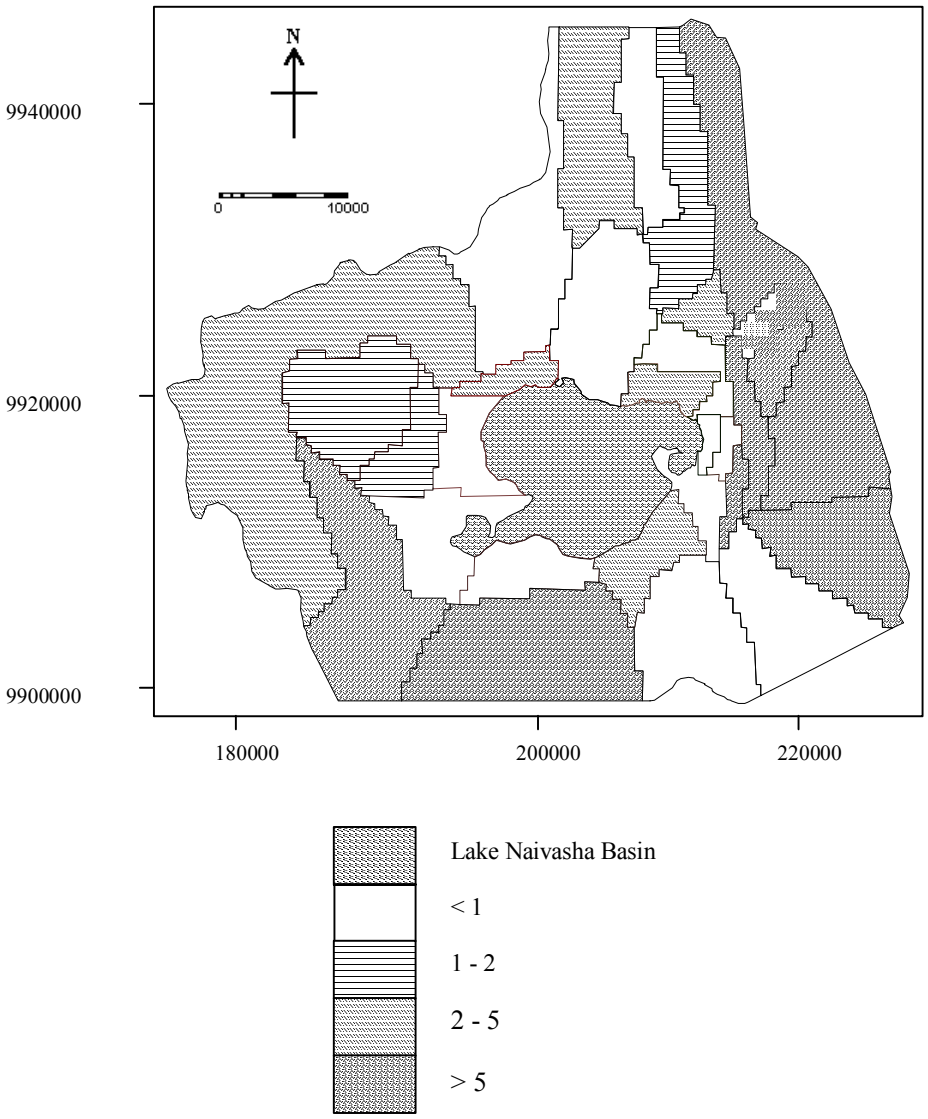

Figure 6.19: Residual head distribution for the aquifer heads for the steady state simulation.

Lakebed Conductance: The lakebed conductivity was initially estimated at 0.25 m/day, taken from an average value for the riverbed sediments quoted by a number of authors including the work of Jolicoeur (MSc 2000) who estimated the saturated hydraulic conductivity of the soils in the lake sediments (Appendix 2). The spatial variability of this parameter is not known and has not been catered for. It has therefore been assumed to be uniform over the whole lake under surface.

6.3.2 Optimisation Results

Table 6.3 shows the parameter estimates for the first final run (storage 1 through 4 for storage coefficients and conductance for the lakebed conductivity), and Table 6.4 shows the second final run where outflow terms were optimised. The storage 1 parameter has been used to estimate the specific yield of the top aquifer (lake sediments) considered to be confined for all the model runs. The outflow term was separately optimised due to computation memory limitations. The analysis of the parameter correlations, the eigen values and eigen vectors provided a great deal of

hydrological insight. These statistics provide a view on the internal essential structure of the inverse problem at hand.

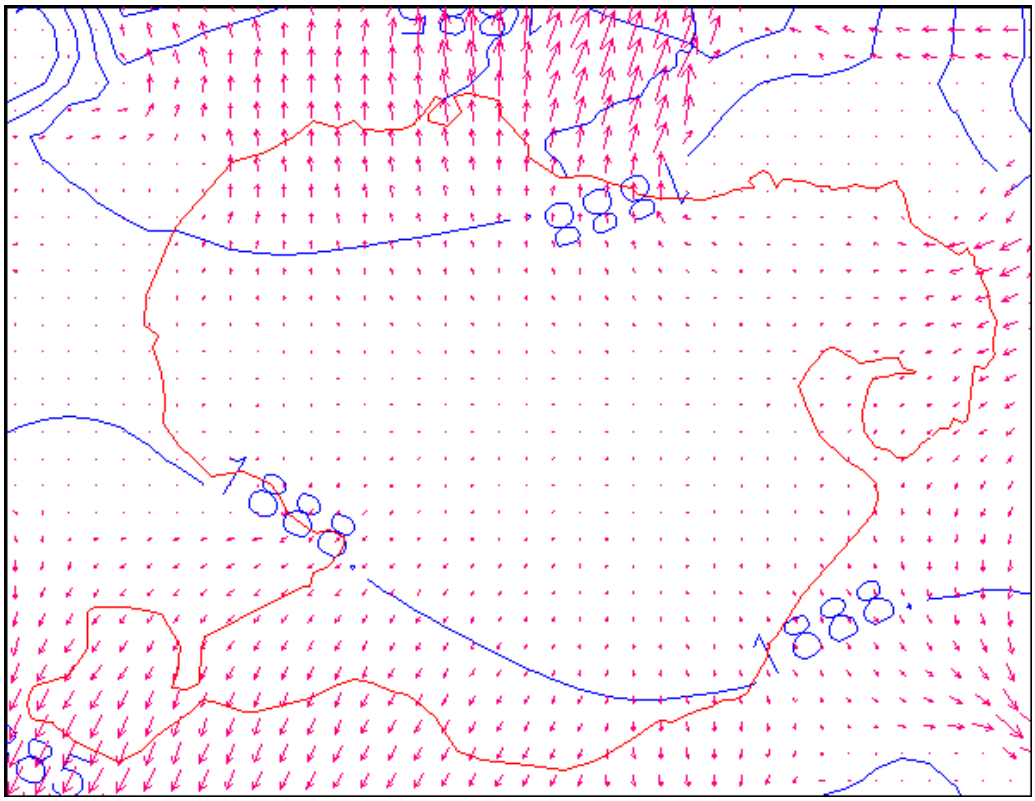

Figure 6.20: Flow vector map showing the main flow paths for the lake area horizons.

Optimisation of storage coefficient and lakebed conductance: The 95% confidence limits for all the parameters are within reasonable ranges. The high objective function (57 000) is due to the big number of observation points (837). The covariance matrix shows very low values (close to zero) of variances of all the adjustable parameters indicating good reliability and certainty of parameter estimation.

The correlation coefficient matrix shows a general lack of correlation between the parameters. The exceptions include a higher degree of correlation between parameters storage 3 and conductance (viz. -0.6999), and between storage 1 and 4 (viz. –0.3605). This explains why, individually, these parameters are determined with a relatively higher degree of uncertainty in the parameter estimation process, as evinced by their wider confidence intervals.

The Normalised Eigenvector of the covariance matrix and the Eigenvalues indicate that the eigenvector of highest eigenvalue is dominated by only one parameter,

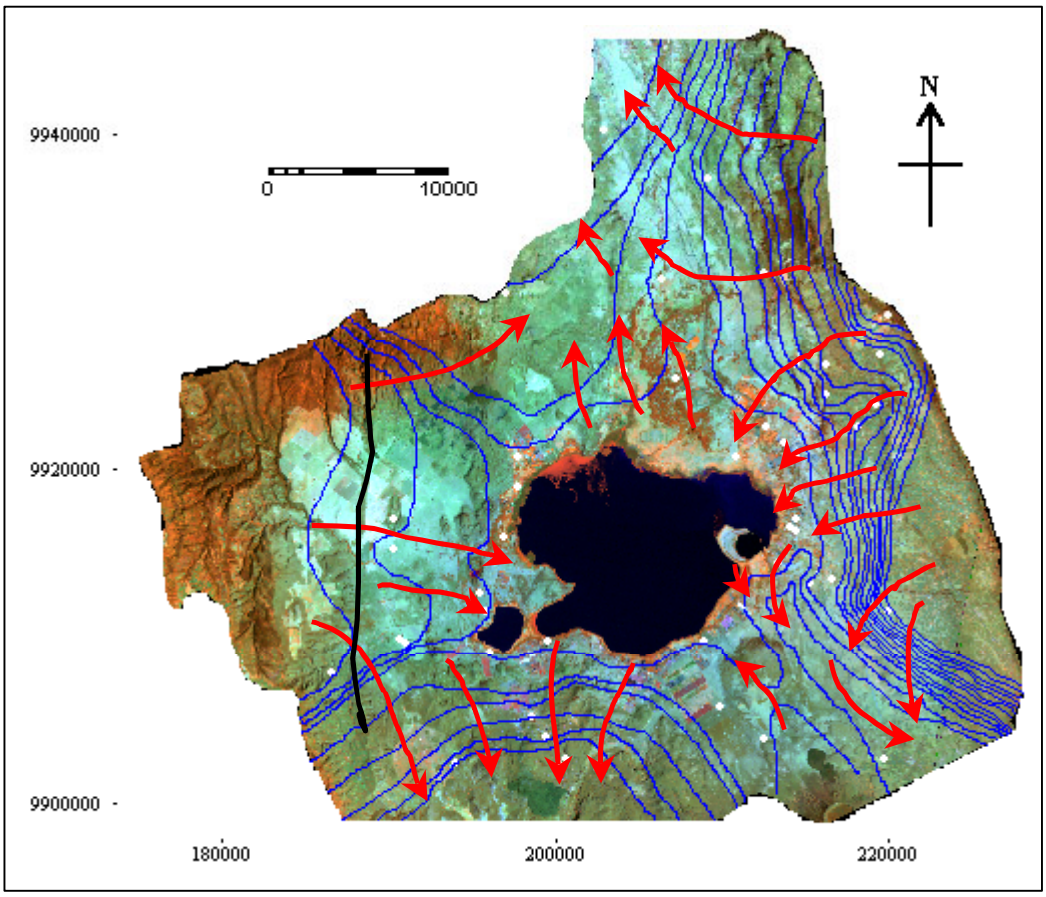

Figure 6.21: Groundwater Flow map for the natural setting prior to 1980.

storage 4 (0.996), which is therefore the most important parameter of the model. Similarly, the next two eigenvectors with the second and third highest eigenvalues are dominated by single parameters, i.e. the second and third
eigenvectors have storage 2 (-0.9984), and storage 3 (-0.9976), respectively. The three storage coefficient parameters determine the amount of water that is released from storage. They thus, regulate the overall elevation of heads in the two aquifers. Therefore, in all the eigenvectors the dominant parameters are well resolved in comparison with the other parameters. Generally the solution indicates a low degree of correlation among the parameters that implies that it is quite unique.

Optimisation of the outflow terms: The 95% confidence limits for all the parameters are within reasonable ranges. The high objective function drops in this run to 43 000. The covariance matrix shows very high values of variances of all the adjustable parameters indicating poor reliability and uncertainty of parameter estimation.
The correlation coefficient matrix shows a general correlation between the parameters. This explains why, individually, these parameters are determined with a relatively higher degree of uncertainty in the parameter estimation process, as evinced by their wider confidence intervals.

The Normalised Eigenvector of the covariance matrix and the Eigenvalues indicate that the the first three eigenvectors of highest eigenvalues are dominated by more than one parameter. Therefore, in all the eigenvectors the dominant parameters are not

well resolved in comparison with the other parameters. Generally the solution indicates a degree of correlation among the parameters that implies that it is not unique.

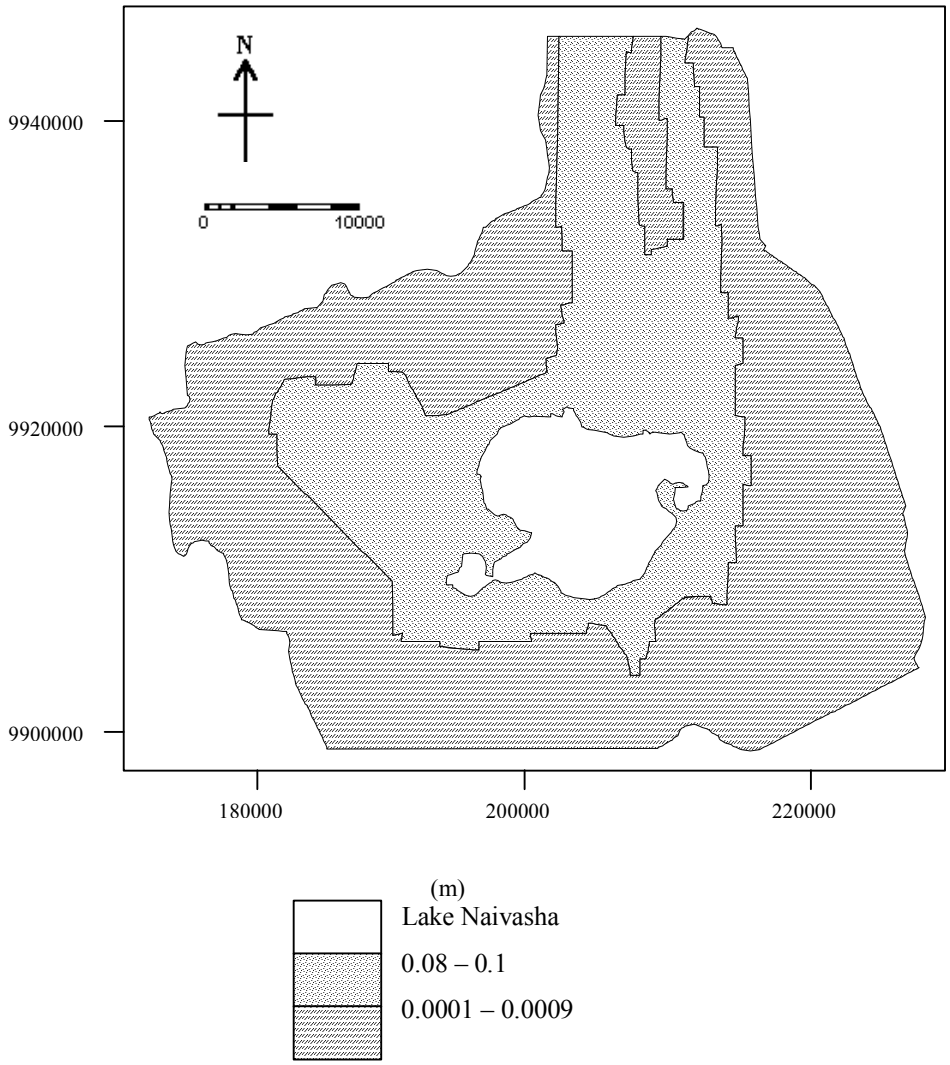

Figure 6.22: Optimised spatial distribution of Storage Coefficient over the modelled area.

The outflow shows a total of 131 mcm/year out of the basin. 83 mcm/year (63%) flow southwards while 48 mcm/year flows northwards. Previous workers estimate a shallow groundwater outflow up to 500m depth from the basin to range from 52-295 mcm/year. South of the basin it ranges from 27-270 mcm/year with a geometric mean of 89 mcm/mth and to the north averages 11 mcm/year.

A scatter plot of observed points for the last 10 years (averaged) for the transient runs is shown in Figure 6.23. Notable is that most of the simulated points are way above the observed, as expected. The transient run does not account for the extra abstractions of water that characterise the period after 1980. So that to correctly fit this period of the simulation, the stresses have had to be stepped up as was done during the predictions discussed hereafter.

The simulated lake levels have already been discussed in section 6.1. The calculated mean error, mean absolute error and root mean square error for the period up to 1980 when there is good correlation between the observed and simulated levels are 0.31m, 0.42m, 0.52m, respectively.

Final Run (Optimizing Storage Coefficients and Conductance)				
Parameter	Estimated value	95% confidence limits		
		lower	upper	
storage 1	0.105142	9.60E-02	0.11427	
storage 2	3.42E-04	1.95E-04	4.89E-04	
storage 3	1.68E-03	6.58E-04	2.70E-03	
storage 4	5.31E-05	-2.09E-03	2.20E-03	
conductance	0.215152	0.141544	0.288761	
Objective Function				
Sum of squared weighte residuals (phi)				5.27E+04
Covariance Matrix				
2.17E-05	9.23E-09	-1.59E-07	-1.84E-06	-1.15E-06
9.23E-09	5.60E-09	-6.26E-09	7.51E-10	-1.28E-07
-1.59E-07	-6.26E-09	2.72E-07	-5.42E-08	-1.37E-05
-1.84E-06	7.51E-10	-5.42E-08	1.20E-06	3.52E-06
-1.15E-06	-1.28E-07	-1.37E-05	3.52E-06	1.41E-03
Correlation Coefficient Matrix				
1	2.65E-02	-6.55E-02	-0.3605	-6.58E-03
2.65E-02	1	-0.1603	9.15E-03	-4.57E-02
-6.55E-02	-0.1603	1	-9.48E-02	-0.6999
-0.3605	9.15E-03	-9.48E-02	1	8.55E-02
-6.58E-03	-4.57E-02	-0.6999	8.55E-02	1
Normalized eigenvectors of covariance matrix				
-2.81E-05	-1.12E-02	8.82E-02	0.996	-8.31E-04
-0.9984	5.60E-02	2.11E-03	4.14E-04	-9.09E-05
-5.61E-02	-0.9976	-3.92E-02	-7.75E-03	-9.73E-03
-8.60E-05	-3.84E-02	0.9953	-8.86E-02	2.50E-03
-6.36E-04	-9.61E-03	-2.80E-03	9.74E-04	0.9999
Eigenvalues				
5.17E-09	1.37E-07	1.03E-06	2.19E-05	1.41E-03

Table 6.3: Optimisation parameters for the final transient mode run (storage coefficient and lakebed conductance).

6.4 Groundwater Head and Flow Fluctuations

6.4.1 The Groundwater Head Response

The groundwater head fluctuations (hydrographs) in response to lake fluctuations were evaluated in the four major directions around the lake. The Time-head distribution utility in PMWIN was used to assess this. The positions of the wells are shown in Figure 6.24. The response was evaluated for wells located at distances of up to 2.5km perpendicular to the lake shores. Graphs for groundwater head fluctuation against time, and for head fluctuation against distance from the lake for selected times were drawn.

Final Run (Optimising Outflow)					
Parameter	Estimated value	95% confidence limits			
		lower	upper		
outflow term 1	-3493.31	-4248.12	-2738.5		
outflow term 2	-4294.77	-4904.77	-3684.78		
outflow term 3	-3500	-4223.13	-2776.87		
outflow term 4	-9749.84	-11000.4	-8499.24		
outflow term 5	-14546.4	-15608.2	-13484.6		
outflow term 6	-5000	-5995	-4005		
Objective Function					
Sum of squared weighte residuals (phi)				4.36E+04	
Covariance Matrix					
1.48E+05	-2.71E+04	-2.20E+04	-6.65E+04	1.60E+04	-6.42E+04
-2.71E+04	9.69E+04	7020	-1.57E+04	-5.75E+04	-2.75E+04
-2.20E+04	7020	1.36E+05	-3.49E+04	2.44E+04	-1.26E+05
-6.65E+04	-1.57E+04	-3.49E+04	4.07E+05	-2.70E+05	6.24E+04
1.60E+04	-5.75E+04	2.44E+04	-2.70E+05	2.93E+05	-3.67E+04
-6.42E+04	-2.75E+04	-1.26E+05	6.24E+04	-3.67E+04	2.58E+05
Correlation Coefficient Matrix					
1	-0.2265	-0.155	-0.2706	7.67E-02	-0.3283
-0.2265	1	6.11E-02	-7.91E-02	-0.3413	-0.1741
-0.155	6.11E-02	1	-0.1483	0.1221	-0.6733
-0.2706	-7.91E-02	-0.1483	1	-0.781	0.1927
7.67E-02	-0.3413	0.1221	-0.781	1	-0.1334
-0.3283	-0.1741	-0.6733	0.1927	-0.1334	1
Normalized eigenvectors of covariance matrix					
0.4194	0.1877	2.53E-02	0.8665	0.1325	-0.141
0.5231	-0.3227	-0.7534	-0.1783	0.1471	3.39E-02
0.3683	0.6516	0.162	-0.4171	0.4728	-0.1267
0.3592	-0.2984	0.4472	-2.47E-02	0.1564	0.7463
0.4274	-0.4145	0.4454	-0.1899	-0.2412	-0.5941
0.3211	0.4187	-8.45E-02	-8.24E-02	-0.8091	0.2304
Eigenvalues					
5368	4.57E+04	1.37E+05	1.69E+05	3.24E+05	6.59E+05

Table 6.4: Optimisation parameters for the final transient mode run (outflow terms).

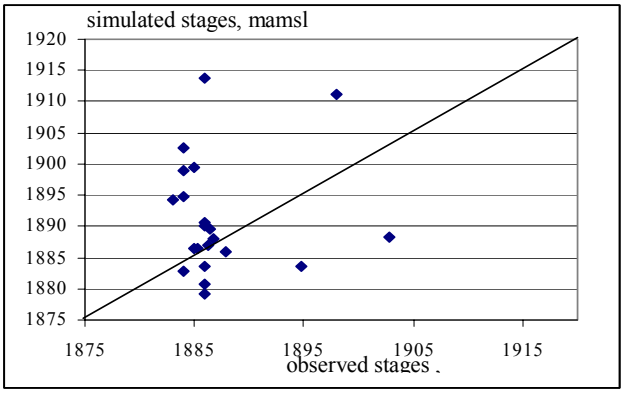

Figure 6.23: Scatter Plot of Observed and simulated aquifer heads for the last 10 years of the transient run.

Figures 6.25 through 6.27 indicate head-time fluctuations of groundwater in response to three selected periods:
i) when the lake level dropped to its lowest level (November 1951 to December 1953), Figure 6.25;
ii) when the lake rose to its maximum level (October 1961 to March 1965), Figure 6.26;
iii) when the lake level was stable (September 1969 to December 1971), Figure 6.27.

During the period of lake level fall, the groundwater levels showed a similar but subdued response in unison. The degree of response decreases with distance from the lake. This lends support to the findings of Behar, MSc 1999 who similarly found out that the wells around the lake mimic the lake level changes. There is a time lag between the response of the peak events in the lake and groundwater levels that varies from 30 to 90 days. This could be attributed to bank storage within the aquifer during these peak periods that take time to be dissipated when the lake level starts to drop. The magnitude and distance of response of the wells is more significant to the west and least to the north of the lake. The heterogeneity of the conductance of the saturated materials plays a major role in defining how far this zone of direct influence extends.

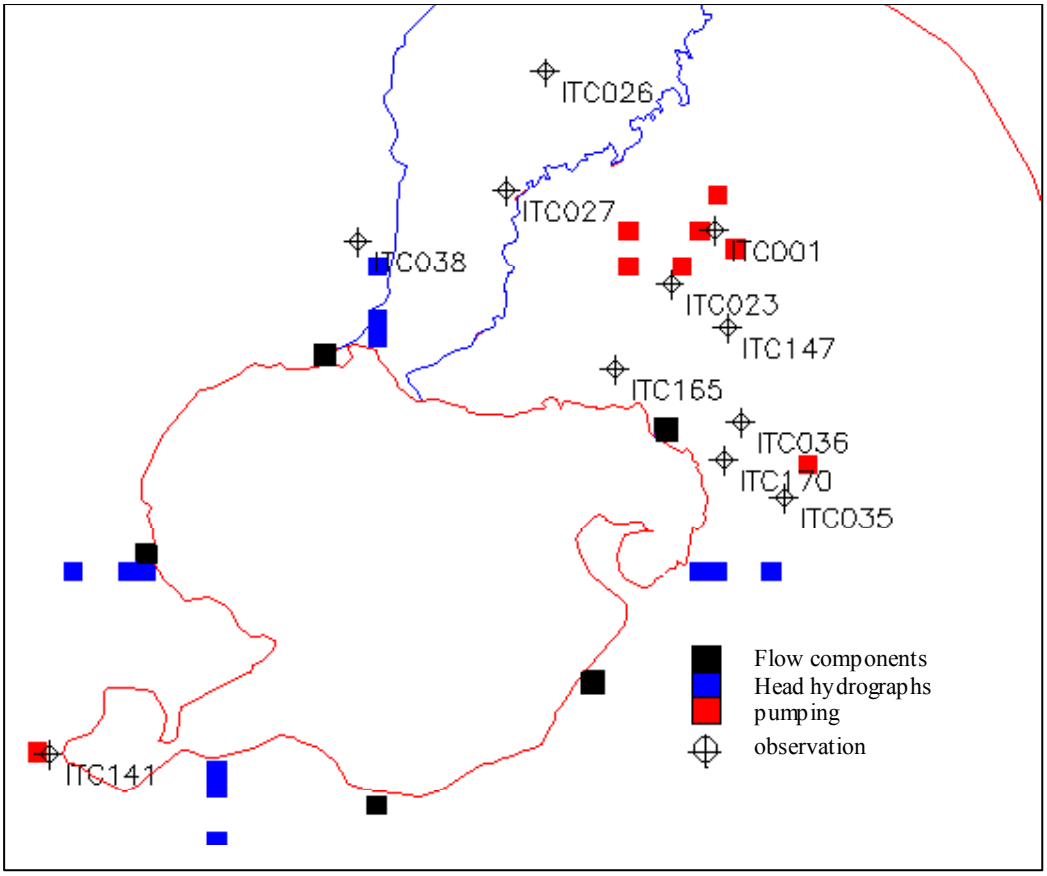

Figure 6.24: The locations of the wells for deriving the flow components, head hydrographs, and for pumping and observation.

When the lake rises, the groundwater levels take a similar time as before to peak in response to the peak lake levels. The eastern part of the lake has the least distance of response to these peak events. During periods of stable lake levels, the

response of the two systems has the least time lag and is more evenly distributed around the lake.

It is expected that when the lake level rises, there is a general outflow to the groundwater and the reverse during the fall in the areas within its immediate vicinity. In order to check these dynamics, plots were made for the three described periods of wells located up to 2.5km from the lake at the four principal points already considered, Figure 6.28. This intricate mechanism of flow reversals has not been possible to be discerned. The magnitude of these fluctuations is subdued mainly due to the discretisation of the area used in this simulation. In each of the four directions, the groundwater levels during lake level rise are higher than groundwater levels during its fall (mimics lake level fluctuations).

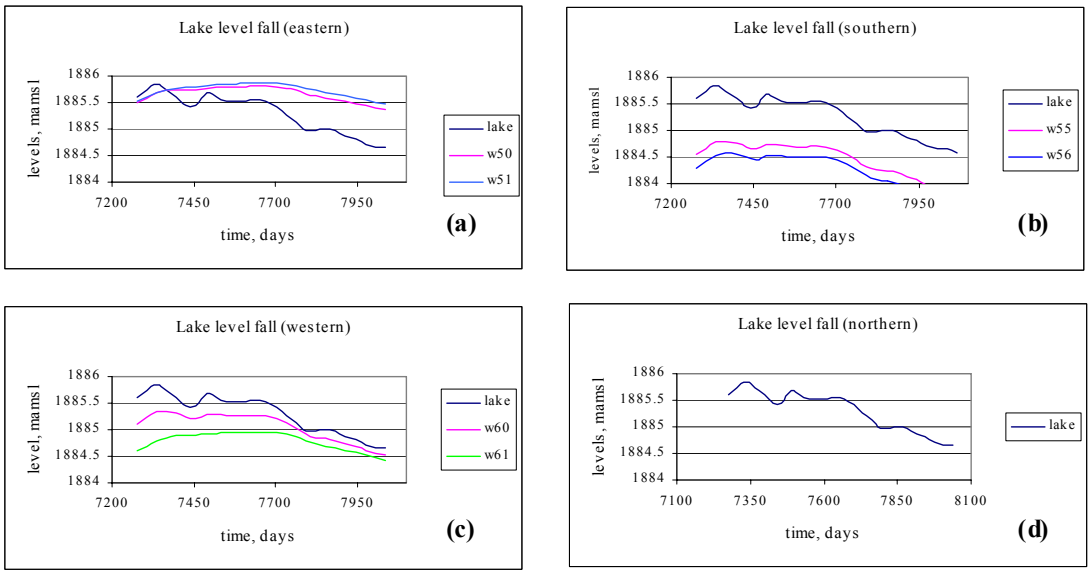

Figure 6.25: Period of Lake level fall: a) eastern part, b) southern part, c) western part, d) northern part.

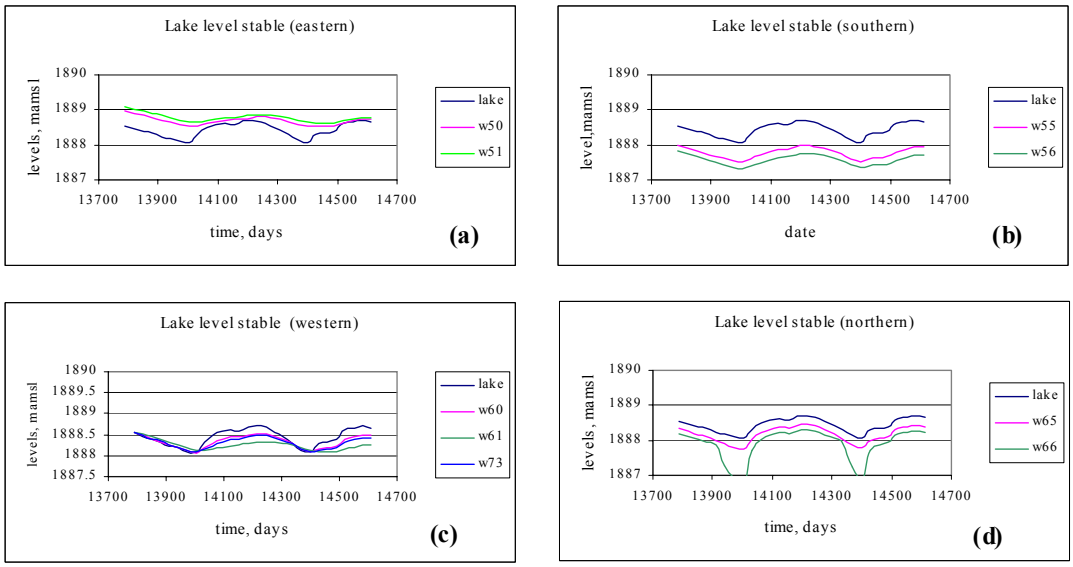

Figure 6.26: Period of stable Lake level: a) eastern part, b) southern part, c) western part, d) northern part.

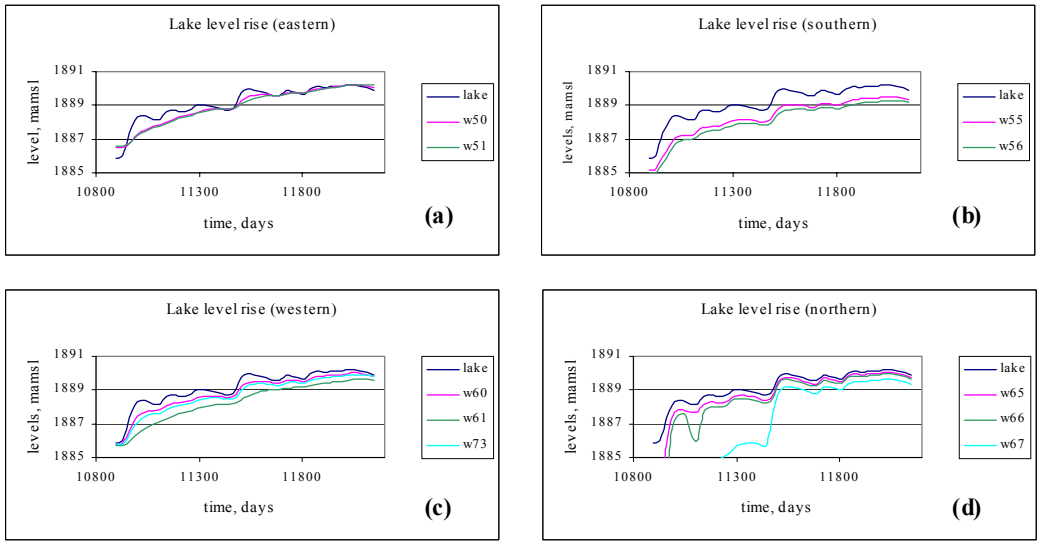

Figure 6.27: Period of Lake level rise: a) eastern part, b) southern part, c) western part, d) northern part.

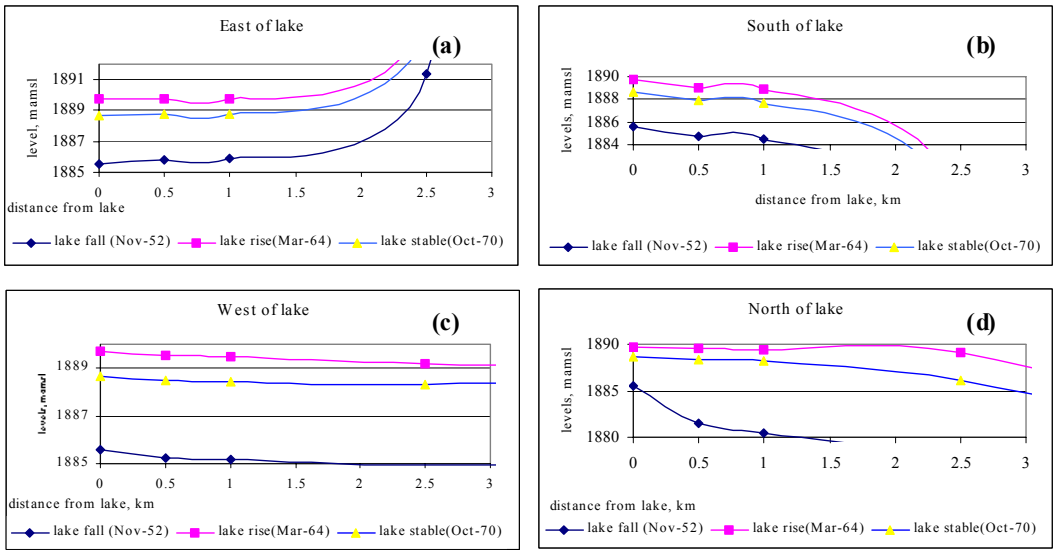

Figure 6.28: The response of the groundwater levels to lake level fluctuations during selected periods of lake level rise (November 1952), lake level fall (November 1952) and stable lake level (October 1970): (a)east, (b) south, (c) west, and (d) north of the lake.

6.4.2 The Groundwater Flow

The groundwater flow was also assessed on a cell-by-cell basis around the lake area. A water budget utility, BUD2HYD was used. The Program reads an unformatted cell-by-cell flow term written in COMPACT form by the MODFLOW version of MODFLOW. It extracts cumulative flow rates within each of a number of user-defined zones within the model domain for all times represented in the cell-by-cell term file. It then records these flow rates on its output file in a format that is readily acceptable to a spreadsheet. Thus flow rates within different parts of the model domain can be plotted against time.
Flow components were extracted from selected points around the lake, Figure 6.24. The plots of the temporal variations in the vertical interaction of the two layers are shown in Figure 6.28.

The most significant fluctuations are observed in the northern, north-eastern, and south-eastern parts of the lake. The flow interchange is most prominent in the north-eastern and south-eastern parts.

The temporal interaction of groundwater with the lake, Figure 6.29, is more pronounced for the top aquifer. A significant exchange of flow between the two domains is seen to the north and west of the lake. Notable is the south-eastern part of the lake where the exchange is least.

The storage change was also considered, Figure 6.30 and is the most dynamic of the three flow components. The most responsive areas are to the northeast, southeast and south of the lake.

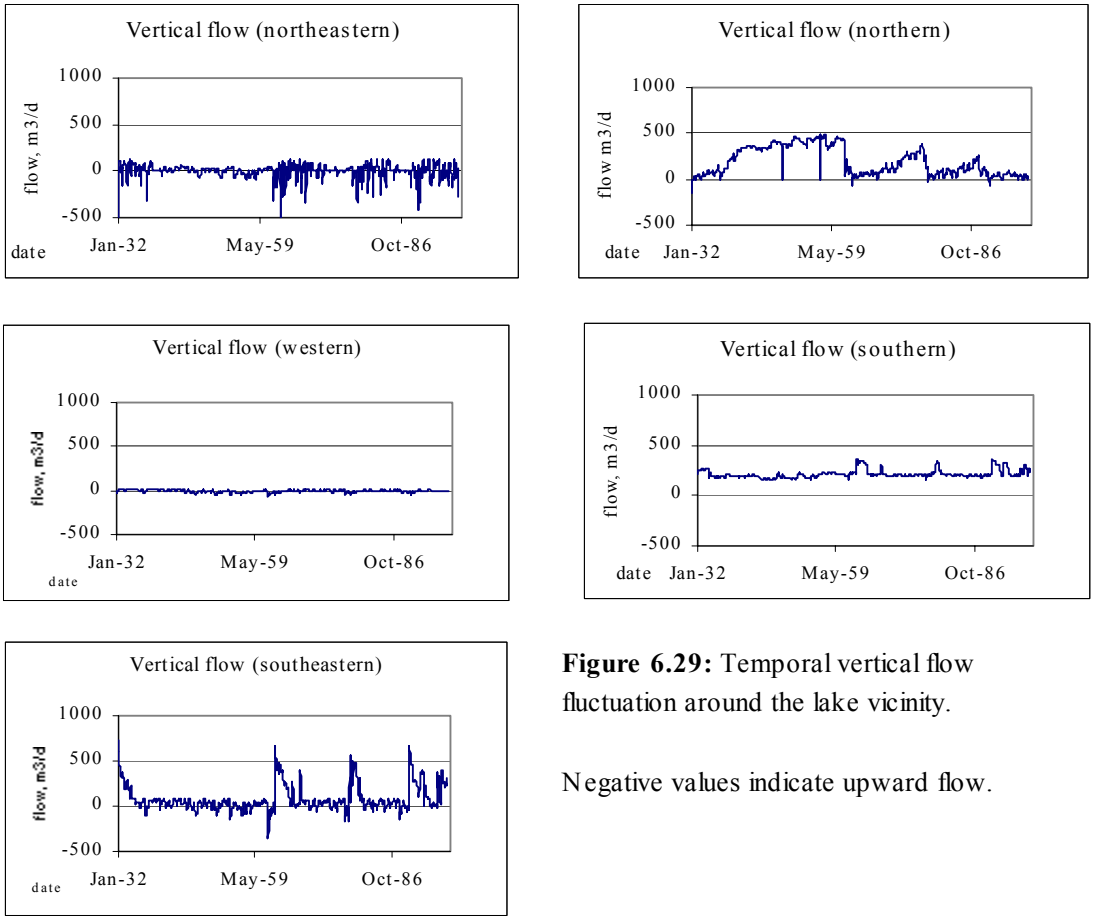

Figure 6.29: Temporal vertical flow fluctuation around the lake vicinity.

Negative values indicate upward flow.

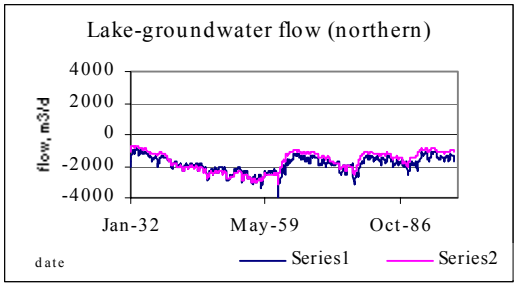

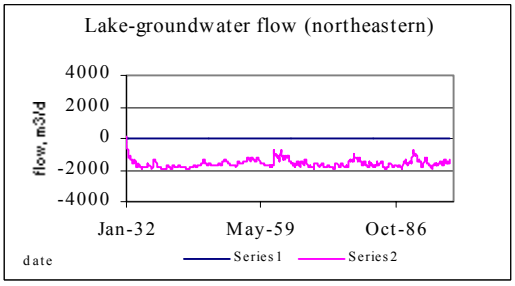

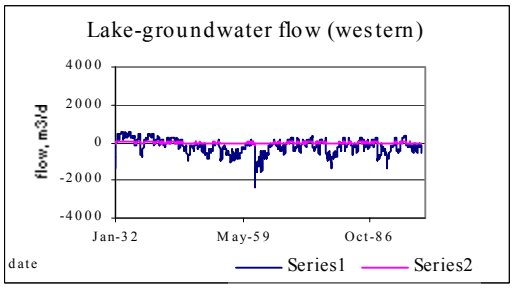

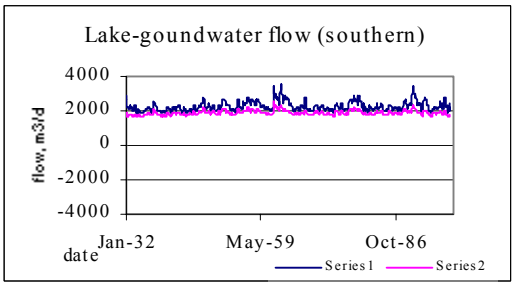

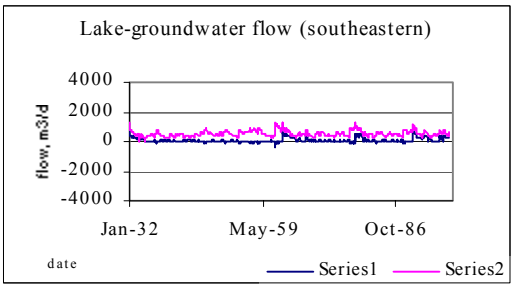

Figure 6.30: Temporal groundwater-lake interaction around the lake vicinity.
Series 1: top layer
series 2: bottom layer
negative values indicate flow into the lake
for the north-east, south-east and southern parts of the lake.

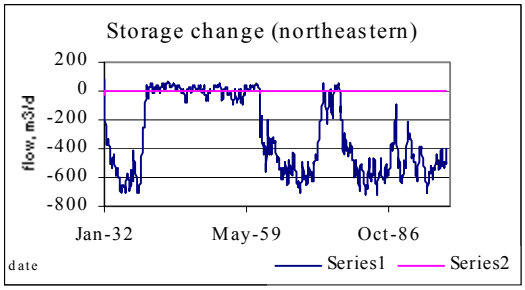

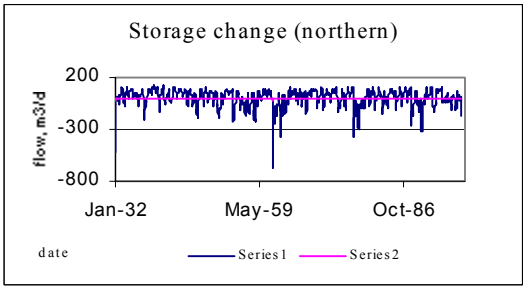

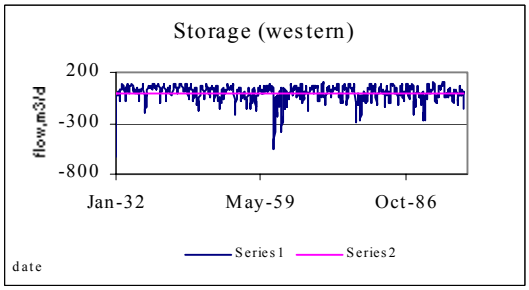

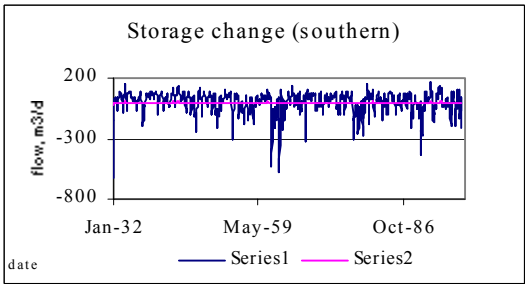

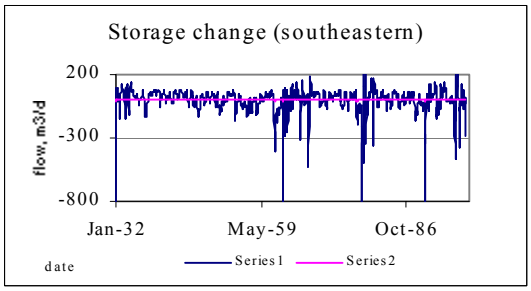

Figure 6.31: Temporal storage change aound the lake vicinity.

Series 1: top layer
series 2: bottom layer

negative values indicate flow out of storage

6.5 Sensitivity Analyses

The uncertainty in modelling exists because of uncertainties in temporal and spatial variation of model parameters, initial and boundary conditions, and subsurface heterogeneity. Sensitivity analyses were carried out firstly in the steady state mode and then in the transient state mode, the results of which are shown in the subsequent figures. The evaluations were made using residuals and "sensitivities" (section 5.8.1).

6.5.1 Steady State

The sensitivity analyses were carried on the effects of a number of parameters on the aquifer heads.
The residuals indicate that the changes in transmissivity and both recharge and transmissivity provide the most response, Figure 6.31b. The vertical conductivity is the least responsive of the parameters, recharge being intermediate. Transmissivity is more sensitive to lower values Figure 6.31c, while recharge is more symmetrical, Figure 6.31d. They both have limits beyond which the response is subdued (20% change). The vertical conductivity does not give a consistent response. Most of the highest magnitudes of deviations were from the wells in the outlying scarp areas.

6.5.2: Transient State

The sensitivities were evaluated for both aquifer heads and lake levels. The aquifer heads are more sensitive to the parameter changes than the lake levels. The residuals for the single changes show least effects by the storage coefficients and most effects by the outflow terms, lakebed conductance being intermediate, Figures 6.32a and b. The sensitivity of each of the terms hits a significant limit at about 20% of actual value, Figures 6.32c and d. They all have a symmetrical effect on the lower and higher changes, save for the lakebed conductance that is more sensitive for the lower values.

The residuals from a combination of changes indicate that changing lakebed conductance and outflow terms give the highest response, while the lakebed conductance with the storage coefficient provide the least response, Figure 6.33a. All the possible double combinations have symmetrical effects save for the lakebed conductance-storage coefficient change that gives better response for lower values, Figures 6.33b, c and d. Again the parameters have a limit of significant (about 20% change) effect beyond which it gets subdued.

6.5.3 Sensitivity of the Objective Function

SENSAN was used in conjunction with PEST to study the dependence of the objective function on certain parameters. SENSAN does not compute an objective function because it does not read an observation dataset, and hence cannot compare model outputs with corresponding observations to calculate residuals. Where there are only two parameters, this can be used to contour the objective function in parameter value space. Time limitations could not enable exploring all these interesting possibilities.

The specific yield of the top aquifer was varied and the resulting objective function generated for each run. No change in the value was realised, Figure 6.34. This was confirmed by the sensitivity of the storage coefficient that showed the least effect on the observations.

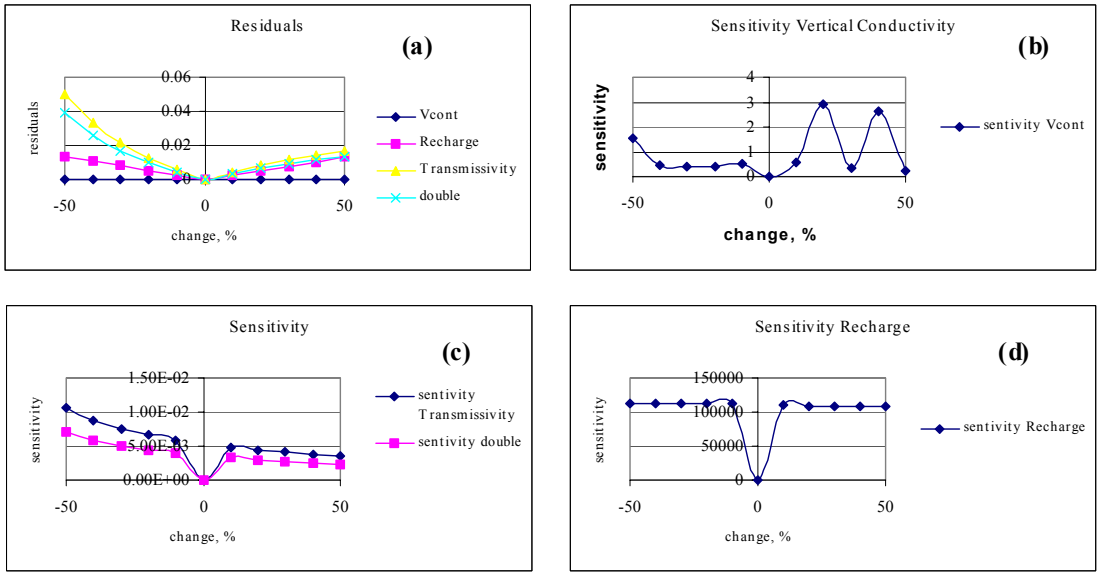

Figure 6.32: Steady State: a) sensitivity of vertical conductivity, b) residuals of all parameters, c) sensitivity of transmissivity and both recharge and transmissivity, d) sensitivity of recharge.

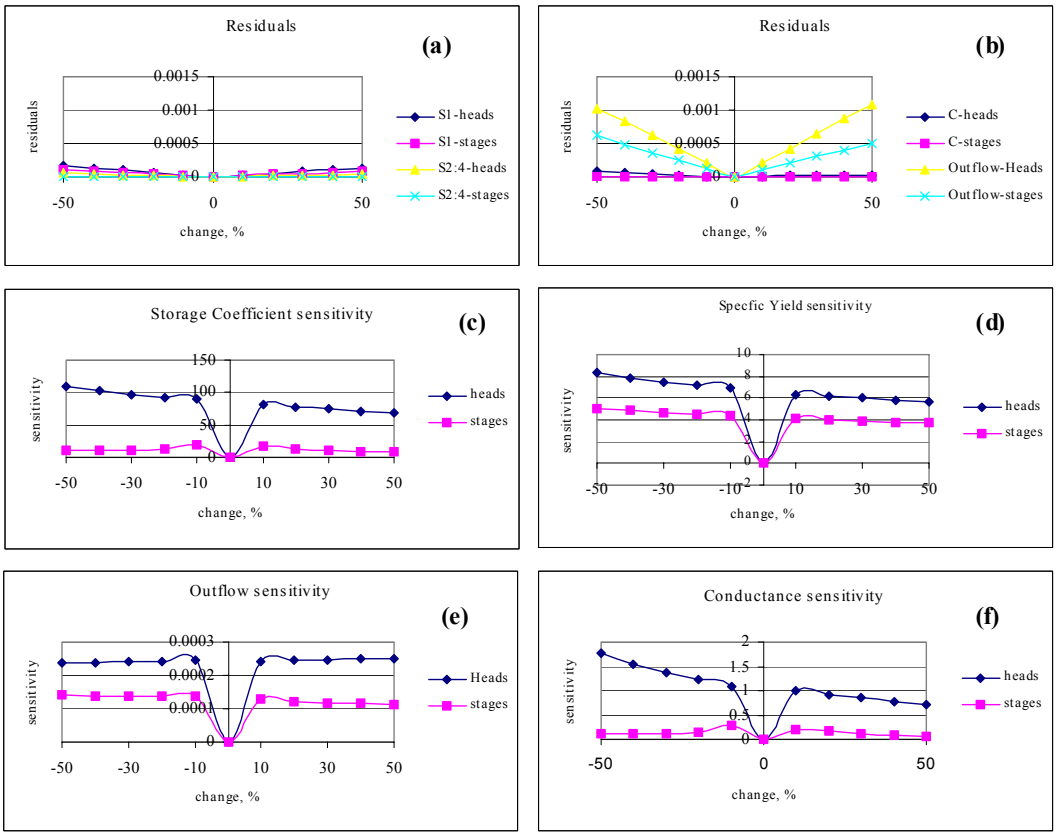

Figure 6.33: Single changes of heads and stages in Transient State: a) residuals of storage coefficients, b) residuals of conductance and outflow, c) sensitivity of storage coefficient, d) sensitivity of specific yield, e) sensitivity of outflow, f) sensitivity of lakebed

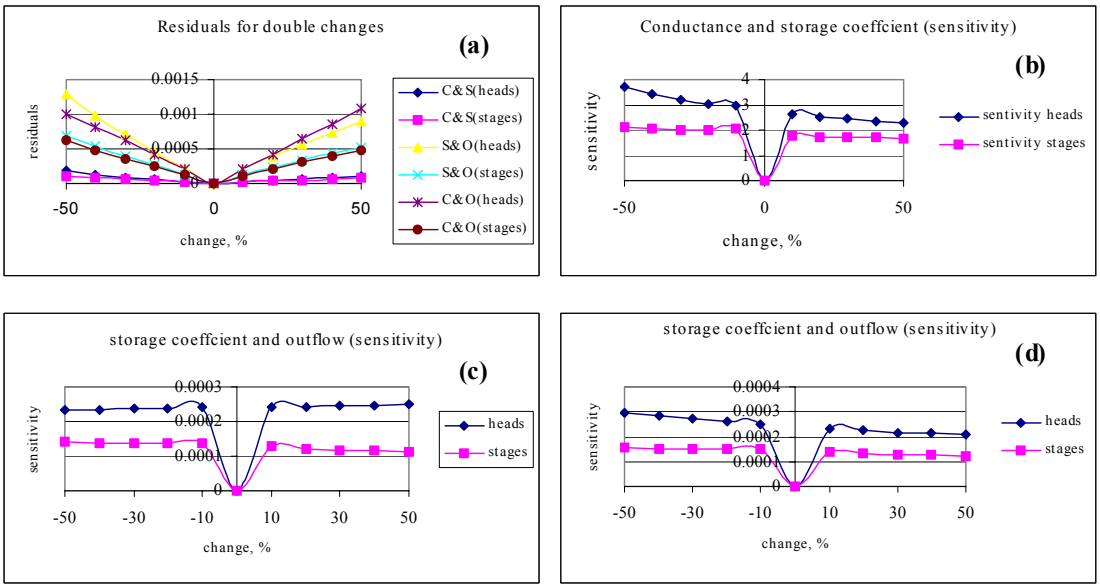

Figure 6.34: Double changes of heads and stages in Transient State: a) residuals of double changes, b) sensitivity of conductance and storage coefficient, c) sensitivity storage coefficient and outflow, d) sensitivity of storage coefficient and outflow.

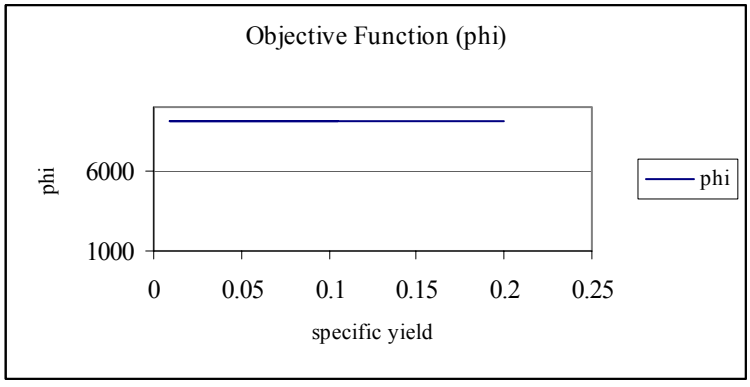

Figure 6.35: The sensitivity of the objective function on the storage coefficient.

6.6 Predictions

Predictive runs were carried out to ascertain the effects of extra pumping being imposed in the very active parts of the region, Figure 6.24. There were two scenarios that were considered: a) pumping a constant outflow from 1980 to 1997 while monitoring the lake and groundwater levels, b) stepping up the outflow in each subsequent run from 1980 to 1997 to estimate the average abstraction rates within this period.

6.6.1 Constant Outflow

Pumping was imposed using a value of 14 000 m^3/day (estimated by Kibona, MSc 2000) for the area to the north-east of the lake. An extra 4000 m^3/day was added to total 18 000 m3/day (Ramirez, MSc 1999) to cater for the areas to the south-east and south-west of the lake. The normal transient run was undertaken with the extra pumpage imposed after 1980 and thereafter maintained constant. It was presumed that the aquifer domain characteristics would not be altered by these new stresses. The calibrated transient run was used as the base reference lake levels for observing the effect of the pumping. The observed groundwater levels were compared to the final levels of the simulated ones.

Results: The lake levels shown in Figure 6.35, has a maximum reduction of 0.84m and rise of 0.18m, mean drop of 0.11m and a standard deviation of 0.178m. The deviations in the aquifer heads are plotted in Figure 6.37.

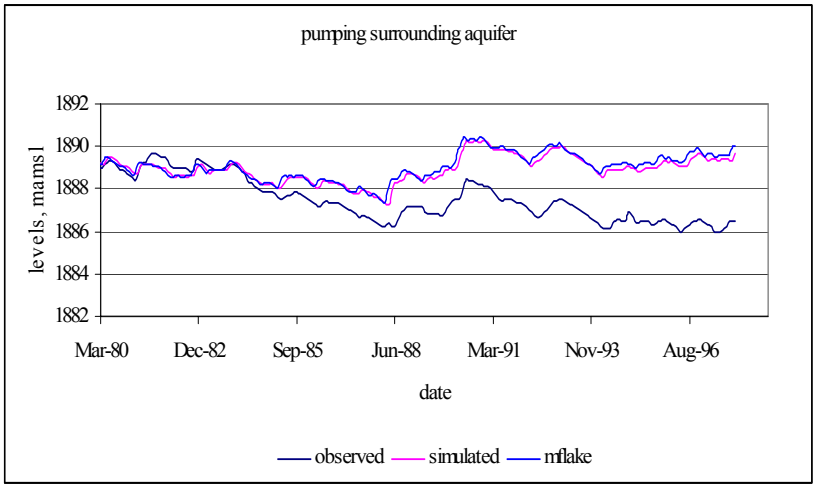

Figure 6.36: The effect of constant pumping after 1980 on the lake levels. Mflake, the calibrated run is used as reference base levels.

The maximum drawdown is observed in wells ITC035 and ITC026. The first one is close to the pumping well in the south-east and is most likely affected by this proximity. The latter is way down the basin and drops much lower than even the wells close to the pimping wells. This is due its being in a very transmissive zone that easily conducts the water. The influence of this characteristic is clearly more significant as also observed in the other wells, affecting them more than their proximity to the pumping wells.

6.6.2 Increasing Abstraction Rates

In this scenario, pumping was carried out at the same points used in the previous case, Figure 6.24. In each subsequent run from 1980 to 1997, the abstraction rates were increased and the resultant levels compared with the observed ones. In each of these simulations, the aquifer characteristics were assumed to be stable and the influence of the extra pumping was not propagated far enough to modify the boundary conditions.

The results are shown in Figure 6.39 (see Appendix 2 for the table of the results). Minimum deviations between the simulated and observed levels are noticed between abstraction rates of 18 000 and 25 000 m^3/day. This is fair enough within the limitations of estimate that is constrained by lack of adequate abstraction records to back this value, and the shortcomings of the model discretization and water level data. This concurs with the estimates quoted by the preceding studies.

The response of the lake levels to a similar input of stresses is shown in Figure 6.39. Increased pumping from 18 000 m3/day were exerted up to a maximum of 64 000 m3/day. The maximum observed fall in lake level is 2 m.

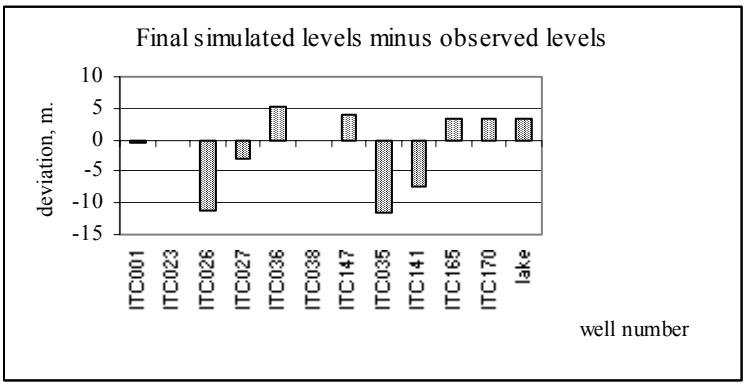

Figure 6.37: The deviations from the observed values of the final transient run with constant pumpage.

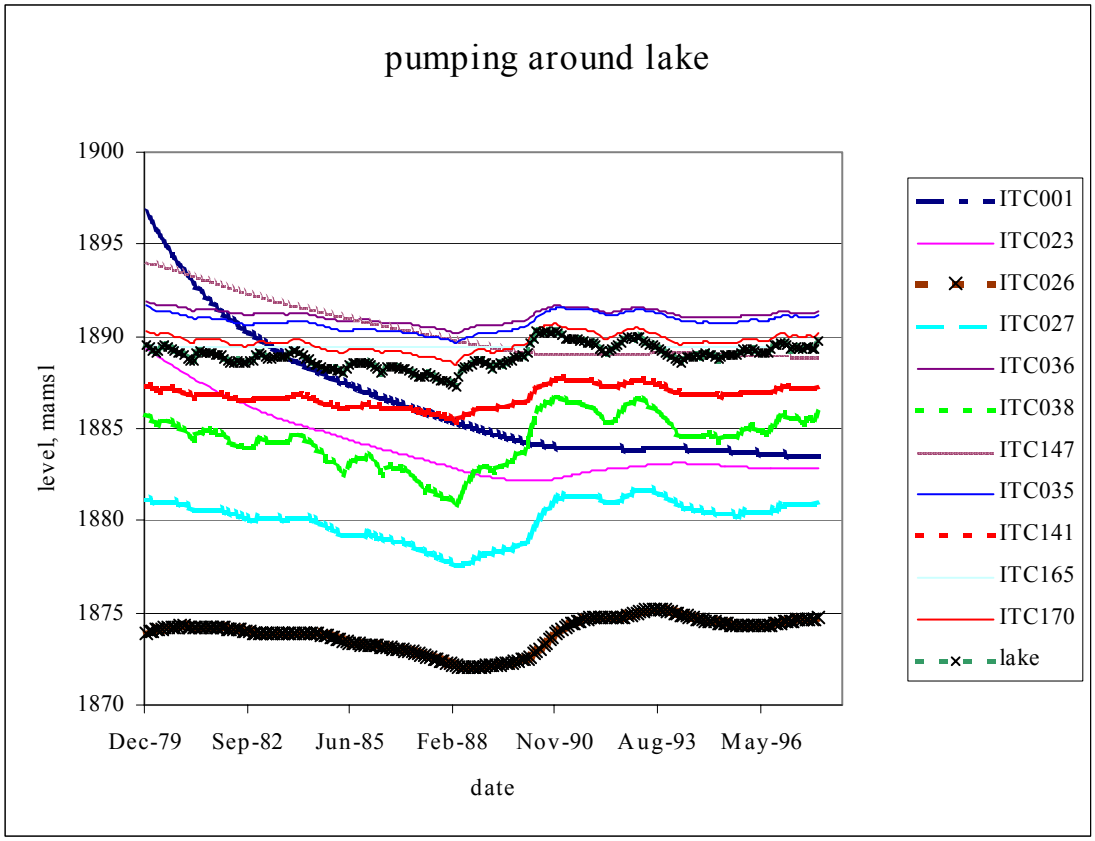

Figure 6.38: The effect of abstracting 18 000m3/day from the aquifer from 1980-1997.

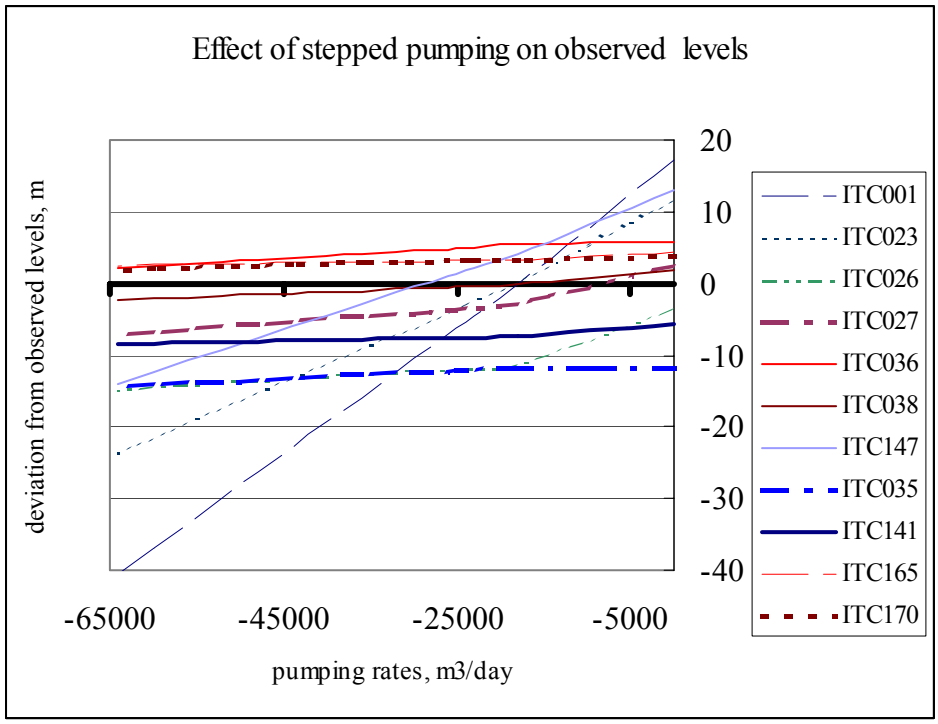

Figure 6.39: The drawdown curves for stepped-up abstractions from 1980 to 1997. Initial values are those simulated by the normal Mflake transient runs and the zero line corresponds to the observed groundwater levels.

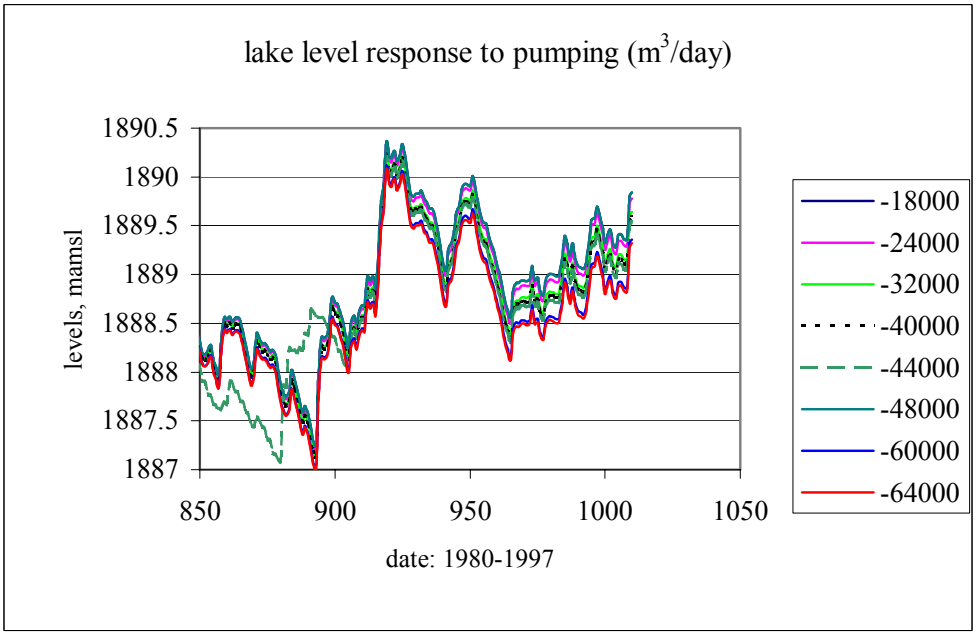

Figure 6.40: The response of the lake to increased pumping from 1980 – 1997.

Chapter 7

DISCUSSION AND CONCLUSIONS

7.1 Discussion

The results of the steady state numerical simulations have shown the existence of particular flow systems around the lake. The transient run indicates temporal differences of flow around the lake area. Such transient effects make it difficult to estimate average annual groundwater components of the lake budget. Previous modelling studies showed that the factors controlling groundwater flow near lakes include geometry and heterogeneity of the geologic framework, anisotropy and hydraulic conductivity of geologic units, lake depth, distribution of recharge, as reflected by the configuration of the water table. Of these factors, distribution of recharge is a dynamic phenomenon; therefore a combination of steady and transient states account for changes in the water table, which makes it more realistic for the geologic and climatic setting of the lake.

Winter (1983), in the study of variably saturated porous media indicates that groundwater recharge is variable in time and space, depending on the thickness of the unsaturated zone through which infiltrating water must move. The resulting complex, transient groundwater flow systems have significant impact on contiguous surface water. In very permeable media, small, local, closed groundwater flow systems can develop and dissipate within a few weeks to several months after major recharge. These have direct effect on contiguous surface water by alternately causing seepage to and seepage from the surface water. The transient nature of these flow systems indicates that reversals of direction of groundwater flow may be common.

Morgan, MSc 1998 found high electrical conductivity values in the waters to the southwest and southeast of the lake. Figure 6.21 indicates that there are water divides in these areas where water could be stagnating. It is probable that this could provide more insight on the rich chemistry of waters in these areas. The possibility of small, local groundwater flow systems forming and disappearing within the groundwater system could lead to very complex geochemical systems.

Lake Naivasha is considered to be a through-flow lake i.e. one that both receives and releases water to the groundwater flow (Born ET al., 1974, 1979).

If the water table is higher than the lake level on a seepage lake, groundwater will seep into the lake. There is a stagnation zone beneath the lake, indicating both local and regional groundwater flow. Upward seepage takes place through the lake bottom. As long as the stagnation zone is present, the lake will not lose water through the bottom. However, should an aquifer or a high-conductivity layer underlie the lake, the stagnation zone could be eliminated (Winter, 1976). Without the stagnation zone, the lake will lose water through part or the entire bottom, even with the presence of a water-table mound downslope.

7.2 Limitations

7.2.1 Data Limitations

Stream Flow Data: The stream flow data seems to be inconsistent during a number of periods. Data evaluation was made for the entries archived at the database in Nairobi that included the actual raw data. Save for short periods with missing data, all the inputs were continuous. There were no data entry anomalies or inconsistencies discernible. It is inferred that the problem is likely to be right from the source (gauge readers). The discrepancy in the data in the 1960s and 1980s were most likely due to wrong gauge readings. The fit of the temporal lake level fluctuations during the simulations of this study were quite suspect for the 1960s. The stream flow gauging stations need to be well monitored for better reliability of results, Plate 1, Appendix 4.

Rainfall/Evaporation Data: Better and more reliable estimates of these two climatic parameters is essential in understanding the dynamics of the system given the intensity of activities taking place at present. Data that has been used in this study requires to be married with what is presently available for a better reliability. Data loggers are already in place and need only be monitored to update the hydrologic database for a more comprehensive study.

7.2.2 Model and Result Limitations

Calibration methods: The automatic calibration methods that were used were instrumental in calibrating a model of this complexity. It was not possible to take enough time in manually trying to obtain a fit because it was simply too time consuming besides its not being able to quantify the degree of uncertainty in the final parameter selection.. Nonetheless, the limitations of the automatic calibration methods have had to be lived with:

Small random errors in observed/measured data result in larger errors in the computed derivatives, and these errors cause excessive spatial variation in the computed parameters. Sometimes, the computed values are even sensitive to the precision of the derivatives.

Subjective input data (groundwater recharge, non-metered groundwater pumping, etc.) is used to simulate model output. And, this output is compared with the observed data by the automatic calibration tools in order to compute model parameters.

Conceptualisation, numerical, truncation and modelling errors are always introduced during the development of a groundwater model.

There are many different ways available to formulate the objective function (calibration criterion) to represent the error of calibration and the computed calibration parameters are largely influenced by how the objective function is formed. As such, model parameters which are computed by these tools, are based on the spurious data rather than by the useful data.

The non-linear behaviour on the groundwater flow equation makes it difficult to discriminate between parameters (important parameters, unimportant parameters or irrelevant parameters) to which the objective function is relatively sensitive, as the sensitivity of the parameter changes with its value.

For all types of parameter estimation problems, but particularly for highly non-linear problems, the closer are user-supplied initial parameter values to optimal parameter values, the more chance does the process have of working. Guo ET al., 1998, indicated that probably the most important and practical way to control uncertainty in model calibration is to set a global calibration target that involves measured hydraulic heads, potentiometric surface, measured or estimate flux, water budget, aquifer test results, according to specific modelling objectives and data availability.

Lake and Aquifer Parameters: The uncertainty in the lake and aquifer parameters is considered to be a major factor in the discrepancies of the results. This could have been as a result of inadequate conceptualisation of the hydrogeologic system and poor estimation of hydrogeologic parameters and hydrological stresses. A consistent and manageable monitoring strategy is necessary to properly estimate these characteristics.

Numerical Codes: Convergence problems were the most difficult problem to overcome in the course of the runs. Most often than not, the runs failed because of its sensitivity to parameter values that were simply unacceptable. The steady state run was most especially cumbersome to calibrate and used up most of the modelling time. Even then it was not possible to adequately fit the outlying areas. It is essential to have more flexibility in the numerical codes especially the Lake Package.

Conceptual Framework: It was expected at the outset of the exercise to test and use the steady state model of Ramirez, MSc 1999. However, this was not possible due to differences in the modalities of conceptual model set up, numerical codes, and a new understanding of the dynamics of the system. Thus the study approach had to be redefined to set up a new conceptual model. This contributed to limitations in time that did not enable the refining and exploring of a number of scenarios with the results.

Results: The results obtained are subject to the accuracy of the DTM that can still be better defined. The spatial and temporal distribution of the parameter estimates and set up of the conceptual model can still be improved. The degree of uncertainty of the predictive simulations can be reduced subject to the availability of more intensive observation data. In general, there is not as yet sufficient certainty in the model calibration and predictive simulations to use the modelling results to make management decisions. However, the results provide more insight into the interactions within the system than has been perceived so far. From this point onwards lots of interesting possibilities can be explored to make the model more reliable.

7.3 Conclusions

The accuracy of the digital terrain model is important to consider so as to safeguard the integrity of the ensuring hydrologic model and its applications. Although overgeneralization poses a risk to the accuracy of hydrologic models, data with too many nodes often need to be generalised to reduce their computational (processing) time. A trade-off has to be made between accuracy and the required resolution, depending on the nature of the study and system used.

Optimisation of the parameters show a low degree of uncertainty in the estimates of the storage coefficient and lakebed conductance compared to the outflow. Calibrating

an integrated model requires a more expanded hydrologic approach than traditionally used for calibrating either a surface water or a groundwater model, Davis, 1998. The dynamic interaction of surface water and groundwater regimes requires a balanced, or integrated, approach to calibrating the model. Simplifying assumptions can no longer be made about the "other" regime, thus minimising the number of calibration parameters. Parameters in both regimes must be adjusted in unison, taking into account potential interactions on water levels, flows and water budgets. The benefit of this integrated approach is an increased level of confidence that can be placed on the long-term calibration of the integrated model.

The Mflake model performs better than the Spreadsheet model in terms of its ability to describe the temporal and spatial fluctuations in groundwater seepage. This has a bearing on the long-term average monthly net seepage from the lake to the groundwater. The two models concur in the estimates of long-term lake water balance.

The long-term water balance shows that the steady state components are close to the long-term average transient values. The steady state and average transient levels and storage volumes are 1888.4 and 1888.2 mamsl, and 7.1 and 6.9 mcm/mth, respectively. It is possible that the system had reached a dynamic cyclic steady state prior to the onset of the present activities. Groundwater outflow from the basin to the north, (Gilgil and Eburru area) and south (Olkaria and Longonot area) amount to 63% and 37%, respectively.

The temporal variations in groundwater seepage from the lake are important. There is a consistent net seepage of water from the lake, a long-term estimate at 4.76 mcm/mth (Spreadsheet model estimates 4.54 mcm/mth after modification). The steady state groundwater seepage from the lake amounts to 4.48 mcm/mth and seepage into the lake is about 0.22 mcm/mth.

Temporal and spatial variations in groundwater-lake interactions, vertical flow and storage abound around the lake. The extent of the zone of influence of the lake varies with the direction. The northern and western parts of the lake show the highest fluctuations in lake-groundwater flow interactions. The response of the groundwater levels to selected periods of lake level rise, fall and stability shows mimicry (Behar, MSc 1999 findings were similar).

Estimates of abstraction from the basin amounted to between 18 000 and 25 000 m3/day.

The response from the calibration parameters in the sensitivity analyses show that the aquifer heads respond more to the parameter changes than the lake stages. The changes in transmissivity and both recharge and transmissivity provide the most response while the vertical conductivity is the least responsive. The outflow terms provide the most response while the storage coefficient is the least, lakebed conductance being intermediate.

A combined use of measurements of groundwater heads and lake levels from a monitoring network and estimates from a groundwater-lake interaction flow model is

a cost-effective method for providing adequate information on head/stage changes, respectively.

It should be noted that the above simulations of groundwater and lake interaction, cannot be expected to be valid without reliable information of the hydraulic conductivity and thickness of lakebed sediments. Nevertheless, the lake package has been instrumental in providing a more realistic insight into the long-term interaction of the lake and groundwater for this kind of system affected by transience.

7.4 Recommendations

A comprehensive database linking together all previous works done in the region by different divisions and institutes is long overdue. It is essential that this be taken up in the next study so as to harmonise and make more efficient subsequent data searches.

The use of remote sensing to accurately measure lake and river levels with frequent repeat cycles should be vitalised in the not so distant future. Stuttard Et al. (1994) used data from the ERS-1 radar altimeter to estimate levels of Lake Nakuru, Kenya, for April and May 1993. Despite the results obtained, they concluded that at the moment, the application of radar altimetry for routine lake level monitoring of a specific lake is not appropriate on the grounds of cost, complexity and accuracy.

An understanding of the flow regimes is instrumental in developing a water management strategy for the basin. There is need to harness the water flowing out of the basin. Water harvesting and retention techniques could then be utilised to tap these outflow areas. This also goes a long way in better appreciating the flow paths and patterns of regional geochemical characteristics.

The long-term research objective is to conjunctively use isotopic and geochemical techniques, well monitoring networks and remote sensing techniques with numerical flow modelling to adequately describe the spatial and temporal variations in the flow paths and patterns.

The short-term research goal as a follow-up of the present study is to make estimates of spatial variations in recharge. An attempt should also be made to calibrate the abstraction rates so as to fit the aquifer heads to the levels they are at now. The intensive logger data (well levels, stream flow) and other climatic variables (rainfall and evaporation) that has been collected since 1997, should be updated and included to more accurately fit the data for the present period. The stream gauging data and rating curves have to be re-evaluated and improved (echoing Mmbui, MSc 1999 who discussed the poor correlation between the River Gilgil and Karati data). Refinement of the model domain can be done to more intensively monitor the lake-groundwater interactions around the lake vicinity.

The still suspect parameters recharge (spatial and temporal), storage coefficient/specific yield and transmissivity have to be better studied to have a more realistic estimate (echoing recommendations of previous workers).

The groundwater monitoring sites need to be carefully located to define accurately water table configuration, groundwater recharge, direction of seepage through the beds of surface water bodies (rivers and lakes), related to changing directions of groundwater flow.

References

Abiya I. O., 1996. Towards sustainable utilization of Lake Naivasha, Kenya. Paper Presented at the sixth International Conference on the Conservation and management of Lakes, Kasumigaura's 1995. Lakes and Reservoirs: Research and Management 1996.

Anderson, M.P., and W.W. Woessner, 1992. Applied Groundwater modeling; Simulation of flow and Advective Transport. Academic Press, San Diego.

Behar, H. A., 1999; Surface Water- Groundwater Interaction, Lake Naivasha, Kenya, MSc Thesis, ITC. Enschede, The Netherlands.

Cheng, X. and Anderson, M. P.; Simulating the influence of lake position on groundwater fluxes; Water Resources Research, Vol. 30, No. 7, pp 2041-2049, July 1994.

Chiang W. and Kinzelbach W. 1996; Processing Modflow (for Windows). A simulation system for Modelling Groundwater Flow and Pollution.

Clarke A.C.G., D. Allen, G. Darling. 1990. Geological, Volcanological and Hydrogeological Controls on the Occurrence of the Geothermal Activity in the Area Sorrounding Lake Naivasha, Kenya. Ministry of Energy, Republic of Kenya.

Domenico, P. A., and Schwartz, F. W.1990; Physical and Chemical Hydrogeology (Second Edition); John Wiley & Sons, Inc., NewYork.

Fetter, C.W., 1994. Applied Hydrogeology. Prentice Hall, Upper Saddle River, New Jersey.

Freeze, R. A., and J.A. Cherry. 1979. Groundwater. Prentice Hall, Englewood Cliffs, New Jersey.

Graham, A., 1998. Groundwater Recharge Estimation of the Malewa Catchment, Naivasha, Kenya. M.Sc. Thesis, ITC, Enschede, The Netherlands.

Groundwater Survey (Kenya) LTD. 1998. Borehole Site Investigations Naibor Ajijik, Report No. 98/547, Nairobi.

ITC, Water Resources Surveys. 1996. Water Resources Assessment Project Phase v, Mission Report, (WRAP). Water Resources modelling of the Rift valley lake Basins and Laikipia (Groundwater Component).

ITC 1997. The Integrated Land and Water Information System 2.1. User's Guide Manual. ITC, Enschede, The Netherlands.

Lake Naivasha Riparian owners Association. 1993. A Three Phase Environmental Impact Study of the Recent Developments Around Lake Naivasha. Phase I, Executive Summary. John Goldson Associates, Nairobi, Kenya.

Lake Naivasha Management Plan, Lake Naivasha Riparian Owners Association, 1996.

Lake Naivasha Riparian Owners Association, 1993; A Three Phase Environmental Impact Study of Recent Development around Lake Naivasha – Phase I.

Anderson M. P. and Cheng, X.; Long- and short term transience in a groundwater/lake system in Wisconsin, USA; 1993, J. Hydrol., 145: 1-18; Elsevier Science Publishers B. V.

Meijerink, A.M.J., de Brouwer, H.A.M., Mannaerts,C.M. and Valenzuela,C.R. 1994. Introduction to the use of Information Systems for Practical Hydrology. ITC Publication Number 23, ITC, Enschede, The Netherlands.

Mmbui, S. G., 1999; Study of Long-term Waterbalance of Lake Naivasha, Kenya, MSc Thesis, ITC, Enschede, The Netherlands.

MODFLOW ’98 Proceedings, Volumes I and II; Golden Colorado, October 4-8, 1998; Edited by Poeter, E., Zheng, C., and Hill, M.; Golden Colorado, Colorado School of Mines.

Morgan, N. E., 1998; Groundwater Chemistry and Quality Assessment of the Lake Naivasha Area, Kenya, MSc Thesis, ITC, Enschede, The Netherlands.

Ojiambo, B. S., 1992; Hydrogeologic, Hydrochemical and Stable Isotopic Study of Possible Interactions Between Lake Naivasha, Shallow Subsurface and Olkaria Geotherma.

Ojiambo, B. S., 1996; Characterization of Subsurface Outflow from a closed-basin freshwater tropical lake, Rift Valley, Kenya.

Olsthoorn, T. N.; The Power of the Electronic Worksheet: Modeling without special programs; Groundwater, Vol. 23, No. 3; May-June 1985.

PEST; Model Independent Parameter Estimation, 1998; User’s Manual; Watermark Computing, Australia.

Ramirez, 1999; Groundwater Flow Modeling of Lake Naivasha, Kenya, MSc Thesis, ITC, Enschede, The Netherlands.

Salah, A. 1999. Productive and Sustainable Use of Water Among Competitive Sectors, A Study in the Naivasha Catchments, Kenya. M.Sc. Thesis, International Institute for Aerospace Survey and Earth Sciences (ITC), Enschede, The Netherlands.

Stuttard, M.J., J. Hayball, G. Narcos, M. Suppo, R. Catani, L.Isavwa, J. Baraza and A. Oroda. 1995. Monitoring Lakes in Kenya: An Environmental Analysis Methodology for Developing Countries, Final Report to European Commission, Contract

No. TS3*-CT92-0016.

Thompson, A.O. and R. G. Dodson. 1963. Geology of the Naivasha Area. Geological Survey of Kenya, Report. No. 55.

Ase, L. E., Sernbo, K. and Per, S., 1986; Studies of Lake Naivasha, Kenya and its Drainage Area.

Trottman, D. K., 1999; Modeling Groundwater Storage Change in response to Fluctuations of Lake Naivasha, Kenya, MSc Thesis, ITC.

Viak Ltd, 1975; Naivasha Water Supply Project, Ministry of Agriculture, Republic of Kenya.

Wiberg,I. 1976. Naivasha Water Supply Project, Groundwater Investigation, VIAK EA Ltd., Consulting Engineering and Mapping Services.

Winter, T. C.; The Interaction of Lakes With Variably Saturated Porous Media; Water Resources Research, Vol. 19, No. 5, pages 1203-1218, October 1983.

Appendices

Appendix 1: Files and Formats

LAK2 Input File Instructions

INDENTIFICATION LINE

/*LAK2.2
format as exactly shown

SIMULATION DATA

NLAKES ILKCBC IECHO NSUBSTEPS
Format: 5I10
NAME ISIMMODE STSTAGE ITERLAKE CONVCRIT (one line for each lake)
Format: A10, I10, F10.0, I10, F10.0

PHYSICAL DATA
(one set for each lake)

NODES NSTRIN NSTROUT STAGEMX ICONDP
Format: 3I10, F10.0, I10

ISEGIN (one line for each inflow stream)
Format: I10
ISEGOUT NRATEQ |one set for each
Format: 2I10 | outflow
CUTOFF CONST ELEV EXPNT (one line for each rating equation) | stream
Format: 4F10.0 | (sorted by CUTOFF; descending) |

ILAY IROW ICOL TOP BOT AREA COND (one line for each lake node)
Format: 3I10, 4F10.0

STRESS PERIOD DATA
(one set for each stress period)

ITMP
Format: I10

PRECIP EVAP RUNOFF DRYCH IOUTOP STAGE (one line for each lake if ITMP >=0)
Format: 4F10.0, I10, F10.0

VARIABLE DESCRIPTIONS

NLAKES: Number of lakes
ILKCBC: >0 Cell-by-cell unit number, <=0 Do not save cell-by-cell
ILKOUT: >0 Stage/Budget unit number, <=0 Do not write stage /budget records
IECHO: >0 No input echoing, 0 Summary of input, >0 Full echoing of input
NSUBSTEPS: Number of sub-time-steps for simulating lakes in transient mode

NAME: Name (ID) of lake (10 characters)
ISIMMODE: Simulation Mode:
0 Fixed Stage, 1 Interpolated stage, 2 Steady-state, 3 Transient

STSTAGE Starting Stage (not required for ISIMMODE = 0)
ITERLAKE: Max interations for stage solver (ISIMMODE = 2 or 3)
CONVCRIT: Stage solver termination criteria (change in stage in 1 interation, ISIMMODE = 2 or 3)

NODES: Number of lake nodes
NSTRIN: Number of inflow streams
NSTROUT: Number of outflow streams
STAGEMX: maximum lake stage
ICONDOP: <=0 Hydraulic conductivity input, >0 Conductance input

USEGIN: Inflow stream segment (from Stream Routing Package)
ISEGOUT: Outflow stream segment (from Stream Routing Package)
NRATEQ: Number of equations used to define stage-discharge relationship

CUTOFF: Lower stage limit of rating equation
CONST: Rating equation constant
ELEV: Rating equation reference (outfall) equation
EXPNT: Rating equation exponent

Outflow = CONST * (STAGE – ELEV) ^ EXPNT (Above CUTOFF)

ILAY: Lake node model layer (0 for top active layer)
IROW: Lake node model row
ICOL: Lake node model column
TOP: Lakebed top elevation
BOT: Lakebed bottom elevation
AREA: Lake node area
COND: Lakebed hydraulic conductivity or conductance (see ICONDOP above)

ITMP: <0 Use information from last stress period, >=0 read new information
PRECIP: Total-area-dependent flow rate (L/T). The Lake Package budget routine multiplies PRECIP by the total area of the lake (wetted cells + shore cells) and adds the resulting flux to the lake's volumetric budget. Specify a positive number for lake inflow or a negative number for lake outflow
EVAP: Wetted-area-dependent flow rate (L/T). The Lake Package budget routine multiplies EVAP by the wetted area of the lake (excluding shore cells) and adds the resulting flux to the lake's volumetric budget. Specify a positive number for the lake inflow or a negative number for lake outflow
RUNOFF: Fixed lake inflow (L^3/T, positive = inflow to lake, e.g. runoff)
DRYRCH: Recharge rate applied to groundwater beneath dry lake cells (L/T)
IOUTOP: Output option, constructed as follows:
0 = no output
+1 = print cell-by-cell flows in main output file
+2 = print lake budget information in main output file
+4 = write stage to stage/budget output file
+8 = write flows (& stage) to stage/budget output file (e.g. to print lake budget in main output file, write stage record to stage/budget output file)
STAGE: If ISIMMODE = 0, lake stage for the stress period
If ISIMMODE = 1, final lake stage for the stress period.
Ignored for ISIMMODE = 2 or 3

The Structure of the PEST Control File

```
pcf
* control data
RSTFLE
NPAR NOBS NPARGP NPRIOR NOBSGP
NTPLFLE NINSFLE PRECIS DPOINT
RLAMBDA1 RLAMFAC PHIRATSUF PHIREDLAM NUMLAM
RELPARMAX FACPARMAX FACORIG
PHIREDSWH
```

```
NOPTMAX PHIREDSTP NPHISTP NPHINORED RELPARSTP NRELPAR
ICOV ICOR IEIG
* parameter groups
PARGPNME INCTYP DERINC DERINCLB FORCEN DERINCMUL DERMTHD
(one such line for each of the NPARGP parameter groups)
* parameter data
PARNME PARTRANS PARCHGLIM PARVAL1 PARLBND PARUBND PARGP SCALE OFFSET
(one such line for each of the NPAR parameters)
PARNME PARTIED
(one such line for each tied parameter)
* observation groups
OBGNME
(one such line for each observation group)
* observation data
OBSNME OBSVAL WEIGHT OBGNME
(one such line for each of the NOBS observations)
* model command line
write the command which PEST must use to run the model
* model input/output
TEMPFLE INFLE
(one such line for each model input file containing parameters)
INSFLE OUTFLE
(one such line for each model output file containing observations)
* prior information
PILBL PIFAC * PARNME + PIFAC * log(PARNME) ... = PIVAL WEIGHT
(one such line for each of the NPRIOR articles of prior information)
```

The Structure of the SENSAN Control File

```
scf
* control data
SCREENDISP
NPAR NOBS
NTPLFLE NINSFLE PRECIS DPOINT
* sensan files
VARFLE
ABSFLE
RELFLE
SENSFLE
* model command line
write the command which SENSAN must use to run the model
* model input/output
TEMPFLE INFLE
(one such line for NTPLFLE template files)
INSFLE OUTFLE
(one such line for NINSFLE instruction files
```

A Sensan Control File For Evaluating The Objective Function

```
scf*
control data
verbose
6 1
1 1 single point
* sensan files
parvar.dat
out1.txt
out2.txt
out3.txt
* model command line
spest ves4
* model input/output
pst.tpl ves4.pst
  rec.ins  ves4.rec
```

Appendix 2: Hydrologic Characteristics Data Tables

The Transmissivity and Hydraulic Conductivity of the wells

Borehole No.	Source	X co-ordinates	Y co-ordinates	Transmissivity
C1482	McCann (1974)	214316	9917024	1330
BH	Ramirez (MSc 1999)	207698	9925728	220
BH 1	VIAK (1975)	212921	9923339	233.28
BH 3	VIAK	212995	9923310	224.64
BH 4	VIAK	212936	9923318	198.72
BH 9	Ramirez	211434	9921380	670
BH A	Ramirez	213712	9925550	1020
BH C	Kibona (MSc 2000)	213459	9924929	1150 (462)**
C1063	McCann	197600	9929926	38.9
C2071	Ojiambo (1992)	202800	9909500	155
C2534	Ojiambo	209050	9910000	166
C2557	Ojiambo	195300	9912500	696
C2638	Ojiambo	210050	9911100	166
C2657	McCann	193901	9913327	307
C2660	Ojiambo	196950	9911950	166
C2701	Ojiambo	195760	9909300	261
C2997	Ojiambo	209900	9899950	21
C3924	Ojiambo	205100	9908100	377
C4397	Ojiambo	204900	9908300	1055
C4420	Ojiambo	204800	9908250	671
C4500	Ojiambo	198300	9914500	309
C4501	Ojiambo	196100	9913900	267
C4989	Ojiambo	208800	9909260	1382
C575	Ojiambo	203050	9905900	6019
C579	Ojiambo	201332	9911484	292
C630	Ojiambo	197700	9906200	127
C630D	Ojiambo	197700	9906200	3
KCC	Ramirez	209037	9925717	75
LB	Ramirez	214151	9920906	1000
UBH	Ojiambo	203950	9909450	10660
well5	Behar (MSc 1999)	214151	9918303	0.014947*
well7	Behar	214340	9918801	0.083722*
KMT1	Kibona	211900	9927739	0.26*
KMT2	Kibona	212717	9928025	0.25*
KMT3	Kibona	211489	9927104	0.38*

* :indicates the wells for which hydraulic conductivities were measured in m/d.
The rest of wells have had the transmissivities determined in m^2/d.
** :Hantush method and Cooper & Jacob, respectively.

Observed Lake level data (mamsl) over 66 years (whole simulation period)

Jan-32	1890.98	Aug-36	1888.69	Mar-41	1886.88	Oct-45	1884.84	May-50	1884.69
Feb-32	1890.98	Sep-36	1888.65	Apr-41	1886.83	Nov-45	1884.72	Jun-50	1884.82
Mar-32	1890.98	Oct-36	1888.6	May-41	1886.82	Dec-45	1884.57	Jul-50	1884.95
Apr-32	1890.98	Nov-36	1888.51	Jun-41	1886.79	Jan-46	1884.39	Aug-50	1884.93
May-32	1890.98	Dec-36	1888.42	Jul-41	1886.75	Feb-46	1884.26	Sep-50	1884.85
Jun-32	1890.89	Jan-37	1888.31	Aug-41	1886.71	Mar-46	1884.43	Oct-50	1884.72

Jul-32	1890.86	Feb-37	1888.15	Sep-41	1886.66	Apr-46	1884.44	Nov-50	1884.62
Aug-32	1890.83	Mar-37	1888.31	Oct-41	1886.6	May-46	1884.46	Dec-50	1884.5
Sep-32	1890.86	Apr-37	1888.79	Nov-41	1886.55	Jun-46	1884.62	Jan-51	1884.56
Oct-32	1890.83	May-37	1889.15	Dec-41	1886.5	Jul-46	1884.86	Feb-51	1885.05
Nov-32	1890.77	Jun-37	1889.55	Jan-42	1886.54	Aug-46	1884.89	Mar-51	1885.28
Dec-32	1890.67	Jul-37	1889.95	Feb-42	1886.78	Sep-46	1884.91	Apr-51	1885.47
Jan-33	1890.55	Aug-37	1889.91	Mar-42	1887.03	Oct-46	1884.85	May-51	1885.51
Feb-33	1890.49	Sep-37	1889.78	Apr-42	1887.26	Nov-46	1884.79	Jun-51	1885.66
Mar-33	1890.37	Oct-37	1889.8	May-42	1887.16	Dec-46	1884.78	Jul-51	1885.82
Apr-33	1890.22	Nov-37	1889.81	Jun-42	1887.2	Jan-47	1884.97	Aug-51	1885.88
May-33	1890.16	Dec-37	1889.7	Jul-42	1887.07	Feb-47	1885.58	Sep-51	1885.99
Jun-33	1890.06	Jan-38	1889.57	Aug-42	1886.87	Mar-47	1886.29	Oct-51	1886.15
Jul-33	1890.06	Feb-38	1889.46	Sep-42	1886.7	Apr-47	1886.48	Nov-51	1886.19
Aug-33	1890.06	Mar-38	1889.34	Oct-42	1886.63	May-47	1886.58	Dec-51	1886.09
Sep-33	1890.06	Apr-38	1889.24	Nov-42	1886.56	Jun-47	1886.66	Jan-52	1885.98
Oct-33	1890.06	May-38	1889.14	Dec-42	1886.47	Jul-47	1886.55	Feb-52	1885.85
Nov-33	1890.10	Jun-38	1889.04	Jan-43	1886.34	Aug-47	1886.48	Mar-52	1885.94
Dec-33	1890.10	Jul-38	1888.96	Feb-43	1886.24	Sep-47	1886.47	Apr-52	1886.01
Jan-34	1889.82	Aug-38	1888.92	Mar-43	1886.17	Oct-47	1886.37	May-52	1885.93
Feb-34	1889.59	Sep-38	1888.88	Apr-43	1886.09	Nov-47	1886.18	Jun-52	1885.87
Mar-34	1889.52	Oct-38	1888.82	May-43	1886.12	Dec-47	1886.11	Jul-52	1885.87
Apr-34	1889.44	Nov-38	1888.69	Jun-43	1886.15	Jan-48	1886.02	Aug-52	1885.86
May-34	1889.36	Dec-38	1888.55	Jul-43	1886.12	Feb-48	1885.85	Sep-52	1885.81
Jun-34	1889.29	Jan-39	1888.43	Aug-43	1886.05	Mar-48	1885.83	Oct-52	1885.71
Jul-34	1889.21	Feb-39	1888.35	Sep-43	1885.94	Apr-48	1885.81	Nov-52	1885.58
Aug-34	1889.13	Mar-39	1888.28	Oct-43	1885.82	May-48	1885.88	Dec-52	1885.4
Sep-34	1889.06	Apr-39	1888.15	Nov-43	1885.64	Jun-48	1885.99	Jan-53	1885.23
Oct-34	1888.98	May-39	1888.01	Dec-43	1885.53	Jul-48	1886.04	Feb-53	1885.14
Nov-34	1888.91	Jun-39	1887.92	Jan-44	1885.43	Aug-48	1885.92	Mar-53	1885.08
Dec-34	1888.84	Jul-39	1887.85	Feb-44	1885.35	Sep-48	1885.85	Apr-53	1885.01
Jan-35	1888.78	Aug-39	1887.72	Mar-44	1885.3	Oct-48	1885.76	May-53	1884.99
Feb-35	1888.72	Sep-39	1887.6	Apr-44	1885.25	Nov-48	1885.63	Jun-53	1884.94
Mar-35	1888.65	Oct-39	1887.45	May-44	1885.2	Dec-48	1885.5	Jul-53	1884.84
Apr-35	1888.57	Nov-39	1887.25	Jun-44	1885.2	Jan-49	1885.39	Aug-53	1884.74
May-35	1888.5	Dec-39	1887.12	Jul-44	1885.19	Feb-49	1885.31	Sep-53	1884.7
Jun-35	1888.44	Jan-40	1887.06	Aug-44	1885.18	Mar-49	1885.27	Oct-53	1884.69
Jul-35	1888.38	Feb-40	1887.02	Sep-44	1885.02	Apr-49	1885.19	Nov-53	1884.58
Aug-35	1888.32	Mar-40	1887.26	Oct-44	1884.81	May-49	1885.19	Dec-53	1884.42
Sep-35	1888.28	Apr-40	1887.47	Nov-44	1884.7	Jun-49	1885.31	Jan-54	1884.25
Oct-35	1888.25	May-40	1887.38	Dec-44	1884.62	Jul-49	1885.34	Feb-54	1884.25
Nov-35	1888.21	Jun-40	1887.25	Jan-45	1884.59	Aug-49	1885.25	Mar-54	1884.5
Dec-35	1888.19	Jul-40	1887.14	Feb-45	1884.61	Sep-49	1885.16	Apr-54	1884.83
Jan-36	1888.18	Aug-40	1886.99	Mar-45	1884.61	Oct-49	1885.1	May-54	1885.19
Feb-36	1888.18	Sep-40	1886.79	Apr-45	1884.63	Nov-49	1884.94	Jun-54	1885.32
Mar-36	1888.27	Oct-40	1886.69	May-45	1884.83	Dec-49	1884.74	Jul-54	1885.42
Apr-36	1888.67	Nov-40	1886.56	Jun-45	1885.07	Jan-50	1884.79	Aug-54	1885.48
May-36	1888.75	Dec-40	1886.43	Jul-45	1885.03	Feb-50	1884.77	Sep-54	1885.43
Jun-36	1888.74	Jan-41	1886.64	Aug-45	1884.97	Mar-50	1884.68	Oct-54	1885.37
Jul-36	1888.73	Feb-41	1886.89	Sep-45	1884.9	Apr-50	1884.64	Nov-54	1885.27
Dec-54	1885.17	Jul-59	1886.73	Feb-64	1889.52	Sep-68	1889.81	Apr-73	1888.03
Jan-55	1885.12	Aug-59	1886.73	Mar-64	1889.39	Oct-68	1889.79	May-73	1887.95
Feb-55	1885.01	Sep-59	1886.74	Apr-64	1889.33	Nov-68	1889.75	Jun-73	1887.93
Mar-55	1884.94	Oct-59	1886.72	May-64	1889.52	Dec-68	1889.75	Jul-73	1887.85
Apr-55	1884.9	Nov-59	1886.66	Jun-64	1889.62	Jan-69	1889.69	Aug-73	1887.80
May-55	1884.82	Dec-59	1886.63	Jul-64	1889.61	Feb-69	1889.61	Sep-73	1887.80

Jun-55	1884.75	Jan-60	1886.55	Aug-64	1889.61	Mar-69	1889.56	Oct-73	1887.77
Jul-55	1884.92	Feb-60	1886.25	Sep-64	1889.72	Apr-69	1889.48	Nov-73	1887.73
Aug-55	1885.12	Mar-60	1886.05	Oct-64	1889.88	May-69	1889.50	Dec-73	1887.63
Sep-55	1885.23	Apr-60	1885.99	Nov-64	1890.07	Jun-69	1889.45	Jan-74	1887.50
Oct-55	1885.18	May-60	1885.92	Dec-64	1890.22	Jul-69	1889.32	Feb-74	1887.33
Nov-55	1885.21	Jun-60	1885.84	Jan-65	1890.16	Aug-69	1889.12	Mar-74	1887.21
Dec-55	1885.29	Jul-60	1885.92	Feb-65	1890.08	Sep-69	1889.11	Apr-74	1887.25
Jan-56	1885.31	Aug-60	1885.87	Mar-65	1890.01	Oct-69	1889.01	May-74	1887.33
Feb-56	1885.27	Sep-60	1885.91	Apr-65	1889.91	Nov-69	1888.91	Jun-74	1887.32
Mar-56	1885.28	Oct-60	1885.92	May-65	1889.77	Dec-69	1888.86	Jul-74	1887.47
Apr-56	1885.45	Nov-60	1885.95	Jun-65	1889.71	Jan-70	1888.79	Aug-74	1887.55
May-56	1885.53	Dec-60	1885.96	Jul-65	1889.76	Feb-70	1888.74	Sep-74	1887.72
Jun-56	1885.61	Jan-61	1885.85	Aug-65	1889.68	Mar-70	1888.63	Oct-74	1887.82
Jul-56	1885.82	Feb-61	1885.73	Sep-65	1889.6	Apr-70	1888.72	Nov-74	1887.83
Aug-56	1886.13	Mar-61	1885.6	Oct-65	1889.53	May-70	1888.90	Dec-74	1887.78
Sep-56	1886.24	Apr-61	1885.47	Nov-65	1889.44	Jun-70	1888.99	Jan-75	1887.62
Oct-56	1886.23	May-61	1885.38	Dec-65	1889.34	Jul-70	1889.03	Feb-75	1887.47
Nov-56	1886.13	Jun-61	1885.37	Jan-66	1889.24	Aug-70	1888.99	Mar-75	1887.34
Dec-56	1886.03	Jul-61	1885.29	Feb-66	1889.14	Sep-70	1889.07	Apr-75	1887.20
Jan-57	1885.92	Aug-61	1885.18	Mar-66	1889.04	Oct-70	1889.15	May-75	1886.99
Feb-57	1885.86	Sep-61	1885.15	Apr-66	1888.94	Nov-70	1889.12	Jun-75	1887.03
Mar-57	1885.95	Oct-61	1885.27	May-66	1888.86	Dec-70	1889.03	Jul-75	1887.08
Apr-57	1886.13	Nov-61	1885.86	Jun-66	1888.94	Jan-71	1888.89	Aug-75	1887.27
May-57	1886.37	Dec-61	1887.16	Jul-66	1888.96	Feb-71	1888.78	Sep-75	1887.66
Jun-57	1886.5	Jan-62	1887.82	Aug-66	1888.9	Mar-71	1888.61	Oct-75	1887.86
Jul-57	1886.63	Feb-62	1888.17	Sep-66	1888.82	Apr-71	1888.50	Nov-75	1887.89
Aug-57	1886.73	Mar-62	1888.05	Oct-66	1888.83	May-71	1888.50	Dec-75	1887.79
Sep-57	1886.68	Apr-62	1887.89	Nov-66	1888.9	Jun-71	1888.61	Jan-76	1887.64
Oct-57	1886.59	May-62	1887.84	Dec-66	1888.89	Jul-71	1888.72	Feb-76	1887.49
Nov-57	1886.51	Jun-62	1888.15	Jan-67	1888.92	Aug-71	1888.89	Mar-76	1887.32
Dec-57	1886.49	Jul-62	1888.17	Feb-67	1888.83	Sep-71	1889.23	Apr-76	1887.16
Jan-58	1886.47	Aug-62	1888.15	Mar-67	1888.7	Oct-71	1889.21	May-76	1887.06
Feb-58	1886.46	Sep-62	1888.21	Apr-67	1888.57	Nov-71	1889.21	Jun-76	1887.00
Mar-58	1886.45	Oct-62	1888.42	May-67	1888.43	Dec-71	1889.11	Jul-76	1886.93
Apr-58	1886.53	Nov-62	1888.59	Jun-67	1888.54	Jan-72	1889.04	Aug-76	1886.82
May-58	1886.73	Dec-62	1888.59	Jul-67	1888.75	Feb-72	1888.98	Sep-76	1887.06
Jun-58	1887.07	Jan-63	1888.52	Aug-67	1888.85	Mar-72	1888.90	Oct-76	1886.87
Jul-58	1887.33	Feb-63	1888.45	Sep-67	1888.92	Apr-72	1888.75	Nov-76	1886.60
Aug-58	1887.4	Mar-63	1888.4	Oct-67	1888.94	May-72	1888.66	Dec-76	1886.73
Sep-58	1887.39	Apr-63	1888.38	Nov-67	1888.92	Jun-72	1888.59	Jan-77	1886.50
Oct-58	1887.36	May-63	1888.59	Dec-67	1888.89	Jul-72	1888.57	Feb-77	1886.34
Nov-58	1887.28	Jun-63	1889	Jan-68	1888.87	Aug-72	1888.52	Mar-77	1886.37
Dec-58	1887.25	Jul-63	1889.36	Feb-68	1888.81	Sep-72	1888.51	Apr-77	1886.53
Jan-59	1887.14	Aug-63	1889.31	Mar-68	1888.719	Oct-72	1888.44	May-77	1887.41
Feb-59	1887.02	Sep-63	1889.19	Apr-68	1888.59	Nov-72	1888.50	Jun-77	1887.62
Mar-59	1886.95	Oct-63	1889.2	May-68	1889.75	Dec-72	1888.47	Jul-77	1887.81
Apr-59	1886.88	Nov-63	1889.12	Jun-68	1889.80	Jan-73	1888.38	Aug-77	1888.02
May-59	1886.86	Dec-63	1889.07	Jul-68	1889.82	Feb-73	1888.27	Sep-77	1888.06
Jun-59	1886.85	Jan-64	1889.43	Aug-68	1889.75	Mar-73	1888.16	Oct-77	1887.95
Nov-77	1888.03	Jun-82	1889.009	Jan-87	1887.194	Aug-91	1887.525	Mar-96	1886.3
Dec-77	1888.26	Jul-82	1888.949	Feb-87	1887.111	Sep-91	1887.478	Apr-96	1886.2
Jan-78	1888.31	Aug-82	1888.945	Mar-87	1887.027	Oct-91	1887.432	May-96	1886.07
Feb-78	1888.29	Sep-82	1888.891	Apr-87	1886.944	Nov-91	1887.385	Jun-96	1886
Mar-78	1888.45	Oct-82	1888.845	May-87	1886.808	Dec-91	1887.338	Jul-96	1886.1
Apr-78	1888.96	Nov-82	1888.89	Jun-87	1886.631	Jan-92	1887.283	Aug-96	1886.24

May-78	1889.28	Dec-82	1889.405	Jul-87	1886.7	Feb-92	1887.155	Sep-96	1886.3
Jun-78	1889.16	Jan-83	1889.346	Aug-87	1886.746	Mar-92	1887.027	Oct-96	1886.5
Jul-78	1889.15	Feb-83	1889.249	Sep-87	1886.659	Apr-92	1886.899	Nov-96	1886.5
Aug-78	1889.20	Mar-83	1889.177	Oct-87	1886.573	May-92	1886.771	Dec-96	1886.56
Sep-78	1889.25	Apr-83	1889.088	Nov-87	1886.486	Jun-92	1886.643	Jan-97	1886.5
Oct-78	1889.42	May-83	1889	Dec-87	1886.399	Jul-92	1886.77	Feb-97	1886.4
Nov-78	1889.47	Jun-83	1888.931	Jan-88	1886.313	Aug-92	1886.906	Mar-97	1886.3
Dec-78	1889.44	Jul-83	1888.916	Feb-88	1886.226	Sep-92	1887.043	Apr-97	1886.2
Jan-79	1889.36	Aug-83	1888.92	Mar-88	1886.22	Oct-92	1887.179	May-97	1886
Feb-79	1889.52	Sep-83	1888.973	Apr-88	1886.383	Nov-92	1887.316	Jun-97	1886
Mar-79	1889.51	Oct-83	1889.079	May-88	1886.232	Dec-92	1887.45	Jul-97	1886
Apr-79	1889.57	Nov-83	1889.191	Jun-88	1886.211	Jan-93	1887.559	Aug-97	1886.07
May-79	1889.64	Dec-83	1889.149	Jul-88	1886.501	Feb-93	1887.479	Sep-97	1886.25
Jun-79	1889.73	Jan-84	1889.086	Aug-88	1886.753	Mar-93	1887.399	Oct-97	1886.5
Jul-79	1889.79	Feb-84	1888.967	Sep-88	1886.968	Apr-93	1887.319	Nov-97	1886.5
Aug-79	1889.79	Mar-84	1888.791	Oct-88	1887.186	May-93	1887.239	Dec-97	1886.5
Sep-79	1889.73	Apr-84	1888.687	Nov-88	1887.179	Jun-93	1887.159		
Oct-79	1889.61	May-84	1888.371	Dec-88	1887.173	Jul-93	1887.079		
Nov-79	1889.55	Jun-84	1888.255	Jan-89	1887.167	Aug-93	1886.999		
Dec-79	1889.46	Jul-84	1888.14	Feb-89	1887.161	Sep-93	1886.919		
Jan-80	1889.32	Aug-84	1888.024	Mar-89	1887.154	Oct-93	1886.839		
Feb-80	1889.20	Sep-84	1887.909	Apr-89	1886.888	Nov-93	1886.759		
Mar-80	1889.09	Oct-84	1887.896	May-89	1886.865	Dec-93	1886.54		
Apr-80	1888.98	Nov-84	1887.882	Jun-89	1886.842	Jan-94	1886.5		
May-80	1889.13	Dec-84	1887.869	Jul-89	1886.819	Feb-94	1886.4		
Jun-80	1889.28	Jan-85	1887.855	Aug-89	1886.796	Mar-94	1886.23		
Jul-80	1889.33	Feb-85	1887.807	Sep-89	1886.773	Apr-94	1886.1		
Aug-80	1889.20	Mar-85	1887.568	Oct-89	1886.75	May-94	1886.1		
Sep-80	1889.08	Apr-85	1887.557	Nov-89	1886.927	Jun-94	1886.16		
Oct-80	1888.93	May-85	1887.612	Dec-89	1887.125	Jul-94	1886.4		
Nov-80	1888.88	Jun-85	1887.666	Jan-90	1887.323	Aug-94	1886.5		
Dec-80	1888.82	Jul-85	1887.72	Feb-90	1887.483	Sep-94	1886.6		
Jan-81	1888.67	Aug-85	1887.775	Mar-90	1887.489	Oct-94	1886.5		
Feb-81	1888.53	Sep-85	1887.829	Apr-90	1887.601	Nov-94	1886.5		
Mar-81	1888.37	Oct-85	1887.809	May-90	1888.016	Dec-94	1886.92		
Apr-81	1888.63	Nov-85	1887.722	Jun-90	1888.431	Jan-95	1886.8		
May-81	1889.04	Dec-85	1887.635	Jul-90	1888.397	Feb-95	1886.64		
Jun-81	1889.23	Jan-86	1887.548	Aug-90	1888.347	Mar-95	1886.4		
Jul-81	1889.25	Feb-86	1887.461	Sep-90	1888.296	Apr-95	1886.4		
Aug-81	1889.56	Mar-86	1887.375	Oct-90	1888.245	May-95	1886.47		
Sep-81	1889.64	Apr-86	1887.288	Nov-90	1888.194	Jun-95	1886.5		
Oct-81	1889.65	May-86	1887.201	Dec-90	1888.143	Jul-95	1886.51		
Nov-81	1889.59	Jun-86	1887.376	Jan-91	1888.093	Aug-95	1886.3		
Dec-81	1889.54	Jul-86	1887.401	Feb-91	1888.042	Sep-95	1886.3		
Jan-82	1889.53	Aug-86	1887.38	Mar-91	1887.851	Oct-95	1886.4		
Feb-82	1889.309	Sep-86	1887.36	Apr-91	1887.657	Nov-95	1886.45		
Mar-82	1889.04	Oct-86	1887.34	May-91	1887.516	Dec-95	1886.56		
Apr-82	1888.975	Nov-86	1887.32	Jun-91	1887.441	Jan-96	1886.5		
May-82	1889.008	Dec-86	1887.277	Jul-91	1887.477	Feb-96	1886.4		

The Augur transects made by Behar, MSc 1999 (monitored, developed and new augers made at the same sites)

Name	x	y	Surface elevation	Water level (Behar, MSc 1999)	Auger Depth	Well status	Waterlevel (2000)

Lake	210519	9919689	1888.7	1888.7	1888.7		-
BA	210644	9920323	1889.19	1887.85	1886.68	Old well	1886.41
BA2	210713	9920651	1888.96	1886.8	1884.71	Old well	1884.86
BA3	210884	9920823	1888.78	1885.66	1884.61	Old well	1884.54
BA4	210973	9921029	1888.5	1885.27	1884.13	Old well	1884.13
BA5	211194	9921180	1888.32	1885.45	1884.57	Old well	1884.52
Well3	211434	9921380	1890.3	1885.64			-

Table 1: Description of Manera Farm Transect (Behar, MSc 1999)

Name	x	y	Auger Depth	Surface elevation	Water Level, (Behar, MSc 1999)	Well status	Water Level, (2000)
Lake	213620	9918120	1888.7	1888.7	1888.7	-	-
Well 1	213725	9918128	1886.7	1889.71	1888.16	New well	1886.86
Well 2	213751	9918121	1886.7	1890.02	1888.13	New well	1884.89
Well 3	213884	9918174	1883.4	1890.27	1888.07	New well	1884.5
Well 4	214014	9918202	1885.5	1890.4	1887.98	Behar well	1883.86
Well 5	214151	9918303	1884.3	1891.04	1887.57	-	-
Well 6	214271	9918436	1883.9	1892.21	1887.51	-	-
Well 7	214309	9918588	1881.7	1893.65	1887.38	-	-
Well 8	214340	9918801	1879.7	1893.15	1887.45	-	-

Table 2: Description of KWS Annex Transect (Behar, MSc 1999).

Piezometric Heads of observation wells prior to 1980 (natural setting)

well number	XUTM co-ordinate	YUTM co-ordinte	piezometric Head, m
C1926	209700	9905700	1889
ITC057	216171	9926241	2037
ITC058	218032	9922558	1999
ITC055	214375	9916225	1889
ITC059	216171	9924404	2006
26	200130	9902275	1594
30	200480	9902580	1643
C0466	190189	9917009	1907
ITC092	219888	9911496	2135
301	193940	9902400	1774
ITC043	210769	9920726	1887
ITC027	207680	9925645	1888
ITC048	212459	9931771	1958
ITC074	213600	9921500	1888
ITC136	219659	9902553	1872
ITC083	214310	9926240	1910
ITC084	214313	9920708	1895
C1404	190190	9915161	1894
ITC047	208988	9937384	1934
ITC042	207165	9925364	1886
701	199340	9903960	1734
C2300	190500	9909750	1914
C733	202750	9940250	1819
N40	216441	9913361	1910
N54	219848	9929261	2168
N52	219411	9926765	2064
ITC076	212463	9922555	1894

C2557	195300	9912500	1892
N57	219112	9923847	1995
C2709	186474	9907789	2114
ITC156	214009	9917763	1888
C2586(X-2)	198500	9905140	1842
EW1	196900	9930575	1852
ITC072	197605	9920698	1886
ITC157	213271	9914310	1886
ITC097	195762	9911480	1893
ITC082	206306	9931350	1886
ITC102	199473	9909635	1878
ITC107	212412	9903826	1899
ITC133	208751	9909641	1883
ITC159	195974	9908951	1887
ITC160	196851	9915861	1888
ITC161	197660	9918954	1888
N24	204040	9925879	1882
N41	190925	9909573	1912

The observation wells used after 1980 (present period).

well no.	Xcoordinate	Ycoordinate
ITC001	213518	9924527
ITC002	213735	9925528
ITC023	212267	9923041
ITC026	208752	9928952
ITC027	207680	9925645
ITC032	211300	9924682
ITC036	214224	9919179
ITC037	214078	9920423
ITC038	203516	9924230
ITC147	213850	9921800
ITC029	204034	9928849
ITC040	201591	9926461
ITC035	215467	9917087
ITC139	214338	9913285
ITC141	194855	9909913
ITC142	208383	9909763
ITC145	212664	9915091
ITC149	217150	9918100
ITC154	211200	9912475
ITC162	215784	9912357
ITC163	215884	9913478
ITC165	210713	9920651
ITC170	213751	9918121

The effects of stepped pumping on the observed groundwater levels

pumping m3/day	ITC001	ITC023	ITC026	ITC027	ITC036
0	17.34	11.67	-3.55	2.45	5.65
-18000	-0.02	0.14	-11.26	-2.96	5.36

-24000	-5.3	-2.94	-11.74	-3.53	5.02
-28000	-8.82	-5	-12.06	-3.91	4.75
-32000	-12.35	-7.05	-12.34	-4.23	4.47
-36000	-15.88	-9.11	-12.66	-4.63	4.19
-40000	-19.4	-11.17	-12.95	-4.97	3.91
-44000	-22.93	-13.22	-13.24	-5.32	3.61
-48000	-26.46	-15.29	-13.56	-5.69	3.32
-52000	-29.98	-17.35	-13.84	-6.02	3.03
-56000	-33.53	-19.43	-14.16	-6.44	2.72
-60000	-37.06	-21.48	-14.46	-6.79	2.42
-64000	-40.6	-23.56	-14.78	-7.21	2.12

pumping m3/day	ITC038	ITC147	ITC035	ITC141	ITC165	ITC170
0	1.99	13.06	-11.75	-5.8	4.33	3.8
-18000	-0.13	4.1	-11.7	-7.43	3.24	3.39
-24000	-0.38	1.78	-12.02	-7.56	3.16	3.23
-28000	-0.64	0.22	-12.25	-7.65	3.08	3.11
-32000	-0.76	-1.34	-12.48	-7.73	3.02	2.99
-36000	-1.08	-2.91	-12.71	-7.82	2.94	2.87
-40000	-1.23	-4.48	-12.95	-7.91	2.89	2.75
-44000	-1.39	-6.05	-13.18	-8	2.85	2.62
-48000	-1.55	-7.63	-13.42	-8.09	2.8	2.5
-52000	-1.7	-9.2	-13.66	-8.18	2.75	2.37
-56000	-1.97	-10.78	-13.9	-8.26	2.67	2.23
-60000	-2.15	-12.36	-14.14	-8.37	2.63	2.1
-64000	-2.41	-13.94	-14.38	-8.46	2.5	1.96

Hydraulic conductivity of different soil types around the lake.

Table 1. Hydraulic conductivity and soil types at Aberdare, after Jolicoeur (MSc 2000)

Depth Range (in cm)	Saturated Hydraulic conductivity in cm/day	Soil types
0-80	37.2	Loam to clay
80-600	26.6	Sandy loam

Table 2. Hydraulic conductivity and soil types at 3 Ostrich farm, after Jolicoeur (MSc 2000)

Depth range (in cm)	Saturated Hydraulic conductivity in cm/day	Soil types
0-40	4	Clay
40-80	8.9	Loam
80-150	41.6	Silt loam
150-600	46.4	Sandy loam to loamy sand

Table 3. Saturated Hydraulic conductivity and soil types at Oserian farm, after Jolicoeur (MSc 2000)

Depth range (in cm)	Saturated Hydraulic Conductivity (in cm/day)	Soil types
0-80	161	Sandy loam
80-400	29	Silt loam
400-530	41	Silt loam (ash)
530-600	29	Silt loam

Appendix 3: Model and Geodetic Surveys Data Set

The Rating Equations generated by the DTM and the two models

Stage	No. of cells	Cumulative	DTM	Spreadsheet	Mflake

m		%	Area, m^2	Area, m^2	Area, m^2
1881.75	34	0.119318182	26250000	4542009.723	
1882	55	0.181818182	40000000	19073365.04	
1882.25	34	0.220454545	48500000	32577642.22	
1882.5	48	0.275	60500000	45054841.29	
1882.75	23	0.301136364	66250000	56504962.22	
1883	42	0.348863636	76750000	66928005.04	
1883.25	20	0.371590909	81750000	76323969.72	
1883.5	30	0.405681818	89250000	84692856.29	
1883.75	8	0.414772727	91250000	92034664.72	
1884	14	0.430681818	94750000	98349395.04	
1884.25	9	0.440909091	97000000	103637047.2	
1884.5	15	0.457954545	100750000	107897621.3	
1884.75	4	0.4625	101750000	111131117.2	
1885	22	0.4875	107250000	113337535	
1885.25	9	0.497727273	109500000	120467131.3	
1885.5	14	0.513636364	113000000	123579675	
1885.75	13	0.528409091	116250000	126658031.3	
1886	12	0.542045455	119250000	129702200	
1886.25	11	0.554545455	122000000	132712181.3	
1886.5	14	0.570454545	125500000	135687975	
1886.75	8	0.579545455	127500000	138629581.3	133250000
1887	23	0.605681818	133250000	141537000	131750000
1887.25	13	0.620454545	136500000	144410231.3	131750000
1887.5	28	0.652272727	143500000	147249275	141500000
1887.75	6	0.659090909	145000000	150054131.3	145500000
1888	11	0.671590909	147750000	152824800	147750000
1888.25	14	0.6875	151250000	155561281.3	152750000
1888.5	17	0.706818182	155500000	158263575	154250000
1888.75	5	0.7125	156750000	160931681.3	156750000
1889	15	0.729545455	160500000	163565600	159250000
1889.25	7	0.7375	162250000	166165331.3	160500000
1889.5	16	0.755681818	166250000	168730875	166250000
1889.75	15	0.772727273	170000000	171262231.3	170000000
1890	12	0.786363636	173000000	173759400	173000000
1890.25	6	0.793181818	174500000	176222381.3	176250000
1890.5	13	0.807954545	177750000	178651175	177750000
1890.75	7	0.815909091	179500000	181045781.3	180750000
1891	12	0.829545455	182500000	188469963.6	180750000
1891.25	6	0.836363636	184000000	191091225.7	185000000
1891.5	12	0.85	187000000	193675092.8	187000000
1891.75	10	0.861363636	189500000	196221565.1	191250000
1892	12	0.875	192500000	198730642.4	192500000
1892.25	10	0.886363636	195000000	201202324.9	196500000
1892.5	15	0.903409091	198750000	203636612.5	198500000
1892.75	11	0.915909091	201500000	206033505.2	201500000
1893	12	0.929545455	204500000	208393003	204500000
1893.25	6	0.936363636	206000000	210715106	206000000
1893.5	8	0.945454545	208000000	212999814	208000000
1893.75	7	0.953409091	209750000	215247127.2	209750000
1894	13	0.968181818	213000000	217457045.5	213000000
1894.25	4	0.972727273	214000000	219629568.8	214000000
1894.5	16	0.990909091	218000000	221764697.3	218000000
1894.75	5	0.996590909	219250000	223862431	219250000
1895	3	1	220000000	225922769.7	220000000

Naivasha, Kenya Data Set

POINT ID	X-CARTESIAN	Y-CARTESIAN	Z-CARTESIAN
133t7	5134554.6221	3786250.4976	-74703.4992

3PAUSHANDPUMP	5133099.3632	3788186.6853	-75720.7860
3PHOUS-C	5133168.2224	3788098.0663	-75359.5191
BH2	5132992.2301	3788359.2509	-74751.1010
BHB	5133015.0883	3788309.1334	-75327.4539
BM33	5140057.6967	3778901.6976	-74947.5507
C11093	5132525.0210	3788781.1930	-86969.1076
C1154	5139391.3184	3779707.2968	-75062.9534
C11841	5132808.9086	3788364.9239	-88269.9212
C2883	5133425.1683	3787891.3061	-71352.4908
C4155	5132595.9454	3788959.6024	-73660.4972
CRATER LAKE LEVEL	5143991.7125	3773112.2193	-86629.0856
M7	5138778.7444	3780570.9742	71401.3677
M8	5138824.5752	3780373.4514	76134.3001
M9	5139023.4669	3780107.3396	76050.0684
MULLA 1	5146168.2653	3770178.6860	91546.5608
OSTRICHBHA	5132827.1038	3788590.0241	74683.1907
SG	5134141.5388	3786517.9605	86157.5992
TANINI	5133114.7253	3788200.5295	74583.4414
W37	5132980.0750	3788080.9448	90130.4906
bm21	5143987.3555	3773115.8522	89617.0806
bm32	5140571.0395	3778131.7133	76137.9158
bm38	5137786.1177	3781933.9304	69310.0865
bm47	5133390.9805	3787741.3007	77314.2650
bm6	5133220.8495	3787757.8508	87878.5189
bm7	5133854.8091	3786880.3915	88912.6938
bm8	5134588.8343	3785863.5281	89780.2795
bm9	5135373.8238	3784773.1986	90614.7142
c11235	5131165.2479	3790702.5919	86719.0856
c2823	5129406.1966	3793052.5908	97746.2678
c2883	5133425.3183	3787891.4744	71352.4841
c467	5131706.2540	3789937.9923	86524.6308
c567	5132972.6253	3788091.5368	90139.5585
cresciland	5134672.0313	3785857.0987	85287.0856
delapiv2	5134456.3088	3786343.3921	75348.3443
delapivot	5133373.1239	3787811.8201	75592.0158
greatwell	5144321.1666	3772726.2201	85385.5184
kobil	5133598.2070	3787478.9454	76613.4706
manera9	5134276.7892	3786493.9255	78874.2094
milkfact	5134070.5471	3786857.6817	75804.8756
mula2	5145577.4122	3770985.3312	91458.9710
station	5132746.6133	3788571.0339	79422.9382
w65	5131775.2063	3789839.5085	87625.6943
w66	5131559.8003	3790141.8698	87138.2932

Table A3: Co-ordinates of Points in Cartesian WGS84.

Appendix 4: Plates

Plate 1: An old lake level staff gauge at the centre Bushy Islands. It indicates the higher lake levels during the earlier years.

Plate 2: The main River Malewa gauging station. Note the wooden planks and the water diversion at the centre of the foreground.

Plate 3: Transect Auguring at the KWS-Annex station. Note the transition from the light brown, clayey sand to dark grey, sandy clay geologic log in the foreground.

Appendix 5: Web and Library Data Sources

1. A utility program called PMVCRT.EXE was obtained from

http://www.uovs.ac.za/igs/pmwin5.exe. This program is able to translate ASCII data to native PMWIN5 files (including time-dependent information).

2. An installer for the Argus PIE that supports the Lake package was obtained from ftp://srv1rvares.er.usgs.gov/pub/rbwinst/Mt3dgui310.zip. This is a new version of the GUI that was released in November, 1999.

3. The source code for the MODFLOW GUI was obtained from

http://water.usgs.gov/nrp/gwsoftware/modflow-gui/modflow-gui.html.

There is a "customized" version of the GUI that supports the Lake2 package as well as MT3D and the Seepage package.

4. LAK2 can be obtained from the Wisconsin Department of Natural Resources at ftp://www.dnr.state.wi.us/Crandon/MODFLOW. LAK2 has a steady-state solver and LAK1 does not. In addition, LAK2 provides more flexibility in outfall stage-discharge relationships for outlet streams.

You can also obtain the LAK2 package from the following URL:

http://www.hsigeotrans.com/modflowlake.html

Appendix 6: Data and Result Archives

1. Thesis: Final Thesis

2. ILWIS maps:
- Drainage
- Geology
- Lake
- Satellite imagery

Catchment boundary

- Survey data
- DTM maps
- Catchment data
- MFLAKE maps

3. MODEL Inputs:

i) Climatic data:
- evaporation,
- rainfall

ii) Lake data

iii) Stream flow data

4. MODEL outputs:

i) Steady State
- Recharge
- Transmissivity
- wells

iii) Transient State
- Storage coefficient

iii) PEST runs
- First run
- Final runs (optimised)
- Water Budget

iv) Lake data

5. Miscellaneous

i) Transect auger data

ii) Piezometric data:
- Prior 1980
- Post 1980

iii) Library data